



Master Thesis

Chassis, Drivetrain, and Energy Storage Layout for an Electric City Vehicle

Dipl.-Ing. (FH) Stefan Eitzinger

Carried out at the Institute of Automotive Engineering

Director: Prof. Dr. techn. W. Hirschberg

Supervisor: Dipl.-Ing. Haymo Niederkofler

Graz, 01 2011

FTG

Für Andrea, Nina und Julia

STATUTORY DECLARATION

I declare that I have authored this thesis independently, that I have not used other than the declared sources / resources, and that I have explicitly marked all material which has been quoted either literally or by content from the used sources.

.....

date

.....

(signature)

Abstract

Increasing fuel prices, CO₂ taxes, and congestion charges like in London will increase the demand for electric vehicles in the future. As the storage of electrical energy is still the main cost driver, the focus must be on the reduction of energy consumption. A parameter which has a significant influence is the vehicle weight. Additionally it is easier in Europe to homologate lightweight vehicles. In cooperation with four students a concept for a lightweight, electric city vehicle was developed.

The present thesis describes the definition and integration of three major modules in this vehicle. The module chassis includes front and rear suspension, steering system, brakes and tires. The module drivetrain consists of the electric motor with transmission, the drive shafts, the high voltage ECUs, the vehicle control unit and the accelerator pedal. The battery and the high voltage distribution unit are included in the module energy storage. The functional requirements for these components are defined from the full vehicle specifications. Additional geometrical requirements from package or ergonomics are considered. Suitable parts are selected from existing parts or conceptually designed. Finally estimated costs and weights of the parts are compared with target values.

Zusammenfassung

Steigende Treibstoffpreise, CO₂ Steuern, innerstädtische Mautsysteme wie in London werden den Bedarf an Elektrofahrzeugen in der Zukunft steigen lassen. Nachdem die Speicherung der elektrischen Energie noch immer der größte Kostentreiber ist, muss der Focus auf der Reduktion des Energieverbrauchs liegen. Ein Parameter mit einem signifikanten Einfluss ist das Gewicht. Zusätzlich ist es in Europa einfacher Leichtfahrzeuge zu homologieren. In Zusammenarbeit mit vier Studenten wurde ein Konzept eines leichten, elektrischen Stadtfahrzeugs entwickelt.

Die vorliegende Arbeit beschreibt die Definition und Integration von drei Hauptmodulen in dieses Fahrzeug. Das Modul Fahrwerk beinhaltet die vordere und hintere Rad-aufhängung, Lenkung, Bremsen und die Reifen. Das Modul Antriebsstrang besteht aus dem Elektromotor mit Getriebe, den Antriebswellen, den Hochspannungs-ECUs, dem Fahrzeugregler und dem Gaspedal. Die Batterie und die Einheit für die Hochspannungs-Verteilung sind im Modul Energiespeicherung enthalten. Die funktionalen Anforderungen an diese Komponenten werden aus den Gesamtfahrzeug-Anforderungen bestimmt. Zusätzlich werden die geometrischen Anforderungen aus Package und Ergonomie berücksichtigt. Passende Teile werden aus existierenden Teilen ausgewählt oder konzeptionell konstruiert. Abschließend werden die geschätzten Kosten und Gewichte mit Zielwerten verglichen.

Content

1	INTRODUCTION.....	1
2	VEHICLE SPECIFICATION	3
	2.1 BASIC VEHICLE SPECIFICATIONS	3
	2.1.1 <i>Homologation category</i>	3
	2.1.2 <i>Basic vehicle specifications</i>	4
	2.1.3 <i>Basic vehicle layout</i>	6
	2.2 DRIVING PERFORMANCE	8
	2.2.1 <i>Driving resistances.....</i>	8
	2.2.2 <i>Traction force diagram.....</i>	12
	2.2.3 <i>Acceleration performance</i>	15
	2.3 BATTERY CAPACITY	18
	2.3.1 <i>Battery capacity simulation using NEDC</i>	18
	2.3.2 <i>Range calculation with given battery capacity</i>	20
3	DRIVETRAIN AND ENERGY STORAGE.....	22
	3.1 DRIVETRAIN LAYOUT.....	22
	3.1.1 <i>Front or rear wheel drive.....</i>	22
	3.1.2 <i>Central motor or wheel hub motor</i>	24
	3.2 DRIVETRAIN COMPONENTS	25
	3.2.1 <i>Traction motor.....</i>	25
	3.2.2 <i>Transmission.....</i>	32
	3.2.3 <i>Electric Control Units</i>	33
	3.3 ENERGY STORAGE	36
	3.3.1 <i>Battery cell technology.....</i>	37
	3.3.2 <i>Battery system</i>	39
	3.3.3 <i>Battery frame and housing.....</i>	41
	3.3.4 <i>Battery lifetime</i>	44
	3.3.5 <i>Battery cooling</i>	48

4	MAIN CHASSIS COMPONENTS / MODULES	50
4.1	FRONT SUSPENSION	53
4.1.1	<i>Benchmark: Front suspension of small vehicles</i>	53
4.1.2	<i>E-MILA Student front suspension</i>	59
4.1.3	<i>New front suspension design.....</i>	59
4.2	REAR SUSPENSION	64
4.2.1	<i>Benchmark: Rear suspension of small vehicles</i>	65
4.2.2	<i>Suitability of benchmark suspension systems for E-MILA S</i>	70
4.2.3	<i>E-MILA Student rear suspension</i>	73
4.3	STEERING SYSTEM	75
4.3.1	<i>Steering kinematics.....</i>	75
4.3.2	<i>Steering wheel position / Steering uniformity.....</i>	78
4.3.3	<i>Steering wheel torque</i>	81
4.4	BRAKES	82
4.4.1	<i>Recuperation brake.....</i>	82
4.4.2	<i>Friction brake</i>	84
4.4.3	<i>Brake simulation</i>	88
4.5	TIRES.....	90
5	VEHICLE INTEGRATION OF COMPONENTS	92
5.1	FULFILMENT OF VEHICLE TARGETS	92
5.1.1	<i>Costs.....</i>	92
5.1.2	<i>Weight.....</i>	95
5.2	OUTLOOK FOR OPTIMIZATION POTENTIAL	98
6	CONCLUSION	100
	REFERENCES.....	102
	LIST OF FIGURES.....	106
	LIST OF TABLES	109
	ANNEX	A

Abbreviations and Formula Symbols

Abbreviations

ABS	Antilock Braking System
AC	Alternating Current
BLAC	Brushless Alternating Current (operation mode for PM)
BLDC	Brushless Direct Current (operation mode for PM)
CFD	Computational Fluid Dynamics
CoG	Centre of Gravity
DC	Direct Current
ESC	Electronic Stability Control System
EUDC	Extra Urban Driving Cycle
GVW	Gross Vehicle Weight
HVDU	High Voltage Distribution Unit
IM	Induction Machine
L7e	Homologation category for lightweight passenger vehicles according to regulation 70/156/EGW
M1	Homologation category for passenger vehicles according to regulation 70/156/EGW
MILA	MAGNA Innovative Lightweight Auto
NEDC	New European Driving Cycle
PM	Permanent-magnet Machine
UNECE	United Nation European Economic Commission
SEI	Solid Electrolyte Interface
SOC	State of Charge
SRM	Switched Reluctance Machine
SRP	Seat Reference Point
VCU	Vehicle Control Unit

Formula Symbols

Symbol	Unit	Description
A	[m ²]	Vehicle Cross Sectional Area
a_x	[m/s ²]	Acceleration in longitudinal direction
a_y	[m/s ²]	Acceleration in lateral direction [m/s ²]
a_z	[m/s ²]	Acceleration in vertical direction [m/s ²]
c_D	[-]	Aerodynamic Drag Coefficient
C_{loss}	[-]	Capacity Loss
C_{RR}	[-]	Rolling Resistance Coefficient
C_{therm}	[J/K/Cell]	Thermal Capacity of Battery Cell
F	[N]	General Force
F_D	[N]	Aerodynamic Drag
F_g	[N]	Climbing Resistance
F_i	[N]	Inertial Force
F_R	[N]	Total Driving Resistance
F_{RR}	[N]	Rolling Resistance
F_z	[N]	Wheel Load
g	9.81[m/s ²]	Constant for Gravitational Acceleration
i	[-]	Gear Ratio
I	[kgm ²]	Rotational Inertia
I_{eff}	[A]	Effective Current
m	[kg]	Vehicle Mass
m_{add}	[kg]	Equivalent additional mass to consider rotational inertia
n_{cycle}	[-]	Number of Cycles
r_{dyn}	[m]	Dynamic Wheel Radius
r_{stat}	[m]	Static Wheel Radius

Abbreviations and Formula Symbols

t	[s]	Time
T	[K]	Temperature
w	[m]	Width of the Tire
α	[rad]	Angle
$\delta_{i,a}$	[rad]	Steering angle of inner, outer wheel
ρ	[kg/m ³]	Air density

1 Introduction

This thesis is one of five theses all dealing with developing a concept of a small electric city vehicle. At MAGNA this vehicle concept has the project name E-MILA Student, later in the text also abbreviated as E-MILA S. This car shall present the ideal concept for a city vehicle: A lightweight, compact, zero emission three-seater car. The first step for a new vehicle concept is a marketing analysis, which was done by Michael Preiss in his thesis [Pre10]. The results of the marketing analysis were a market scenario with estimated sales volume and rough vehicle specifications. The remaining four theses are based on these results and were carried out in parallel by four students representing the E-MILA Student team. Praveen Madeshi describes the homologation process for the vehicle. Additionally he also took care of the interior and the ergonomics requirements [Mad11]. Veera Muttumula describes the recycling process for the vehicle [Mut11]. The process of a full vehicle development and the targets for the different vehicle functions are described by Lukas Wechselberger [Wec11]. An overview on the content of this thesis is given in the following paragraph.

The integration of electric drivetrain components and a battery into an existing vehicle is strongly restricted by the existing vehicle layout and package. Thus the degrees of freedom in design are limited. Usually the parts have to be modified to fit in the vehicle. In contrast to that the integration of these parts in a newly designed vehicle, as is presented here, offers more degrees of freedom. Besides adapting the parts to the vehicle it is also possible to adapt the vehicle to existing parts. The higher number of possibilities seems to make integration easier initially, but to find an ideal solution is a lot more difficult, as there are many parameters to tune and these parameters also influence each other.

The aim of this thesis is to describe the main steps that are necessary to define a chassis, drivetrain, and battery concept for a small battery electric vehicle and integrate these major modules into the vehicle.

Although the task was to design the vehicle from scratch, some very important prerequisites were defined in advance. The vehicle shall be a small three-seater car that can be homologated in the L7e category in Europe, which means that there is a weight limit for the empty vehicle without batteries of 400 kg and also a power limit of 15 kW.

The first task is to gather all the specifications on a full vehicle level that are necessary to define the specifications of the major modules. As there are different sources for the vehicle specifications it shall be investigated, if they match. For instance if the

desired acceleration performance of the vehicle, defined by customer requirements, can be achieved with the motor power and the weight of the vehicle, limited by law. Thus it will be possible to define some of the specifications of the three major modules independently from each other based on the full vehicle specifications.

Nevertheless there are other specifications like the package space for the modules that cannot be predefined. The design of one module influences the design of another module or/and the vehicle layout. It is the main task of this thesis to define the components in a way to optimize the vehicle layout. The components are either selected from existing production parts or else conceptually designed. For the optimized vehicle layout it is necessary to consider exterior and interior dimensions, ergonomics for the driver and passengers, functional requirements, weight and last but not least costs. Besides the technical specifications it is therefore also necessary to identify the costs of the components.

2 Vehicle Specification

This chapter describes the full vehicle specification of the E-MILA Student city vehicle. To break down the requirements for the chassis and the drivetrain, it is essential to define and understand the specification for the full vehicle. These specifications are based on a marketing analysis, which was carried out by Michael Preiss and documented in his thesis [Pre10]. In a collaboration of four students representing the E-MILA Student team the specifications defined in [Pre10] were reviewed and modified to be technically feasible. This process is described in detail by Lukas Wechselberger [Wec11]. The given work will not show the process of the definition of the complete full vehicle requirements, but present the necessary results to understand the layout of the drivetrain and chassis described in chapter 3 and 4.

2.1 Basic Vehicle Specifications

2.1.1 Homologation category

Europe

For Europe the homologation categories are described by the UNEEC (United Nation European Economic Commission) in the regulation 70/156/EEC. The E-MILA-Student shall be homologated in L7e category. The standard category to homologate a passenger vehicle is the M1 category. It represents the category for common passenger vehicles up to a seating capacity of 8 passengers plus driver. The L7e category is designated to small lightweight vehicles. These vehicles must fulfil the following basic requirements:

- Maximum kerb weight not including the weight of the batteries: 400 kg
- Maximum nominal engine power: 15 kW

These two requirements already show that weight (of the vehicle and therefore also of every single part in the vehicle) must be the main focus for the concept development. Additional detailed requirements for L7e vehicles will be presented in this work, when relevant for the concept decision.

United States / Canada

For the United States the E-MILA Student shall be homologated according to the standard FMVSS500. In Canada the same standard is called CMVSS500. The main basic vehicle requirements of this standard are the following:

- Maximum kerb weight including the weight of the batteries: 3000 lbs (1361 kg)
- Maximum top speed: 25 mph (40 kph)

If the requirements for the homologation in the L7e category in Europe are fulfilled, also the requirements for the homologation according to the FMVSS500/CMVSS500 standard are met. It is only necessary to limit the top speed to 25 mph, which in case of an electric vehicle can be easily realized without any additional parts.

A complete description of all homologation requirements associated with the E-MILA Student can be found in the thesis of Praveen Madeshi [Mad11].

Japan

In Japan there is a category for small cars called “kei”-cars. In order that a vehicle can be homologated as a “kei”-car it has to fulfil the following requirements [SAE83]:

- Max vehicle length: 3.4 m
- Max vehicle width: 1.48 m
- Max vehicle height: 2 m
- Max engine displacement: 660 cc
- Max nominal engine power: 47 kW

The maximum nominal engine power is already limited to 15 kW due to the requirement of fulfilling the European L7e standard. To also fulfil the Japanese standard it is therefore only necessary to stay within the given outer dimensions. Here especially the maximum vehicle width needs a special focus, the other dimensions (length and height) are planned to be smaller anyway (see 2.1.2).

2.1.2 Basic vehicle specifications

The idea behind the vehicle concept is to design a vehicle which is ideal for all daily short distance travels. For instance for a daily commuter, who lives in the surroundings of a city, works in the city and prefers the comfort of individual transport. Of course this vehicle should also perfectly satisfy the demands of someone doing the daily shopping trip or a father or mother bringing his/her kids to kindergarten. The driving performances are dedicated to urban use.

Therefore the main characteristics of the vehicle are:

- Small exterior dimensions:
 - Vehicle length max. 2.55 m, so that cross parking is possible
 - Vehicle width max. 1.48 m, in order to fulfil the Japanese “kei”-car homologation requirements (chapter 2.1.1)
 - Vehicle height max. 1.6 m
- At least 3 seats (so that parents can carry their two children)
- A trunk space large enough to carry a crate of beer and two shopping bags)
- A range of 90 km (for commuters to get to work and also back home)
- A top speed of 90 kph (to drive short distances on motorways)
- A turning circle of less than 7.5 m (for good manoeuvrability and easy parking)
- A more detailed description of the technical specifications is given in Table 2.1.

Table 2.1 Basic vehicle specifications, compare to [Pre10]

Outer Dimensions	
Length [mm]	2550
Width [mm]	1450
Height [mm]	1550
Wheel Base [mm]	1850
Track Width Front [mm]	1300
Track Width Rear [mm]	1300
Turning circle diameter [m]	7.5
Inner Dimensions	
Passenger Compartment	Driver and 2 passengers (adults)
Trunk space [l]	150
Weight	
Curb weight w/o batteries [kg]	400
Curb weight with batteries [kg]	550
Design weight [kg]	640
Gross vehicle weight [kg]	800
Drivetrain	
Driven Axle	Rear Wheels
Drive	Electric Motor
Power [kW]	15
Battery	Li-Ion
Range [km]	90
Performance	
Max. speed [kph]	90
Climbing Performance [-]	25%
Max. time for acceleration 0-50kph [s]	7.8

2.1.3 Basic vehicle layout

Based on the basic vehicle specification a first rough vehicle layout (see Figure 2.1 and Figure 2.2) was defined. The driver is positioned in the centre, which has several advantages:

- No left and right hand drive version necessary
- Free vision field – no disturbance from the A-pillar
- Driver can be moved to the front
- Sufficient leg room for the driver and still very large steering angles possible
- Co-drivers have their leg room beside the driver and can therefore sit close behind the driver. This enables a short overall vehicle length.

The disadvantage of declined accessibility has to be considered in the body layout. In the area of the driver the vehicle body has a reduced width.



Figure 2.1 First vehicle layout – sideview [PSM09]

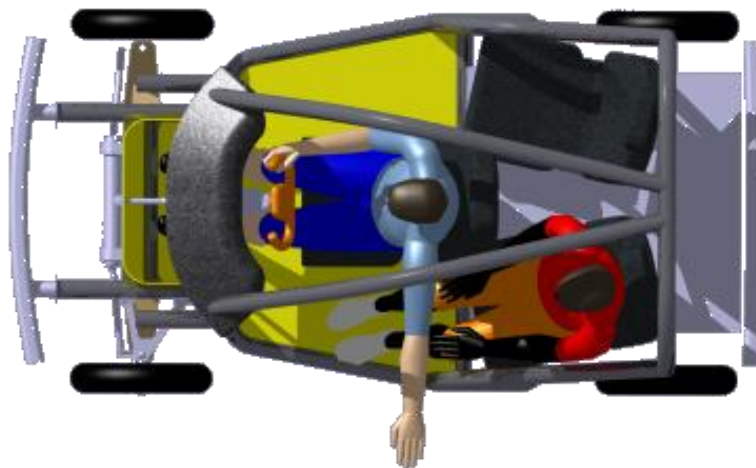


Figure 2.2 First vehicle layout – top view [PSM09]

Especially for package reasons it was decided to position the motor on the rear axle and drive the rear wheels. A central motor in the front would significantly reduce the free deformation length for a front crash. Moreover it would be necessary to move the driver position to the rear, because the drivers leg room uses the package space for the gear and the motor. This results in less space for the passengers, especially in lateral direction because their seating position moves closer to the rear axle and also the trunk space would be reduced. The only possibility to realize a front wheel drive with the given vehicle layout and seating position is to use wheel hub motors. But wheel hub motors would increase the system costs. Therefore it was decided to use a centrally positioned

motor that drives both rear wheels. A more detailed description of the advantages and disadvantages of this concept is given in chapter 3.1.

The package space for the batteries is under the driver and passenger seats it can be seen in Figure 2.1. A detailed description of the battery and the integration in the vehicle is given in chapter 3.3.

2.2 Driving performance

As described in chapter 2.1.1 the nominal motor power is limited to 15 kW. This of course also limits the driving performance. As the vehicle is intended to be mainly use in cities, the focus is not on maximum speed, but more on a reasonable acceleration and climbing performance. It is important that the vehicle is no obstacle in city traffic. An observation during daily city driving showed, that the average time for acceleration from 0 to 50 kph is 7.8 seconds. The vehicle should at least have the same acceleration performance. The climbing performance was defined with minimum 25% inclination. This is sufficient to be able to climb all usual roads.

2.2.1 Driving resistances

To be able to investigate the actual driving performance of the vehicle, it is necessary to define all driving resistances.

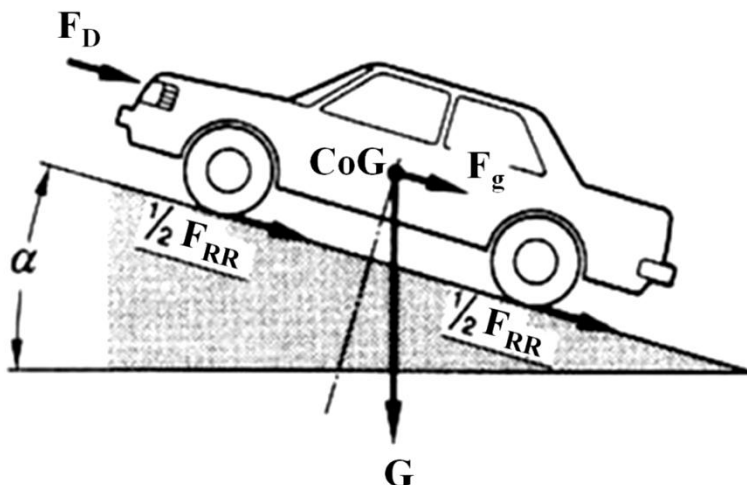


Figure 2.3 Driving resistances at constant speed [BOS07]

The total driving resistance for constant speed is the sum of the inclination and rolling resistance as well as the air drag (see Figure 2.3). In case the vehicle speed is changing the inertia resistance has to be considered additionally (see formula 2-1).

$$F_R = F_{RR} + F_g + F_A + F_I \quad (2-1)$$

The calculation of the single driving resistances is described below.

Inclination Resistance

The inclination resistance is depending on the vehicle weight and inclination of the road.

$$F_g = m \cdot g \cdot \sin \alpha \quad (2-2)$$

Rolling resistance:

The tire is deformed in the contact patch, due to the load acting on it. When rolling, the repeated deformation causes energy loss known as rolling resistance. In [ISO8767] rolling resistance is defined as the energy consumed by a tire per unit of distance covered. The rolling resistance is mainly depending on the tire and the wheel load, but also on the vehicle speed. The speed influence is relevant at higher vehicle speeds. At lower speeds (< 100 kph) the influence can be neglected (see Figure 2.4).

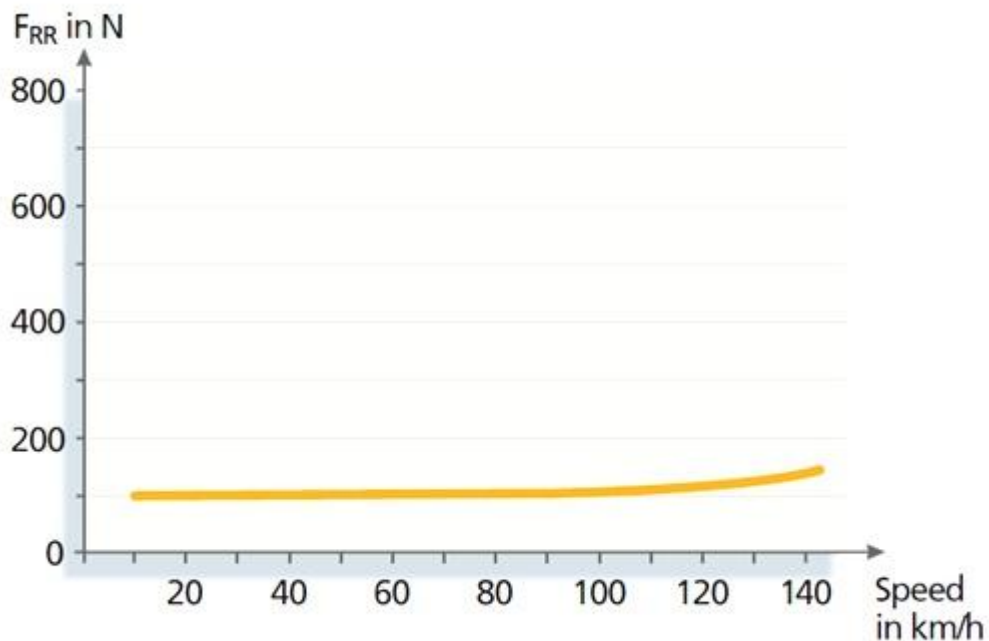


Figure 2.4 Vehicle speed influence on rolling resistance [MIC03]

A simple formula to calculate the rolling resistance can be found in [BOS07] or [Bra01].

$$F_{RR} = C_{RR} \cdot m \cdot g \cdot \cos \alpha \quad (2-3)$$

The rolling resistance F_{RR} is calculated by multiplying the friction coefficient C_{RR} with the wheel load. C_{RR} is depending on various parameters, like the tire dimensions, tire construction, tread design, and rubber compound, tire pressure, temperature, load, and speed. According to [MIC03] volume production passenger car tires available in 2002 have rolling resistance coefficients between 8.5 and 13 kg/t. But there are also tires available, with especially low rolling resistance coefficients of down to 6 kg/t. In the driving performance calculation the rolling resistance coefficient is considered with 10 kg/t because not only the resistance of the tire alone, but also the resistance due to friction in the ball bearings needs to be considered.

Air drag

The air drag F_D is depending on the outer geometry of the vehicle, the air density ρ and the vehicle speed v .

$$F_D = \frac{1}{2} \cdot A \cdot c_D \cdot \rho \cdot v^2 \quad (2-4)$$

The geometry is considered in the formula with two parameters. A represents the vehicles cross sectional area (see Figure 2.5) and c_D is the drag coefficient, which is mainly depending on the body shape. The drag coefficient can be determined by CFD simulation or by experiment in a wind tunnel or less accurate in a coasting test. During the years improvement of vehicle design led to an improvement of the drag coefficient [Hei08]. Typical modern cars have a drag coefficient around 0.3, but the shorter a vehicle is, the more difficult it is to have a low drag coefficient. A Smart for example has a drag coefficient of 0.35 [AMS10]. As the E-MILA Student will have a very similar body shape, also a drag coefficient of 0.35 is considered.

The vehicle speed influences the air drag with the power of 2. Therefore the air drag has only a minor percentage of the total driving resistance at lower speed, like in city traffic (see Figure 2.6).

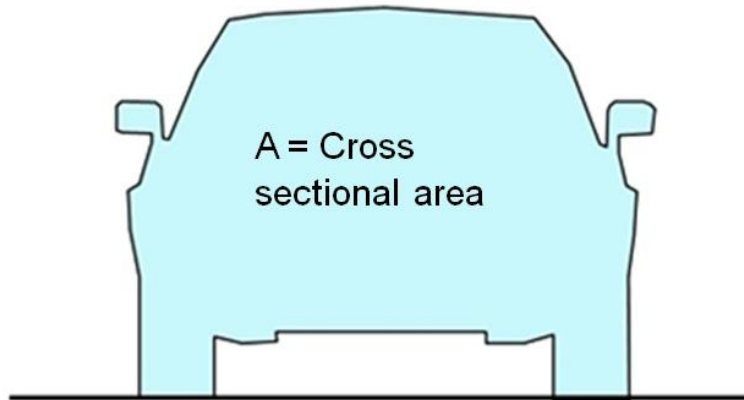


Figure 2.5 Vehicle cross sectional area

Inertia resistance

Due to the mass of the vehicle m and the rotational inertia I of all rotating parts (like the motor or the wheels), the motor also has to overcome the inertial force F_I , when accelerating the vehicle. The rotational inertia of all rotating parts can be considered as an additional mass, which is added to the vehicle mass, to calculate the inertial force (see formula 2-6).

$$m_{add} = \frac{I \cdot i}{r_{dyn}^2} \quad (2-5)$$

$$F_I = (m + \sum_{i=0}^n m_{add,i}) \cdot a_x \quad (2-6)$$

For the E-MILA Student it is planned to use a transmission with a fixed gear ratio. Therefore there are only two types of rotating parts in the vehicle. Parts like the wheels, drive shafts and the output gear of the transmission are rotating at wheel speed, which is equivalent to the vehicle speed divided by the dynamic wheel radius (r_{dyn}). The rotor of the motor and the input gear of the transmission are rotating at motor speed, which is equivalent to the wheel speed times the gear ratio.

The inertia of these rotating parts is considered in the acceleration calculation with the additional masses calculated in Table 2.2. The gear ratio considered in the calculation is defined in Table 2.3.

Table 2.2 Inertia of rotating parts

	Inertia [kg m ²] per Wheel	Additional mass [kg]
Wheels, Brake Disk/Drum, Drive Shaft, Output Gear	4.500E-01	23.46
Rotor, Input Gear	1.811E-03	3.99

It can be seen that the wheels account for the main part of the additional mass. The calculated additional mass is reasonable, when compared to the rule of thumb given in [MIC03], that the additional mass from the wheels is approximately 50% of the mass of the wheels. So choosing light wheels with a small diameter is beneficial in terms of inertial resistance.

Figure 2.6 shows that during city driving the rolling resistance force and the inertial force have the main impact on the total driving resistance.

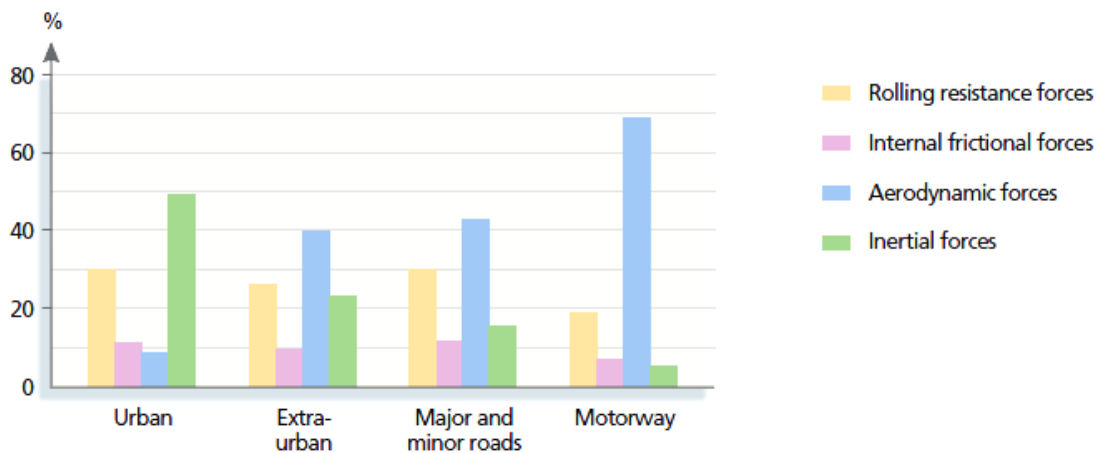


Figure 2.6 Percentage of resistive forces in different driving cycles [MIC03]

Aerodynamic forces soon become relevant when the vehicle is driving at higher speeds. In case of the E-MILA Student the maximum velocity is 90 kph, furthermore the vehicle is intended to be driven in cities, where the average speed will be below 50 kph, so the aerodynamic drag will be less significant. A low c_D value is therefore not the highest priority target in the vehicle development.

More important is a low rolling resistance and low inertial force. Both can be advantageously influenced with a low vehicle mass. Additionally the maximum mass is limited by regulations (see 2.1.1). The mass is therefore the most important technical vehicle target.

2.2.2 Traction force diagram

The driving performance at constant speed is investigated with the use of a traction force diagram (see Figure 2.8). This diagram shows the traction force depending on the vehicle speed. By adding the driving resistances at constant speed, several important vehicle specification parameters can be determined.

The following vehicle parameters are used for the traction force diagram:

Table 2.3 Vehicle parameters for traction force diagram

GVW [kg]	800
vmax [kph]	90
motor nom./peak power [kW]	15
motor nom. torque [Nm]	55
motor peak torque [Nm]	90
rdyn [mm]	265
gear ratio [-]	13
gear efficiency [-]	0.97
drivetrain efficiency [-]	0.95
cross sectional area [m²]	2.1
drag coefficient [-]	0.35
air density [kg/m³]	1.1
rolling resistance coefficient [-]	0.01

The maximum motor power is given from the homologation criteria (see chapter 2.1.1). The gear ratio was chosen in a way that the motor can achieve its maximum power until the maximum vehicle speed of 90 kph. The maximum speed of the motor was defined with 12,000 rpm, because this is also the maximum speed of a motor with a very similar nominal power, which is available at MAGNA. The corner speed, which is the speed where the motor has its nominal power and nominal torque, was defined with 2,600 rpm. Thus the motor has a nominal torque of 55 Nm and an area of field weakening of 1:5. More details on motor definition can be found in chapter 3.2.1. The result is a motor characteristic as shown in Figure 2.7. Due to the limitation of the output power of 15 kW, the peak torque is not really relevant and cannot be used at higher speeds. At lower speeds the higher peak torque can be used for a higher starting torque, pull-out torque, or to increase the climbing performance, but only for a period of 30 sec.

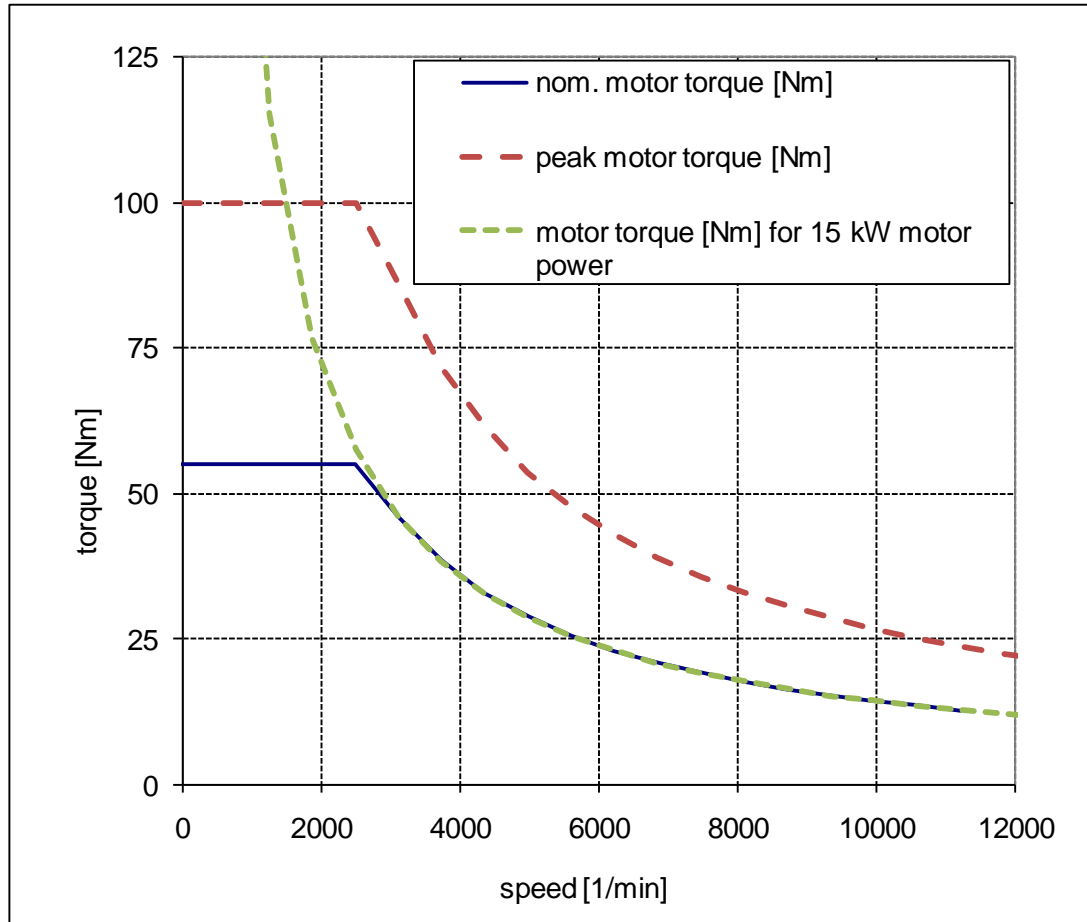


Figure 2.7 Motor characteristic for driving performance calculation

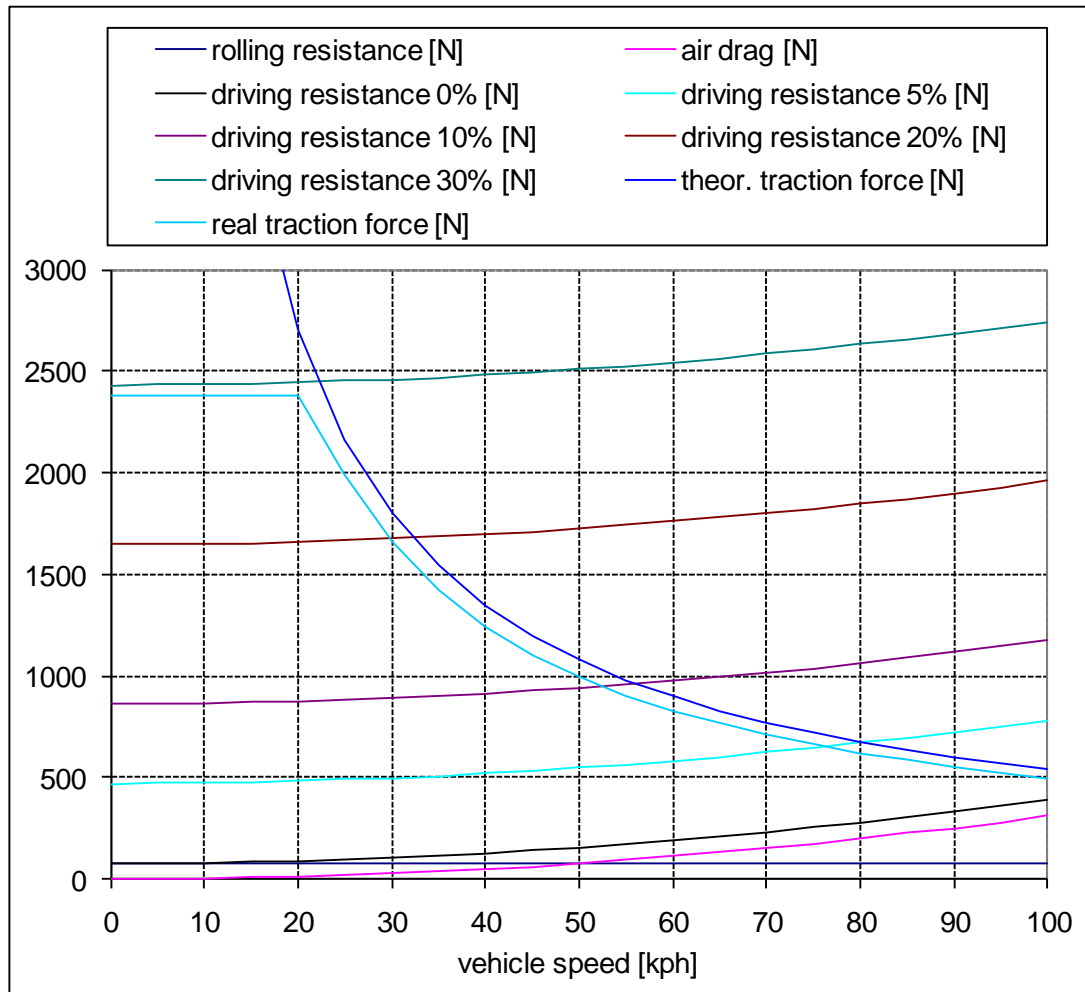


Figure 2.8 Traction force diagram

Results from the traction force diagram:

- Maximum vehicle speed of 90 kph will be reached up to road inclination of maximum 2.8%.
- The vehicle speed on flat road would be higher than 90 kph and thus needs to be limited electronically.
- The vehicle will meet the requirement to climb a road with an inclination of at least 25%. Theoretically the maximum possible inclination for the vehicle to climb would be 29%.
- At 50 kph the air drag equals the rolling resistance.

2.2.3 Acceleration performance

The traction force diagram only considers the vehicle at constant speed. Therefore it is necessary to have a look at the acceleration performance in a separate diagram (see Figure 2.9). This diagram shows on the one hand the maximum possible acceleration for

different road inclinations depending on the vehicle velocity. On the other hand it shows the time necessary to accelerate the vehicle from standstill to a certain speed for different road inclinations.

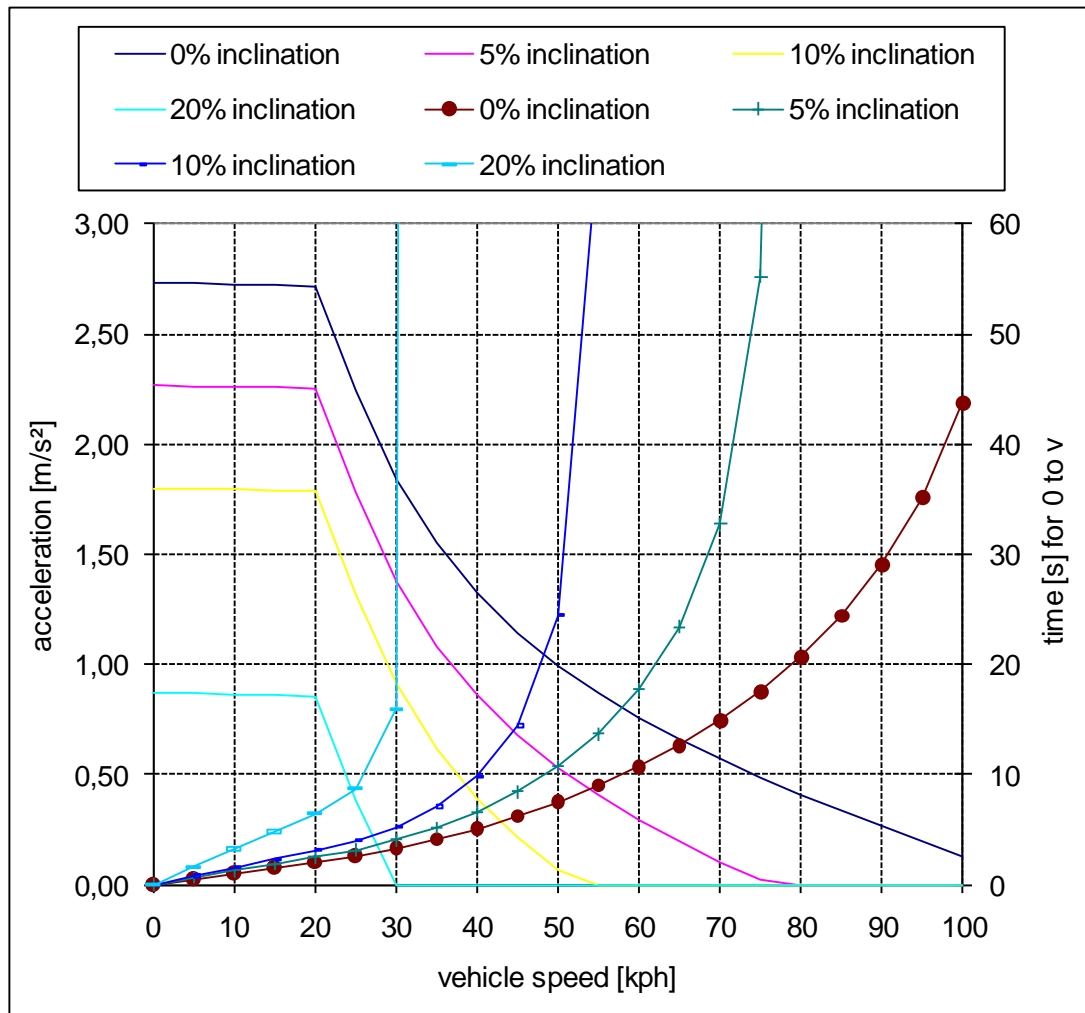


Figure 2.9 Acceleration Performance (continuous torque)

The most important result from this diagram for a city vehicle is the time needed for the acceleration from 0 to 50 kph.

- 0 to 50 kph with 0% road inclination: 7.5 sec
- 0 to 50 kph with 5% road inclination: 10.7 sec

Apart from the driving resistances, the acceleration time is depending on the motor performance. The motor power is limited to 15 kW, but the maximum motor torque is variable and is only depending on the motor and the inverter. The maximum phase current must be limited in order to prevent the motor or/and the inverter from overheating. So not only the motor and inverter design but also the cooling concept are relevant for the maximum phase current and thus the maximum torque.

Nevertheless for a short period of time (usually this time is limited to 30 sec), the motor can deliver a higher torque. This can be used to improve the acceleration performance (see Figure 2.10).

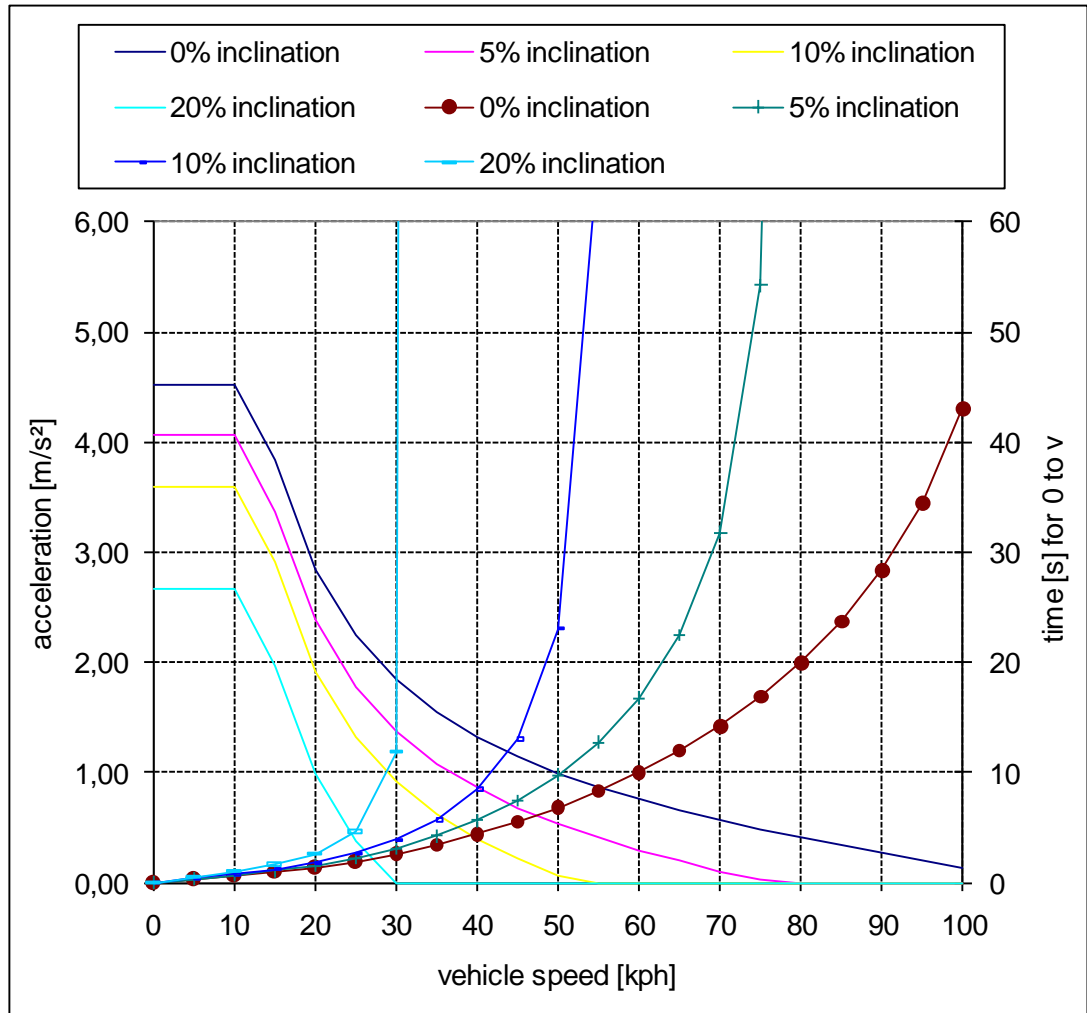


Figure 2.10 Acceleration Performance (peak torque – max. 30 sec)

Due to the fact that, with increased peak torque, the motor is running at its maximum power already at a lower speed (10 instead of 20 kph), the time needed for the acceleration from 0 to 50 kph is decreased.

- 0 to 50 kph with 0% road inclination: 6.7 sec
- 0 to 50 kph with 5% road inclination: 9.7 sec

2.3 Battery capacity

2.3.1 Battery capacity simulation using NEDC

The required battery capacity is calculated as the energy needed to overcome the driving resistances (see chapter 2.2.1) in a driving cycle over a certain distance. The regulation ECE-R 101 describes the test procedure to measure the range for electric M1 vehicles. This test procedure is used for the E-MILA Student to determine the required battery capacity from a demanded minimum range. The driving cycle used in the test procedure is the NEDC (New European Driving Cycle). The NEDC is a sequence of four times the ECE 15 (see Figure 2.11) cycle and one time the EUDC (Extra Urban Driving Cycle) [ECE-R101]. If the vehicle as in our case cannot reach the maximum speed of the EUDC, then the vehicle must drive with its maximum speed whenever the driving cycle velocity is exceeding the maximum speed of the vehicle (see Figure 2.12). One NEDC cycle is 10.7 km long. The vehicle drives the NEDC in succession to reach the required range of 90 km. The NEDC does not consider an inclination of the road. The efficiency of the drivetrain (from the battery to the wheels) is estimated with 80%. From the experience at MAGNA E-Car this efficiency can be achieved with a high efficient electric motor like a PM-motor (see chapter 3.2.1 for details). The recuperation efficiency is estimated with 70%. This efficiency describes the amount of energy, which can be stored back into the battery while braking. For headlights, wiper, radio and so on an additional constant power consumption of 400 W is considered.

Not according to the test procedure in the requirements, the simulation is done with the vehicle loaded to its gross vehicle weight of 800 kg, instead of kerb weight plus 100 kg. An additional simulation is done with the test weight given in the requirements to determine the range of the vehicle according to the requirements (see chapter 2.3.2).

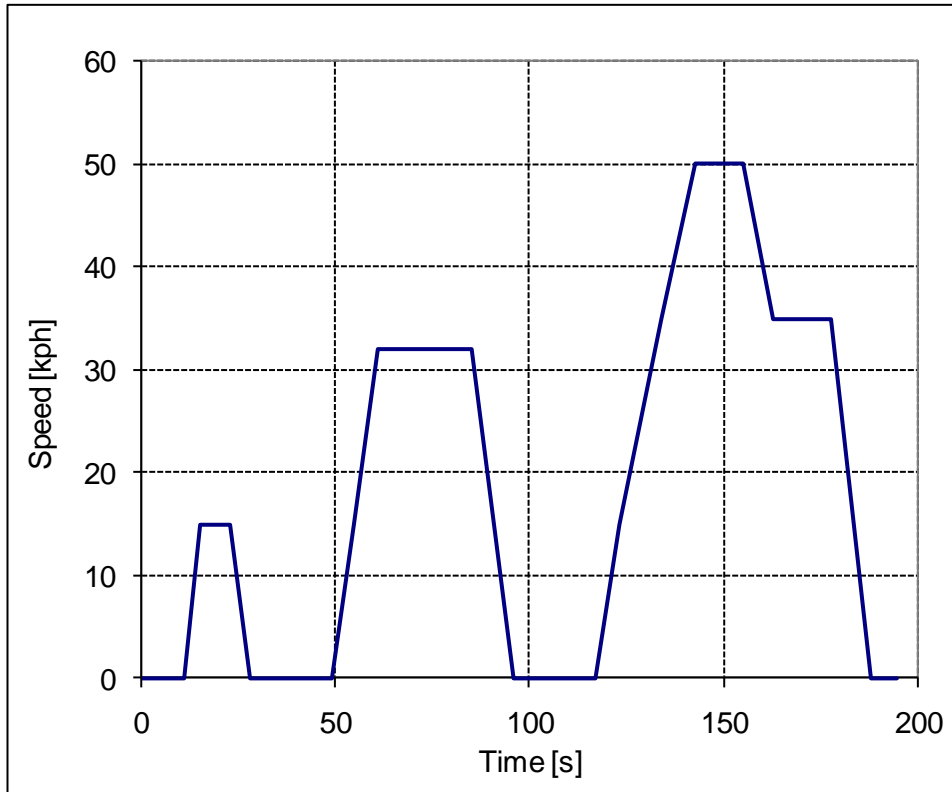


Figure 2.11 ECE 15 driving cycle [ECE-R 101]

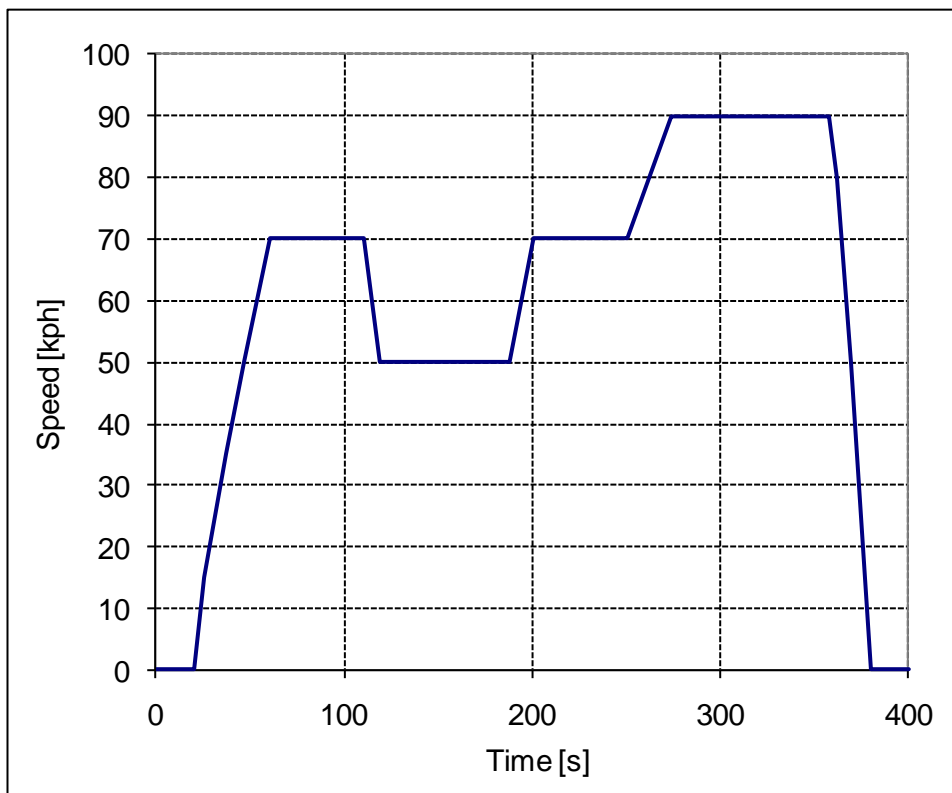


Figure 2.12 EUDC for low powered vehicles [ECE-R 101]

The results of the battery capacity simulation are shown in Table 2.4.

Table 2.4 Energy consumption from battery at NEDC

Results (w/o auxiliary power consumption, w/o recuperation)	
Energy consumption [kWh/100km]	9.17
Energy consumption for a range of 90 km [kWh]	8.25
Required installed battery capacity for a SOC range of 80%	10.31
Results (with auxiliary power consumption, with recuperation)	
Energy consumption [kWh/100km]	9.19
Energy consumption for a range of 90 km [kWh]	8.27
Required installed battery capacity for a SOC range of 80%	10.34

The target for the vehicle development is to install a battery with a capacity of at least 10.34 kWh.

2.3.2 Range calculation with given battery capacity

Additionally to the calculation of the required installed battery capacity, simulations were carried out with different driving cycles and vehicle conditions to see what range can be achieved with a battery capacity of 10.34 kWh.

NEDC with test weight according to ECE-R 101

According to ECE-R 101 the determination of the vehicle range is measured with the vehicle kerb weight plus an additional weight of 100 kg. With a vehicle kerb weight of 550 kg the test weight is therefore 650 kg.

Resulting range with auxiliary power consumption and including recuperation: 97 km This is 7 km longer than the 90 km range the vehicle reaches with gross vehicle weight (see chapter 2.3.1).

NEDC with design weight

Probably more relevant for the daily use, especially compared to the vehicle loaded to gross weight, will be driving the NEDC with the vehicle loaded to the design weight. Design weight for this vehicle is defined as the vehicle kerb weight plus the weight of the driver with 68 kg plus luggage in the trunk with a weight of 22 kg. The design weight is then 640 kg. Which is very close to test weight (see above), therefore there is also no big difference in the resulting range.

Resulting range with auxiliary power consumption and including recuperation: 98 km This is 8 km longer than the 90 km range the vehicle reaches with gross vehicle weight (see chapter 2.3.1).

ECE 15 driving cycle

ECE 15 driving cycle is the city driving part of the NEDC. So it represents the NEDC but without the extra urban driving cycle.

Resulting range with auxiliary power consumption and including recuperation:

- Design weight: 107 km
- Gross vehicle weight: 94 km

From the range difference between design and gross vehicle weight it can be seen, how important the inertia resistance and thus the vehicle mass is during city driving.

Constant speed

The following list shows the range of the vehicle driving at constant speed on a road without inclination including auxiliary power consumption:

- 50 kph constant speed, design weight: 213 km
- 50 kph constant speed, gross vehicle weight: 196 km
- 90 kph constant speed, design weight: 104 km
- 90 kph constant speed, gross vehicle weight: 100 km

The range at a constant speed of 50 kph is approximately double the range at a constant speed of 90 kph. This is due to the increasing influence of the aerodynamic forces at higher speeds. The vehicle weight has only a minor influence on the range at constant speed. The range is only slightly reduced at gross vehicle weight because the higher weight results in a higher rolling resistance. This is of course different if the vehicle climbs up a road with an inclination or is accelerated and decelerated like in the ECE 15 driving cycle.

3 Drivetrain and Energy Storage

In this chapter the realization of the drivetrain for the E-MILA Student vehicle is investigated. The content is structured according to a top down approach concerning the specification of the systems and components. So the first sub-chapter deals with the full vehicle requirements and the vehicle layout in order to define the requirements for the drivetrain layout. In chapter 3.2 the requirements for the drivetrain system are broken down to the components. The focus of the components is on the traction motor and the battery.

3.1 Drivetrain Layout

The main three questions which shall be answered in this chapter are:

- What wheels are driven (front or rear)?
- Is a single, central traction motor or are two wheel hub motors advantageous for this vehicle concept?
- If a central traction motor is chosen, is a coaxial or offset transmission/motor configuration advantageous?

3.1.1 Front or rear wheel drive

Front or rear wheel drive has an influence on many different vehicle characteristics like weight distribution, self steering behaviour, traction (especially depending on the load), front and especially rear suspension system and many more. But for the E-MILA Student the most important influence of front or rear wheel drive is on the package.

The driver sits in the centre of the vehicle. This has the big advantage that the driver can be moved to the front, because there is no wheelhouse that reduces the required leg room. Moving the driver to the front is necessary to be able to realize 3 full seats within an outer length of 2.55 m.

Although the sketch is very simple and rough, it can be seen in the Figure 2.1 that it is not possible to package a central traction motor in the front without moving the driver and the fire wall. Additionally it is more difficult to package the steering. The steering would need to be mounted behind the wheel centre and therefore also behind the motor, which would require to move the driver and the fire wall even further to the rear. A front wheel drive is therefore only possible with wheel hub motors.

On the rear axle packaging a central traction motor requires a limited length of the battery, which will be positioned under the driver- and passenger seats. Wheel hub motors are also possible on the rear axle.

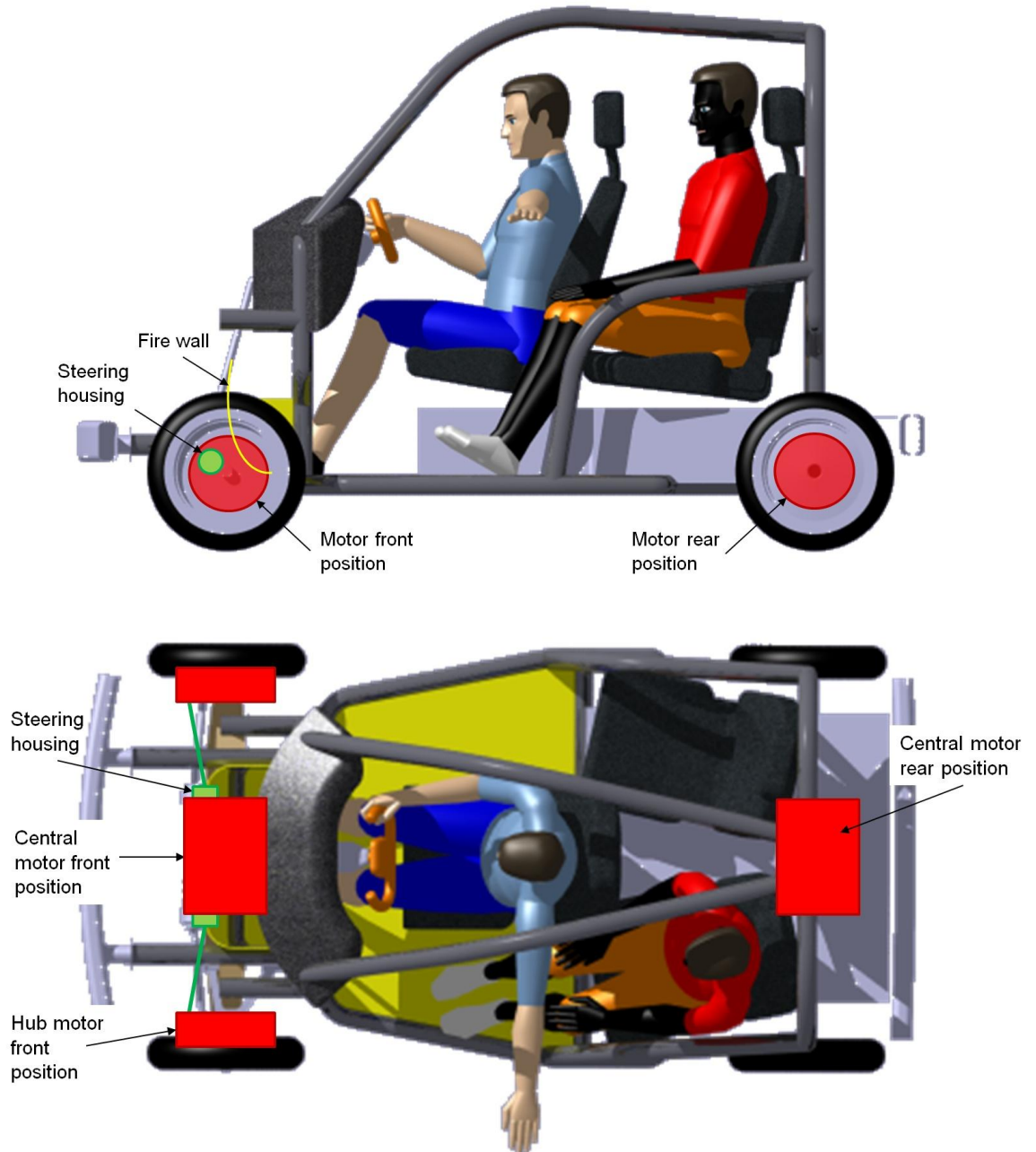


Figure 3.1 Sketch drivetrain layout, side view and top view

So due to package either a central motor in the rear or wheel hub motors either on the front or rear wheels are possible. The advantages and disadvantages of a central motor and a wheel hub motor are described in chapter 3.1.2. Especially due to system costs it was decided to go on with the central motor in the rear.

Except from the package the rear wheel drive has the following characteristics concerning vehicle requirements:

- Weight distribution to the rear with the advantage of reduced steering forces, which is essential when considering that the steering shall work without power assistance (see chapter 4.3.3)
- Simpler driveshafts (no steering of the rear wheels)
- Steering angle of front wheels is not limited by the driveshaft joints
- No influence of traction torque into steering, which is of course not very relevant for this vehicle because of the low power.
- Recuperation potential is rather limited on the rear axle, due to vehicle stability and the dynamic load change to the front while decelerating. But due to the higher rear axle load and due to the limited power of the motor, the recuperation potential can be used in most situations (see chapter 4.4.1)
- Traction is better when fully loaded, but can also be expected to be sufficient when only partially loaded (e.g. only driver), due to rear axle load and low power.
- The disadvantage of an basically instable driving behavior, because the vehicle is pushed by the rear wheels and not pulled by the front wheels, is less relevant due to low power.
- Rear suspension must be drivable. Still also a twist beam axle can be used because there is no propshaft.

All in all the rear wheel drive has more advantages than disadvantages for this vehicle concept and is therefore the basic assumption for all further concept investigations.

3.1.2 Central motor or wheel hub motor

The size of an electric motor is mainly depending on the necessary continuous output torque of the motor. The central motor and the two wheel hub motors need to provide the same output power. If the wheel hub motor is directly driving the wheel without any reduction transmission, it will run with the rotational speed of the wheel. The central motor will have a transmission with a ratio of approximately 10 (see chapter 2.2.2). Although the central motor needs to provide double the power as one wheel hub motor, the output torque is five times lower. As rotor volume of the motor is proportional to the output torque, the size of the central motor is a lot smaller. If for example the length of the motor is the same in both cases, the rotor diameter of the central motor can be roughly $\sqrt{5}$ times smaller than of the wheel hub motor [Mat10].

Therefore it is necessary to use a transmission for each wheel hub motor to reduce the motor torque and thus also reduce the motor size. The argument for the wheel hub motor, that the overall efficiency is better because of the missing transmission is not valid in that case. Another disadvantage of the wheel hub motor is the increase of the unsprung mass. This is especially relevant for this vehicle because of the low vehicle weight. The ratio between the un-sprung masses and the mass of the rest of the vehicle would be very unfavorable. An acceptable ride comfort would be hard to realize. An additional problem with wheel hub motors is cooling. If the motors are liquid cooled, there is the problem with the hose routing to get the coolant from the motors at the wheels to the radiator. If the motors are air cooled, there is the problem with the weight and size of the motors because of the required additional surface (cooling ribs) [Bie10].

To keep the costs, weight and system complexity as low as possible it was decided to use a central motor with a transmission and a differential. The realized concept is described in the following chapter.

3.2 Drivetrain components

3.2.1 Traction motor

Basics

Beside the battery the electric motor is the key component in a battery electric vehicle. Some of the main characteristics, which are relevant for the vehicles driving performance, are already anticipated in chapter 2.2.2. In this chapter the vehicle specific demands on the electric motor are described more in detail. This is the basis to derive the advantaged and disadvantages of the different motor concepts. The following list shows the requirements on the electric motor [Zhu07].

- High torque and power density for a small and lightweight motor design.
- High torque for starting, at low speeds and hill climbing, and high power for high speed cruising.
- Wide spread range, with a constant power operating range of around 3-4 times the base speed being a good compromise between the peak torque requirement of the machine and the volt-ampere rating of the inverter (see Figure 3.3).
- High efficiency over wide speed and torque ranges, including low torque operation.

- Intermittent overload capability, typically twice the rated torque for short durations. This is not really important for the E-MILA Student because of the limited maximum power.
- High reliability and robustness appropriate to the vehicle environment.
- Acceptable cost.
- Low acoustic noise and low torque ripple

When the vehicle needs to be towed, due to some failure, the behaviour of the electric motor is important. In best case the electric motor does not produce a torque, when it is driven through the wheels and the motor phases are not connected [Mat10].

Figure 3.2 shows the broad variety of existing electrical machines. Although there are electric vehicles, like the first Reva, which was built until 2006, that were equipped with a DC-motor, DC-machines are not serious candidates for today's vehicle application due to wear and maintenance problems brought on by the brush-commutator arrangement, and by their modest efficiency. Two types of motors have found application in modern-day electric and hybrid-electric traction: The squirrel cage induction machine (IM), and the permanent-magnet machine (PM). A third candidate, the switched reluctance machine (SRM), might see applications in the future, and has been used in prototypes. [Riz07], [REV10].

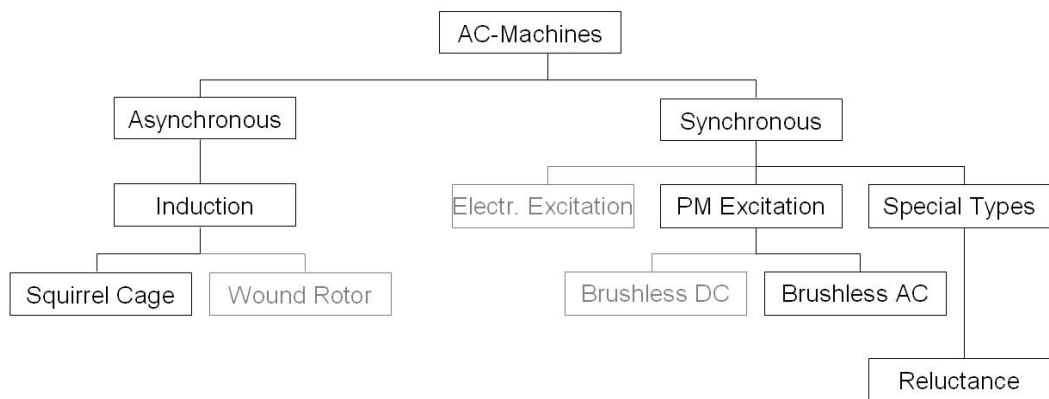


Figure 3.2 Classification of alternating current machines [Bou07], [Riz07]

The three different machine types induction machine (IM), switched reluctance machine (SRM), and permanent-magnet machine (PM) are investigated concerning their potential as traction motor for the E-MILA Student. With the right design and control strategy all three machines can achieve the idealized torque/power-speed characteristics shown in Figure 3.3.

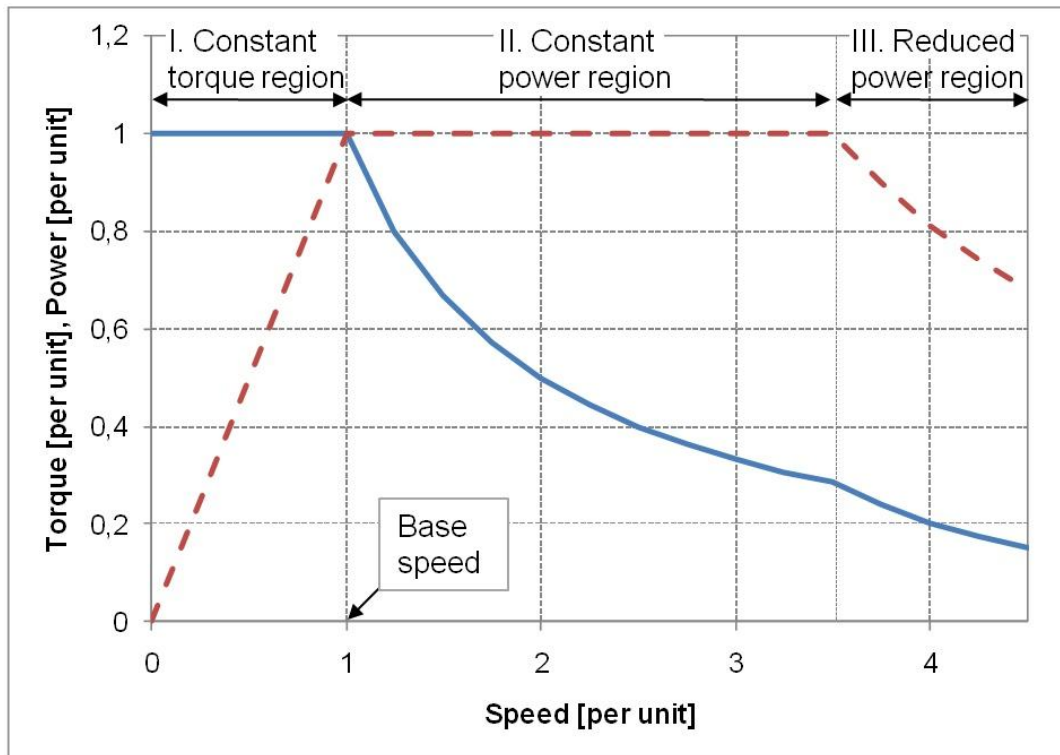


Figure 3.3 Idealized torque/power-speed characteristics [Zhu07]

Induction Machine

An induction motor works similar to a transformer. The stator is the primary side and the rotor the secondary side of the transformer. The current in the rotor is induced by the magnetic field of the stator. This only happens if there is a small difference in the rotating speed of the magnetic field of the stator and the rotor. This so called slip reduces the efficiency of the induction motor. At lower speeds the slip needs to be higher, there the induction machine has an efficiency disadvantage compared to the synchronous motor. At higher speeds the efficiency is similar [Mat10]. With an optimized variable flux control of the motor the efficiency especially at lower speeds in the constant torque region, can be significantly increased [Wil10a].

Of the three electrical machine technologies under consideration, induction machines are the most mature, due to their wide spread industrial applications. Induction machines are robust, relatively low cost, and have well established manufacturing techniques. For conventional IMs the constant power range is 2-3 times the base speed, but for traction machines this can be extended to 4-5 times the base speed, which is generally desirable [Zhu07].

An important advantage of the induction motor is its fail safe characteristic. The rotor is behaving like a simple piece of metal, without producing any torque, when the

stator is not producing a magnetic field [Mat10]. This behaviour is especially important when the motor is used to drive the wheels of an “electric axle” in a so called through the road hybrid. In such a vehicle the electric axle is usually used for pure electric driving at low speeds (e.g. stop and go traffic), to improve traction and for recuperation braking at low to medium speeds. At high speeds the electric motor is usually not used and therefore it is important that the motor does not produce any drag torque [Wil10a], [Bou07].

Table 3.1 Summary of characteristics of IM [Bou07]

Induction Machine	
Advantages	Disadvantages
Robust, suitable for high speeds	Ohms losses in rotor windings
No position sensor necessary	High idle power demand
High overload potential	Lower efficiency at low speeds
No danger of demagnetization	Over dimensioning necessary
Low cost production	Lower power density
Good characteristics in constant power region	
Good fail safe behaviour	
No iron losses at idle speed	

Permanent-magnet Machines

A permanent-magnet motor is a special type of a synchronous machine. This means that the rotational speed of the rotor is the same as the rotational speed of the magnetic field in the stator. It is also often called brushless DC-motor (BLDC), when driven by rectangular shaped current waveforms, or brushless AC-motor (BLAC), when driven by sinusoidal shaped current waveforms. Although the demands on the inverter and the rotational positioning sensor are higher for the BLAC-mode control, it is usually preferred due to the higher efficiency and the lower operation noise [Zhu07].

The PM differentiates itself from other synchronous machines that the excitation winding in the rotor is replaced by permanent magnets. Therefore there are no losses from ohms-resistance in the rotor. By the use of strong lanthanide magnets it is possible to built machines with a high torque and power density, usually higher than with the other two machine types. This means that for a specific power and torque demand, the PM will be the smallest and lightest machine type [Bou07].

The advantage of the constant excitation in the constant torque region becomes a disadvantage in the constant power region. The necessary field weakening at higher speeds requires power consumption even when the machine is not delivering power

[Riz07]. Still the PM is the machine type with the highest efficiency especially in the area of the base speed [Bou07].

The constant excitation is also a significant problem in case of a failure. If the rotor is rotating because e.g. the vehicle is towed the generated electromotive force could damage the inverter, or in case of a short circuit of the stator phases result in high power losses and potential overheating of the machine [Mat10], [Riz07].

Due to the permanent magnets and the higher demands on the rotor position sensor the PM is approximately 20% more expensive than an IM [Bou07].

Table 3.2 Summary of characteristics of PM [Bou07]

Permanent-magnet Machine	
Advantages	Disadvantages
High power and torque density	Iron losses at idle speed
Small machine size	Position sensor necessary
High efficiency	Losses at field weakening operation
Decreasing costs for magnetic material	Magnets can corrode
No ohms losses in rotor	Danger of demagnetization
Low idle power demand	Smaller constant power region
	Fail safe characteristic

Switched Reluctance Machine

The switched reluctance machine is the simplest electric machine that permits variable-speed operation. Some believe that the SRM forms the basis of an ideal electric and hybrid-electric vehicle traction drive because of its low cost and robustness. The SRM does not need a magnet or a winding in the rotor. The operation principal of this machine is based on the difference of the magnetic resistance (reluctance) in the air gap. The rotor and the stator therefore need clearly defined poles (see Figure 3.4). The windings in the stator are similar to that in an IM or PM. The stator can be excited by any multiphase source. The SR machine is excited by discrete current pulses that must be timed with respect to the position feedback. The speed of the rotor is determined by the switching frequency of the stator coil currents. While in principle very easy to control, actual control of SRM is quite challenging with respect to noise vibration control, and the SRM had not yet found commercial vehicle applications [Riz07], [Bou07].

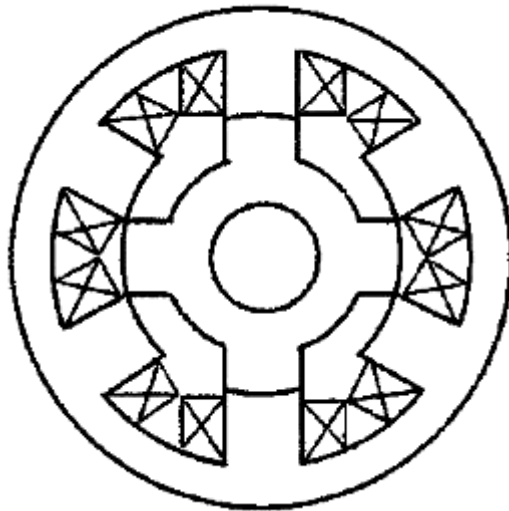


Figure 3.4 Sketch of a simple 3-phase Switched Reluctance Machine [Zhu07]

Basically due to its simple and robust rotor design the SRM has the capability to be used for high maximum rotational speed. A disadvantage is the uneven structure of the rotor and the stator and the resulting higher air drag in the air gap, compared to IM or PM. This can be compensated by filling the gaps with non-magnetic material, which on the other hand may reduce the robustness of the rotor [Bou07].

Power and torque density and thus machine size and weight is comparable to an IM [Bou07].

Table 3.3 Summary of characteristics of SRM [Bou07]

Switched Reluctance Machine	
Advantages	Disadvantages
Simple design	Torque ripple and operation noise
Robust	High idle power demand
Large constant power region	Higher air drag losses in air gap
Low costs	

Traction machine for E-MILA Student

An electric machine is a part which requires high investments for development and tooling, especially for the rotor- and stator sheet production. The basic cost advantage of an induction machine can quickly vanish, if a new IM is compared with a permanent magnet machine, which is already developed and where the tooling costs can be shared between different applications.

In advanced development at MAGNA Powertrain an electric drivetrain for a “through the road” hybrid vehicle is being developed. The drivetrain is available in different

classes for different power requirements. The smallest class fits very well to the requirements of the E-MILA Student. The electric machine is a water-cooled PM-machine. The machine has a constant power output of 20 kW, which is higher than the required 15 kW. On the one hand the machine could be used without modifications and the output power is limited electronically by the inverter. The oversized motor has the disadvantage of higher costs for copper (windings) and the magnets, but the advantage of a higher maximum, constant torque, which improves especially the gradeability. On the other hand the motor could be adapted to the requirements. This can be done by reducing the length of the machine, which is simply done by reducing the number of stacked rotor- and stator sheets. The rotor- and stator sheets could be used without changes, thus the adaption could be done with low investment costs. A detailed comparison which of these two variants is better is not done in this thesis. This would need to be done in series development together with the motor supplier. For this thesis it was estimated that the motor will be used without any modifications and that the maximum output power of the motor will be limited by the inverter. This is also the worst case for package because the motor has its maximum dimensions. Figure 3.5 shows the motor characteristics.

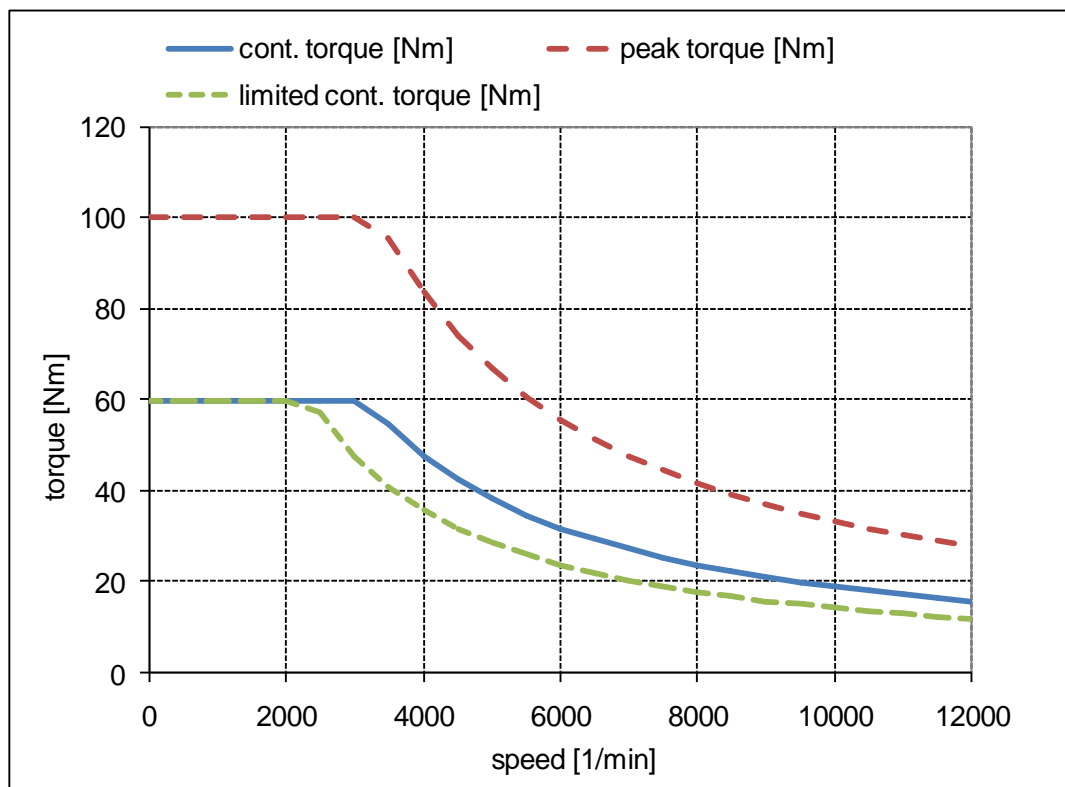


Figure 3.5 Motor characteristics compare [MAG10b]

The motor characteristics are very similar to the estimated motor characteristics shown in Figure 2.7. Only the maximum continuous torque is 60 Nm instead of 55 Nm.

This would result in minor improvements of the driving performance. As the motor characteristic described in [MAG10b] is a result from a simulation, the real achievable torque might vary slightly. To be on the save side, the driving performance results presented in chapter 2.2 are therefore not changed, but will be achieved by the vehicle as presented.

The motor has a hollow shaft design, so the motor can be positioned coaxially to the drive shafts. This is possible because the motor outer diameter is small enough to have sufficient ground clearance. The advantage of the coaxial position is that the surrounding parts like the twist beam of the rear axle (see chapter 4.2) the trunk floor and the rear bumper can be moved closer to the rear wheel centre. A motor positioned behind the rear wheel centre, which would be the only possible position if it is not positioned coaxially, would be harmful to the balanced weight distribution.

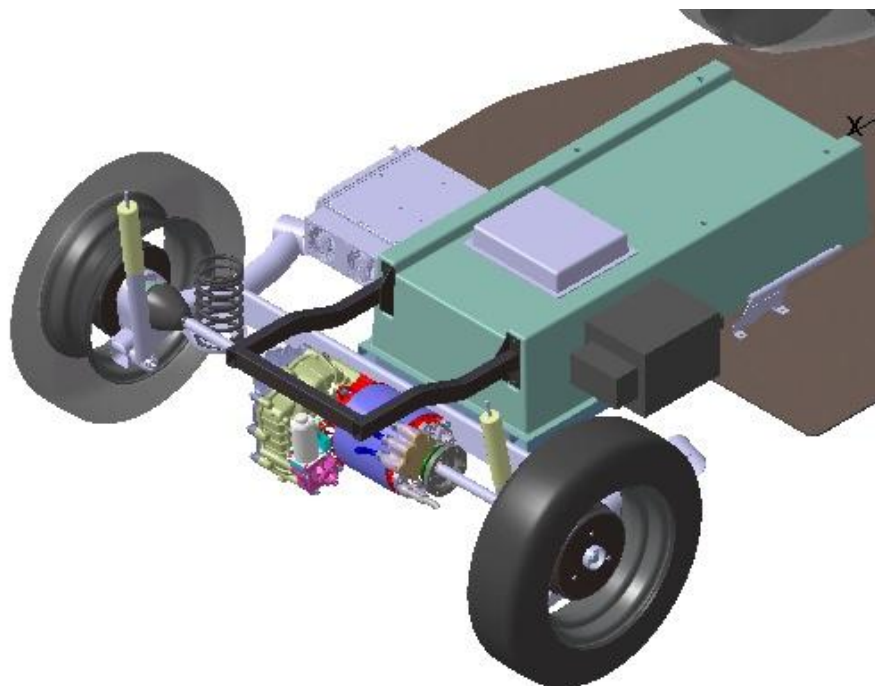


Figure 3.6 Motor and transmission in vehicle package

3.2.2 Transmission

The transmission is a spur-gear unit with a constant ratio. The ratio is chosen so that at the maximum vehicle speed of 90 kph the motor runs at its maximum speed of 12,000 rpm. The required ratio $i=13$ is within the feasible ratio range from 7 to 14 for this concept [MAG10b]. The concept of the MAGNA Powertrain transmission is equipped with an electromechanical actuated parking pawl. Figure 3.6 shows the transmission with the electromechanical actuator. The parking pawl is required for M1 cars, it is not required for

L7e vehicles in Europe, and still it must be installed in the E-MILA Student, as the vehicle shall also be sold in the United States and Japan, where a parking pawl is required [Mad11]. As the roughly estimated costs for the electromechanical actuator for the parking pawl is about EUR 200.-, it was decided to actuate the parking pawl mechanically via a Bowden cable and a lever at the steering wheel.

3.2.3 Electric Control Units

The electronic control units (ECUs) for the electric drivetrain of the E-MILA Student are not the focus for this thesis, therefore only a rough overview over the required components and their basic functions is given. The following ECUs are required for the electric drive:

- An inverter: It converts the high voltage direct current from the battery into a three phase alternating current for the motor. The parameters of the alternating current like the frequency or the voltage amplitude must be fully controllable.
- A DC/DC converter: To drive the standard components like the lights, the windscreen wiper or the radio, the vehicle needs a standard 12 Volt battery besides the high voltage battery. As there is no generator like in a car with combustion engine, the 12 Volt battery needs to be recharged via the DC/DC converter from the high voltage battery.
- A charger: It is needed to recharge the high voltage battery at a common household socket or at a charging station.
- A vehicle control unit (VCU): In the widest sense the VCU has a similar task like the engine control unit in a combustion engine car. It controls the electric motor torque depending on the accelerator pedal position and the speed. Additionally it monitors important parameters of the motor like the motor speed, phase current or the motor temperature and of the high voltage battery like the state of charge or the battery temperature. The VCU is also responsible for the battery monitoring during charging and the charging process.

The first three ECUs are high voltage ECUs because they are connected with the high voltage battery. The connection of the ECUs to the battery is done via a so called high voltage distribution unit (HVDU). Beside the relative simple function to connect the HV-ECUs to the battery, the HVDU has also a safety function and must be able to disconnect

the battery from the ECUs. This is usually realized by a pyrotechnical switch. The HVDU is directly placed on the battery between the passenger seats (see Figure 3.14).

The VCU is not considered as a HV-ECU because it has no high voltage power in- or outputs. Still the VCU is connected to the high voltage battery via the HVDU for instance to monitor the battery voltage.

For the estimated volume of the E-MILA Student of 10,000 vehicles per year, it makes sense to use existing hardware components, due to high development costs for new hardware (see chapter 5.1). Listed below are the main E-MILA Student specific requirements for the high voltage ECUs:

Inverter

- DC Voltage range (min. to max. battery voltage): 165 V to 246 V [MAG10a]
- Continuous power output: 15 kW
- Package requirements
- International protection (also known as ingress protection) class
- Weight

MAGNA E-car has an inverter in their portfolio, which also has an integrated DC/DC converter. Both the inverter and the DC/DC converter fulfil the requirements. In fact the component is capable of switching more than double the required power [Rei10]. As there is no component available at MAGNA, which would be more suitable for the E-MILA Student this component is considered in the vehicle package and for cost evaluation.

DC/DC Converter

- High voltage range (min. to max. battery voltage): 165 V to 246 V [MAG10a]
- Continuous power output: 1 kW
- Package requirements
- International protection (also known as ingress protection) class
- Weight

A DC/DC converter which fulfils the requirements is integrated in the inverter (see above).

Charger

The charger requirements are limited by the specifications of typical household sockets. The voltage in Europe is 220 Volts and the socket is fused with 13 or 16 A. To be able to use the maximum available power from a 220 Volts socket the typical charger

power is 3.3 kW ($= 220 \text{ V} * 15 \text{ A}$, which is the maximum current to make sure that the fuse does not disengage the power supply). With an estimated charging efficiency of 70% the charging time to recharge an empty battery (from 10% to 90% SOC) is less than 4 hours [Rei10].

- High voltage range (min. to max. battery voltage): 165 V to 246 V [MAG10a]
- Continuous power: 3.3 kW
- Package requirements
- International protection (also known as ingress protection) class
- Weight

Also for the charger a suitable component from MAGNA E-car will be available in series production before the planned SOP of the E-MILA Student.

The inverter with the integrated DC/DC converter and the charger will be packaged under the passenger seats. The inverter (2) is positioned under the right passenger seat, which enables a short 3 phase connection to the motor and the charger (1) is positioned under the left seat. The components are mounted to the rear floor. Figure 3.7 shows the package of the high voltage ECUs in the vehicle without the rear floor for a better overview.

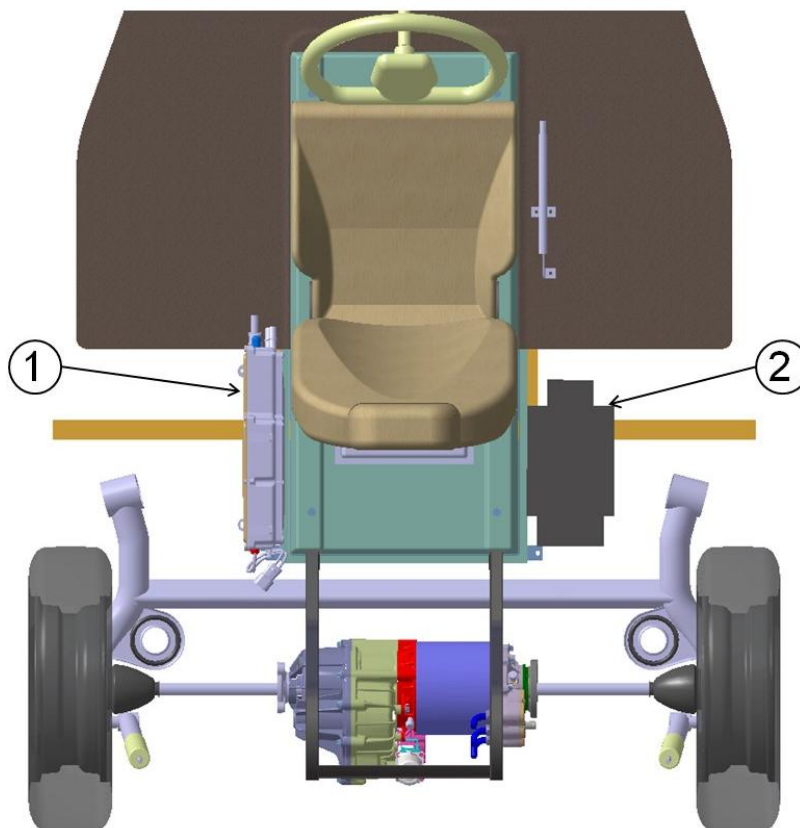


Figure 3.7 Package of high voltage ECUs

3.3 Energy storage

Basically there are several different possibilities for energy storage in electric vehicles like fuel cells, capacitors, high speed flywheels and rechargeable batteries. But a look at recently presented electric vehicles either prototypes (like the Nissan Leaf or the Renault Fluence) or series production vehicles (like the Tesla Roadster or the Mitsubishi iMIEV) shows that they all use batteries for energy storage. The reason is that up to date only the batteries have reached technical maturity at reasonable costs [Cha99]. Therefore only batteries are further investigated as energy storage for the E-MILA Student.

General requirements for a battery system are a high energy capacity, high charging and discharging power, low weight, small volume, long durability and a low price [Koe10]. As not all requirements can be fulfilled at a time it is necessary to find the right compromise for each application. Figure 3.8 shows the demands on energy storage capacity and discharging power of different electric- and hybrid vehicles. Due to the restriction of the maximum motor power the E-MILA Student has comparably low demand on the maximum discharging power. Also the required energy capacity is lower than of other electric vehicles, due to low vehicle weight and due to the limited maximum speed.

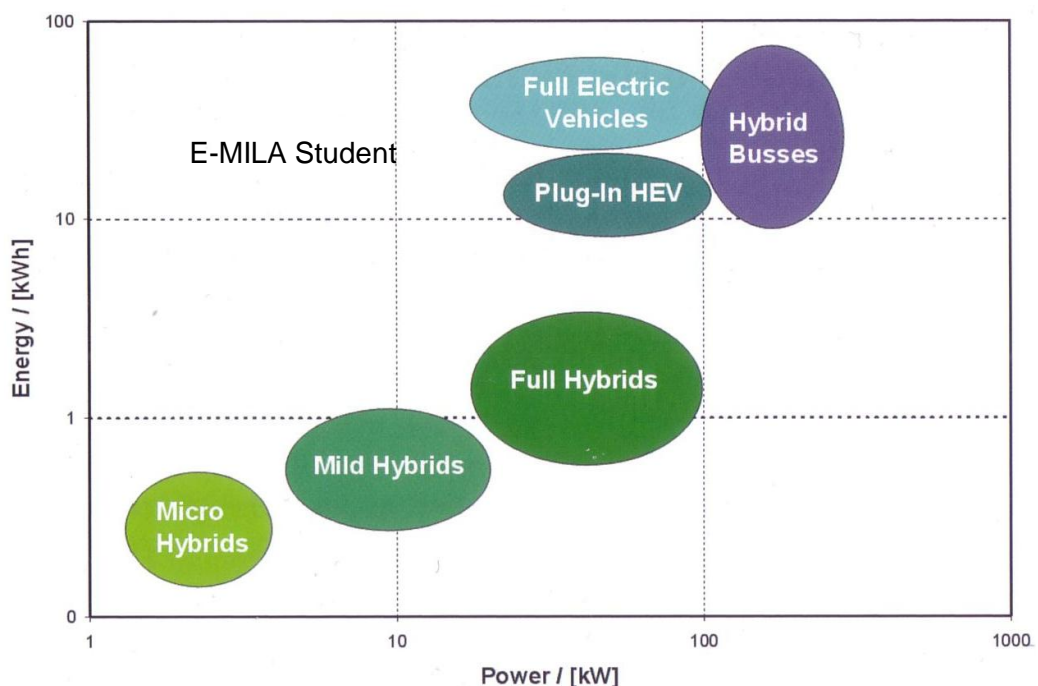


Figure 3.8 Energy and power demand for different drivetrain types [Koe10]

The focus for the battery will be high energy capacity with reasonable weight at low costs. The charging and discharging power is less important.

3.3.1 Battery cell technology

In available production vehicles there are four different battery types in use.

- Lead acid
- Nickel-metal hydrid (Ni-MH)
- Sodium/nickel chloride (Na/NiCl₂)
- Lithium ion (Li-ion)

The performance range of this cell types is shown in Figure 3.9. The figure additionally shows the performance of nickel-cadmium (NiCd) cells, which were also used as traction batteries for electric vehicles (like Peugeot 106 electric [EUR10]). This cell type is no longer used for vehicles because of the carcinogenicity and environmental hazard of cadmium ([Koe10], [Cha99]).

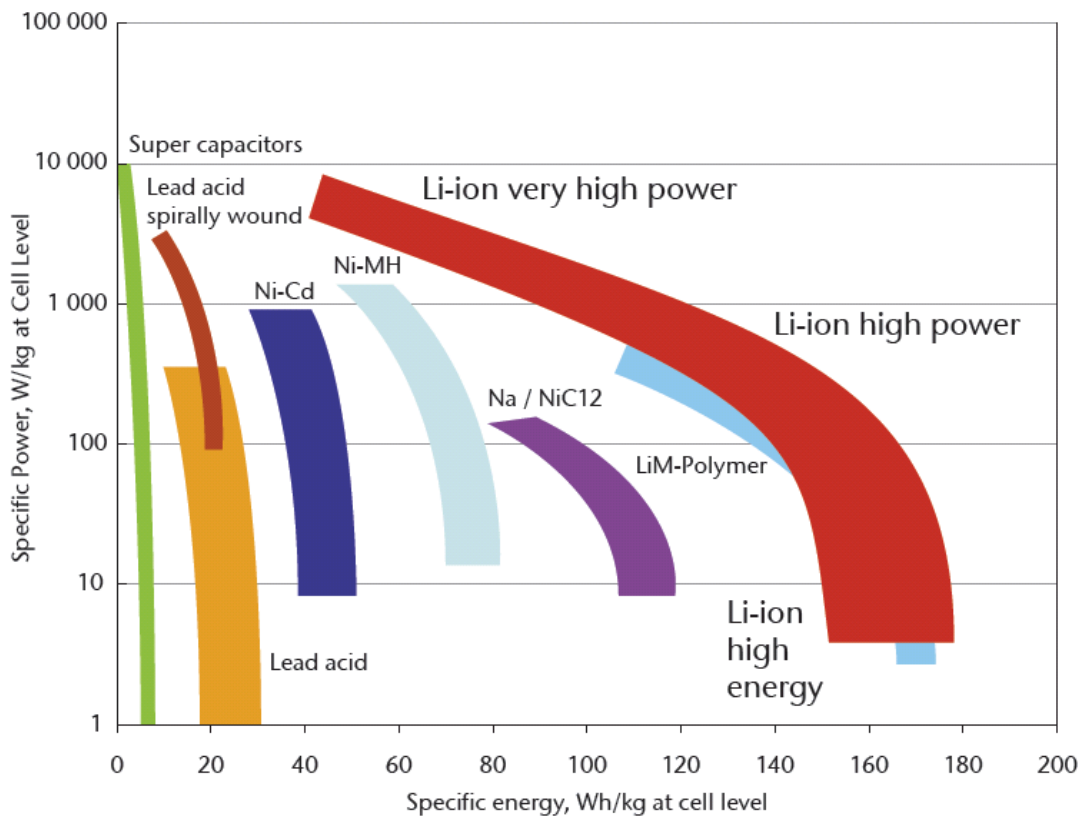


Figure 3.9 Performance of different cell types [Koe10]

Lead acid

Lead acid batteries are the most mature battery technology in vehicles. They are used as starter batteries in vehicles with an internal combustion engine since more than 100 years. And for a long time since the first electric vehicles (like the Lohner Porsche)

were presented, there was also no alternative to lead acid batteries as a traction battery for electric vehicles.

Reasons for the long success were the high specific power of over 200 W/kg (or even more with spirally wounded cell technology), the low costs and the rapid recharge capability. However the main disadvantages are the low specific energy capacity (see Figure 3.9) and the short capacity turnover (about 500 cycles) [Cha99]. This are the reasons why the lead acid battery is not further considered for the E-MILA Student.

Nickel-metal hydrid (Ni-MH)

Nickel-metal hydrid is considered as the successor of the nickel-cadmium batteries. Today the Ni-MH batteries are successfully produced in high volume for different hybrid vehicles (like all Toyota and Lexus hybrid vehicles [PRI10], [LEX10]).

The Ni-MH battery has more than double the specific energy of the lead acid battery (see Figure 3.9). The high specific power together with a long cycle life, especially with low depth of discharge, and a rapid recharge capability makes it so interesting for hybrid vehicles [Koe10], [Cha99].

For pure electric vehicles like the E-MILA Student the specific energy capacity, especially when only low specific power is needed, is not satisfying. This is probably also the reason why Toyota changes to a lithium-ion battery for the Prius plug in hybrid, which will have a longer range in electric mode than the standard Prius hybrid [TOY10].

Sodium/nickel chloride (Na/NiCl₂)

The sodium/nickel chloride battery cell requires an inner operation temperature of approximately 300°C. This battery system also known as Zebra battery is used as a traction battery in the Think City electric vehicle [THI10].

The Na/NiCl₂ battery has an specific energy capacity that significantly supersedes the capacity of the Pb- and Ni-MH systems. The relatively lower specific power compared to the energy together with a long cycle life makes the battery more interesting for electric than hybrid vehicles. The problem is the necessary operating temperature of 300°C. It requires high performing heat insulation and still the thermal losses will be approximately 5W per kWh. To keep the operation temperature the battery needs to be heated. In a fleet use this will not be a big problem, because of the relatively low losses compared to the energy used for driving. But in private use the thermal losses are a significant disadvantage, due to long standing times and short driving times [Koe10].

Think will change the battery for the Think City from Na/NiCl₂ to Li-Ion. With both batteries the vehicle has a range of 160 km, although the new Li-Ion battery has only a capacity of 21.5 kWh compared to 28.3 kWh. The reason is the required compensation of thermal losses to keep the operating temperature of the Na/NiCl₂ battery to 300°C. Interestingly the price for the vehicle in Austria with Li-Ion batteries is nearly EUR 9,000.- cheaper than with Na/NiCl₂ batteries (EUR 35,760.- to EUR 44,400.-) [THI10]. As the Na/NiCl₂ battery has obviously a cost disadvantage compared to the Li-Ion battery the Na/NiCl₂ battery is no longer investigated for the E-MILA Student.

Lithium-ion (Li-ion)

Lithium-ion batteries are the latest battery technology. After Li-ion batteries established in the consumer market (mobile phones, laptops,...) they are now entering the automotive segment.

Lithium-ion batteries have a high cell voltage of 3.6V to 4.2V, depending on the electrode material. The high cell voltage has the advantage to build a battery system with a comparably small number of cells. But for li-ion cells it is important that each cell is operated in a defined voltage range, to ensure the durability of the whole battery system. So it is necessary to monitor the voltage of each cell in a battery system with a control unit and keep the voltage of all cells on one level. Such a battery system has a very high capacity turnover of more than 3000 cycles (at 80% depth of discharge). The main advantage of li-ion batteries is the high specific capacity. A li-ion battery system with 20 kWh has a typical weight of 180 kg compared to more than 300 kg for the nickel-metal hydrid battery system and more than 500 kg for a lead acid battery system [Koe10].

The high specific capacity makes the lithium-ion battery the only battery system which is available today and which can almost fulfill the requirements concerning range of an electric vehicle [Koe10]. For the E-MILA Student all further investigations concerning the energy storage are therefore done with a lithium-ion battery.

3.3.2 Battery system

As described in chapter 2.3.1 the installed battery capacity shall be 10.34 kWh.

Battery cell

At MAGNA for several advanced development projects a prismatic lithium-ion cell with a capacity of 50 Ah is used. The cell has a nominal voltage of 3.75 V. This means that one cell has a theoretical nominal capacity of 187,5 Wh. To get the required capacity of the

battery system of 10.34 kWh it is necessary to use at least 56 cells, which would result in a capacity of 10.50 kWh.

Battery module

MAGNA uses a battery module which consists of a cell carrier made from an extruded aluminum profile that supports 4 cells on the upper and 4 cells on the lower side of the cell carrier. One module therefore consists of 8 cells which are connected in series. Figure 3.10 shows a section cut of the battery module. The cells are glued to the cell carrier. The cell carrier is fixed to the battery frame at two fixation points.

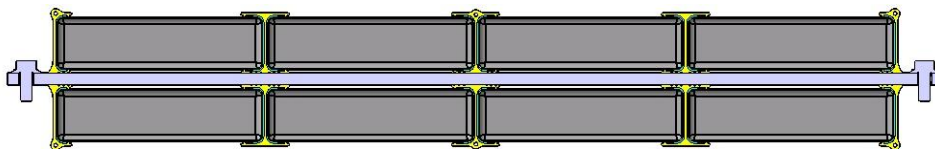


Figure 3.10 Section cut of MAGNA battery module with 8 cells [MAG10e]

For the required capacity of 10.34 kWh it would be necessary to install 7 modules, with an installed capacity of 10.50 kWh, which is very close to the required battery capacity.

It is only possible to package 6 modules under the driver and passenger seats in longitudinal direction. Two modules are placed above each other and three modules besides each other. But as 6 modules do not have sufficient capacity, a seventh module would need to be packaged in lateral direction behind the 6 modules under the passenger seats. The package of the batteries is shown in Figure 3.11. This battery configuration requires a more complex battery frame, compared to a frame with only longitudinally positioned modules. Additionally the package of the charger and inverter is more difficult, due to the required space of the lateral positioned battery module. Still a possible package could be found as shown in Figure 3.11.

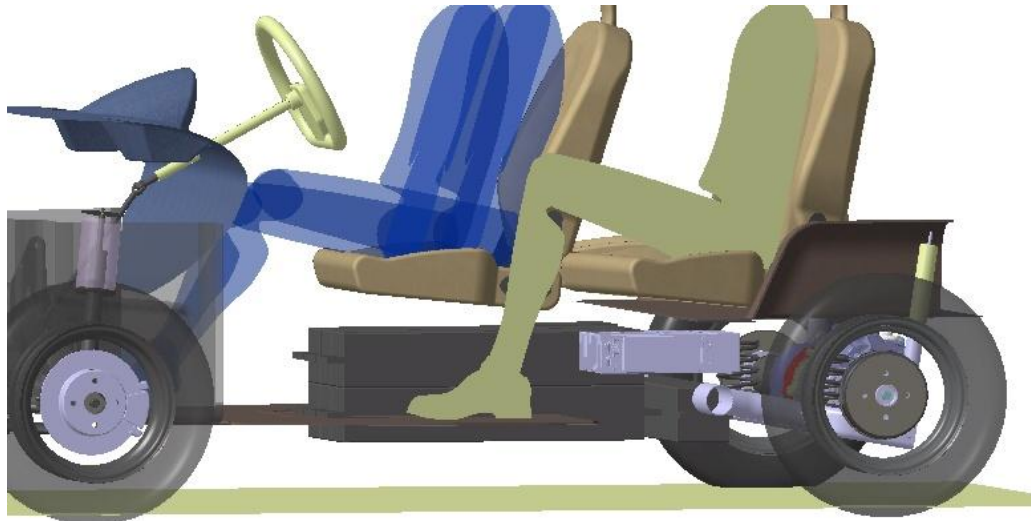


Figure 3.11 Package of 7 battery modules with 8 cells

Nevertheless it seems to be more reasonable to change the battery module. When the length of the battery module is increased to carry 10 instead of 8 cells, it is sufficient to have 6 modules. The 6 modules carry in sum 60 battery cells with a capacity of 11.25 kWh. With this capacity the range of the vehicle at GVW in the NEDC increases from 90 km to 98 km (compare chapter 2.3). The cross section of the modified battery module is shown in Figure 3.12.



Figure 3.12 Section cut of battery module with 10 cells

It is important to pay attention to the maximum deflection of the cell carrier under load of the cell weight and defined maximum acceleration in z-direction. The height of the cell carrier profile needs to be increased in order that the deflection of the module with 10 cells is not more than the deflection of the module with 8 cells.

The I-shaped battery frame for only longitudinal modules is a lot simpler than the necessary T-shaped frame for the 7 modules with 8 cells each.

3.3.3 Battery frame and housing

Frame

The battery and thus also the battery frame does not need to be considered in the weight limit of 400 kg for the empty vehicle (see chapter 2.1.1). Therefore it is obvious to

use the structure of the battery frame also for other functions, besides carrying the battery modules. The weight of the frame is still relevant, because an increased vehicle weight results in decreased vehicle performance and increased energy consumption.

Although a frame made from steel profiles will be heavier than a frame made from aluminium extrusion profiles, it was decided to make the frame from steel because of cost reasons. Aluminium extrusion profiles make sense when flanges can be integrated in the profile and thus the number of parts can be reduced and if weight is very important, like for the vehicle space frame.

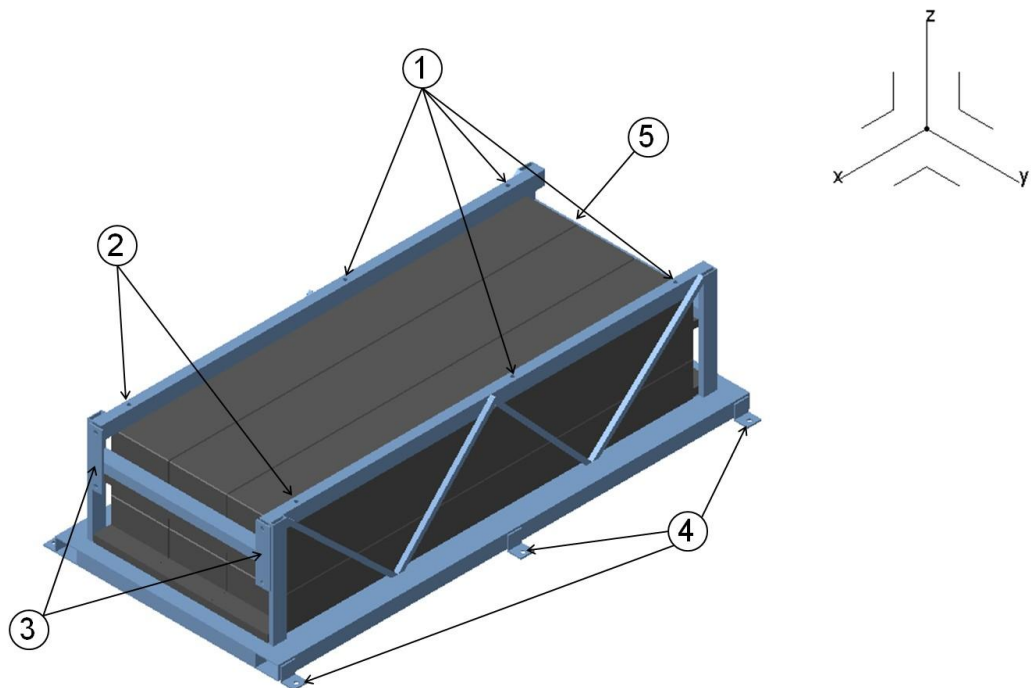


Figure 3.13 Battery frame with battery modules

Figure 3.13 shows the frame with the battery modules. The frame is basically a weld structure. Only the front cross beam (5) that carries the upper 3 modules needs to be removable, to allow the assembly of the battery modules to the frame. The following parts, beside the battery modules, are supported by the battery frame:

- The driver seat rails are connected to the frame at the 4 positions (1).
- At position (2) the passenger seats and the trunk floor are connected.
- The engine frame is mounted to the battery frame at position (3).

The battery frame itself is fixed to the vehicle frame at position (4).

Housing

The battery housing consists of 3 parts (see Figure 3.14). The upper housing (1) covers the upper part of the battery and separates the battery from the interior of the vehicle. The housing must be airtight to prevent battery gases getting in the interior. It must prevent passengers of getting in contact with high voltage parts and isolate the parts. And it should prevent the heat transfer from the interior to the battery, especially in summer, when the vehicle heats up in the sun. An additional reduction of the heat transfer is achieved by the floor carpet. The upper housing is therefore designed as a sheet moulding compound part. The simple part design allows a cost efficient tooling. The holes in pulling direction (4) can be directly integrated in the tool. The holes to mount the motor frame (3) are not in pulling direction and will be drilled after the moulding process to minimize tooling costs.

The lower housing (5) is made from an aluminium sheet metal to allow a good heat transfer from the battery to the surrounding. The concern why a good heat transfer is demanded, is not the self heating of the battery (see chapter 3.3.5), but the heating of the battery, due to heat transfer from the interior. If the heat transfer from the interior can be reduced sufficiently, the lower battery housing could also be a sheet moulding compound part. This would reduce the costs and result in a more constant battery temperature. In both cases the lower battery housing is glued and additionally riveted (not shown in the figure) to the battery frame.

The upper and the lower housing can be glued to the battery frame at the battery manufacturer. The third housing, the high voltage distribution unit (HVDU) cover (5) will be mounted to the battery at the battery manufacturer, for a safe transport. But it needs to be removable to connect the inverter with the integrated DC/DC converter, the charger and the vehicle control unit (VCU) to the battery at the vehicle assembly.

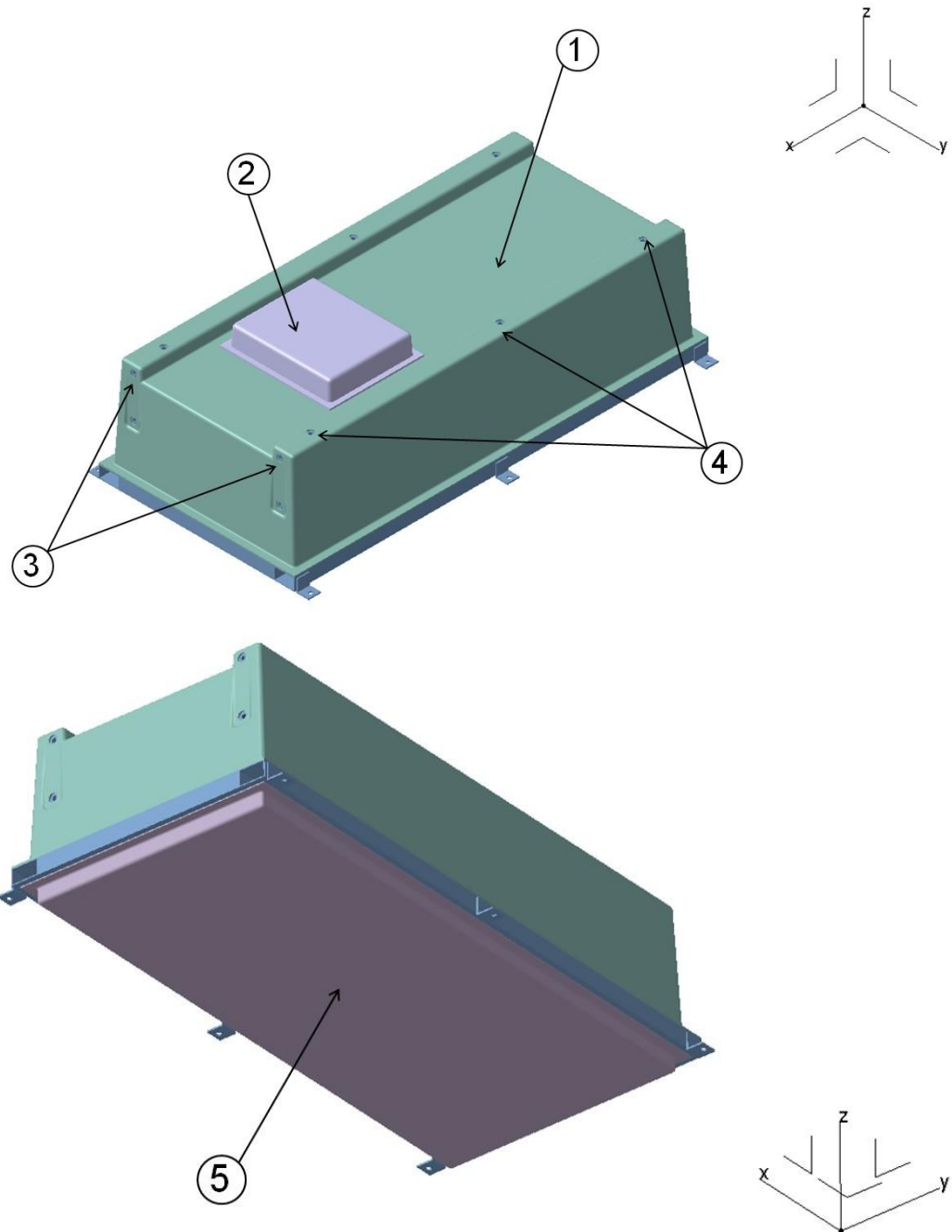


Figure 3.14 Battery Housing

3.3.4 Battery lifetime

The capacity of a battery decreases over time. The main reason is the increase of the internal resistance due to an increase of the thickness of the solid electrolyte interface (SEI), which separates the solid graphite electrode from the liquid electrolyte. The decrease of the battery capacity is depending on two factors, the calendrical age and the cyclic age. So a battery which is not used but just stored loses capacity over time. The

speed of capacity decrease is depending on the storage temperature and on the state of charge (SOC). There are many different models in literature to simulate the battery life. The model presented here is very simple and used at MAGNA for a quick battery life estimation in the concept phase. The necessary data to determine the parameters for this simple model is available for the used 50 Ah cell. The capacity loss depending on time t can be approximated by the formula 3-1. The factor $a(T, SOC)$ is specific for every cell type and depending on the temperature and the SOC level during storage. [Rei10], [Wat10], [MAG10a].

$$C_{loss,time}(t) = a(T, SOC) \cdot \sqrt{t} \quad (3-1)$$

The behaviour of the battery concerning capacity loss due to SOC cycles is similar to the time depending capacity loss, see formula 3-2. The factor $b(\Delta SOC)$ is specific for every cell type and mainly depending on the difference between the maximum SOC, when the battery is fully loaded and the minimum SOC, when the battery is empty. It is usual to use the battery within 10% (minimum SOC) and 90% (maximum SOC), to limit the capacity loss [Rei10], [Wat10].

$$C_{loss,cycle}(n_{cycle}) = b(\Delta SOC) \cdot \sqrt{0.5 \cdot n_{cycle}} \quad (3-2)$$

The number of cycles can also be expressed by time when a user profile is known. From the profile the cycles per time can be derived. And so both capacity losses can be shown depending on the time. With the user profile it is also possible to determine the average SOC, which is relevant for the calendar life.

User profile

For the SOC profile (Figure 3.15) the following estimations were made:

The car is used for the daily drive to work over a distance of 35 km. Every evening during the week the car is connected to the power supply and recharged in the time between midnight and six o'clock in the morning, to load at the cheaper night rate. On Friday the car is also used in the evening for a trip in the city over a distance of 20 km and not charged in the night to Saturday. On Saturday the car is used for a distance of 20 km for a shopping trip. In the night from Saturday to Sunday the battery is reloaded again, to have the full range of the vehicle on Sunday, but the vehicle is not used on Sunday because the family car is used for the family trip. For the calculation of the energy consumption per km the consumption during the NEDC cycle (see Table 2.4) is used.

To be on the safe side the profile was chosen in a way that the average SOC is on the upper level. The average SOC resulting from that profile is 67.4%. To increase the

battery life the recommendation for the customer would be, to load the car only every second day, to reduce the average SOC to 58.6%. Or even to 49.7% if the battery is not reloaded in the night from Saturday to Sunday, but from Sunday to Monday. But in reality the customers will probably tend to reload the car earlier to have to full range available.

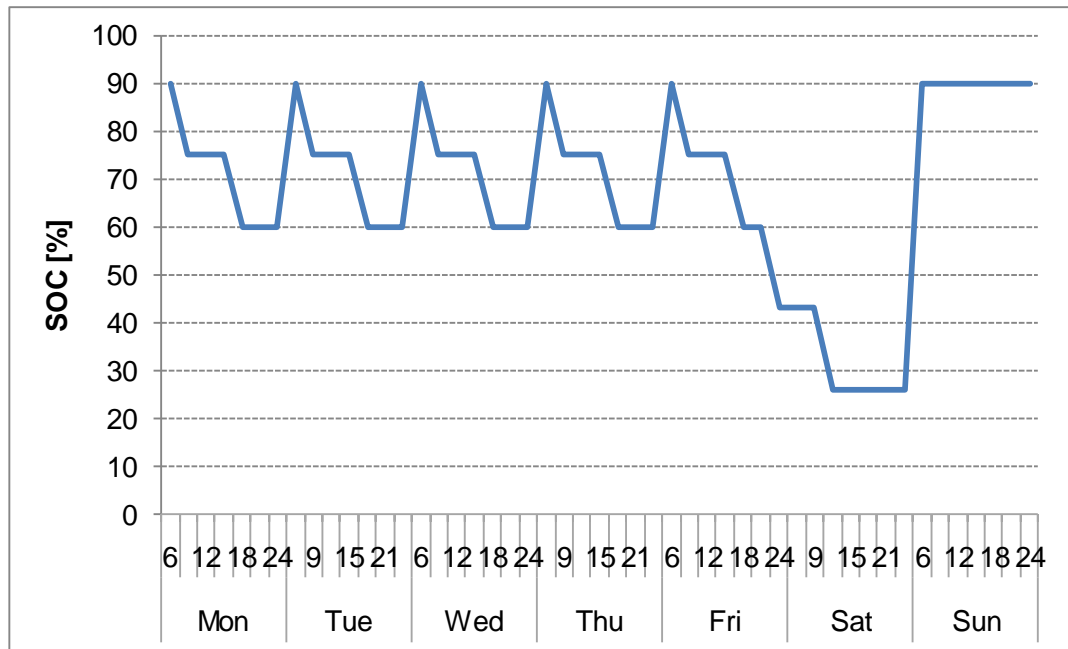


Figure 3.15 Weekly profile of the SOC

Besides the SOC the average temperature of the battery is important for the battery life. The car is used only approximately one hour per day in average and is recharged for maximum 3.5 hours with the onboard 3.3 kW Charger (see chapter 3.2.3). During a one hour drive of the NEDC the temperature increase of the adiabatic cell (worst case) is only 3.8 K. The temperature increase of the adiabatic cell during charging (from 10% to 90% SOC) is 3.5 K. Chapter 3.3.5 explains the details of the thermal simulation. So the theoretical average temperature of the cell will be only 0.7 K higher than the average ambient temperature. Thus for the battery life it is more important where the car is used, than how it is used. As an example the ambient temperatures of 3 European cities are considered:

- Graz: 9,4 °C [ZAM10]
- Malaga: 18 °C [WIK10a]
- Oslo: 5,9 °C [WIK10b]

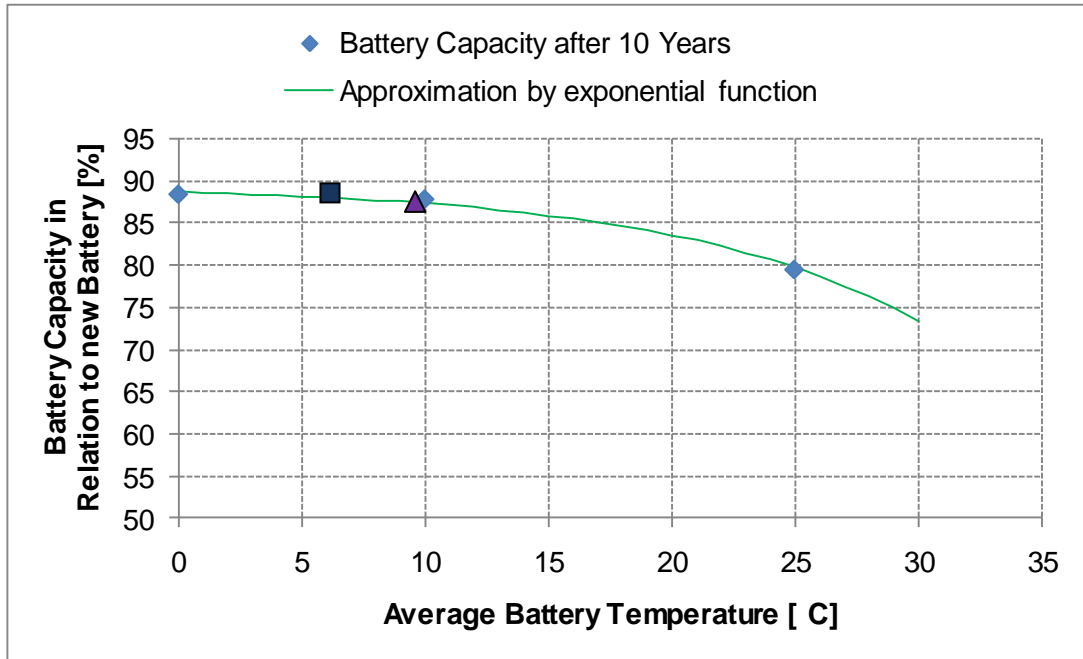


Figure 3.16 Battery capacity after 10 years (no cyclic aging)

The battery capacity after 10 years at the temperature of 0, 10 and 25 °C is given in the battery data sheet [MAG10a].

Battery life

With the profile give in Figure 3.15 the car is used 215 km per week and 11,180 km per year. This is significantly above the estimated mileage per year of 7,000 km [Wec11]. So the calculated battery life should rather be the worst case scenario. With the energy consumption (see Table 2.4) and the installed battery capacity the average cycles per day can be calculated. With that result the cyclic capacity loss can be expressed depending on the time (see formula 3-3).

$$C_{loss,cycle}(t) = b(\Delta SOC) \cdot \sqrt{0.5 \cdot \frac{n_{cycle}}{t} \cdot t} = b^*(\Delta SOC) \cdot \sqrt{t} \quad (3-3)$$

This enables to calculate a combined capacity loss depending on the time, and thus the battery life. As both capacity losses are depending on the square root of the time they cannot be simply added. The derivative of the capacity loss is discretized in time. The capacity loss is then calculated with the formula 3-4.

$$C_{loss,i} = C_{loss,i-1} + (a^2(T, SOC) + b^*{}^2(\Delta SOC)) \cdot \frac{\Delta t}{2 \cdot C_{loss,i-1}} \quad (3-4)$$

With the formula 3-4 the figure can be created to show the capacity change over lifetime of the battery. End of life of the battery usually is defined if the capacity of the battery is 80% of the capacity of the new battery.

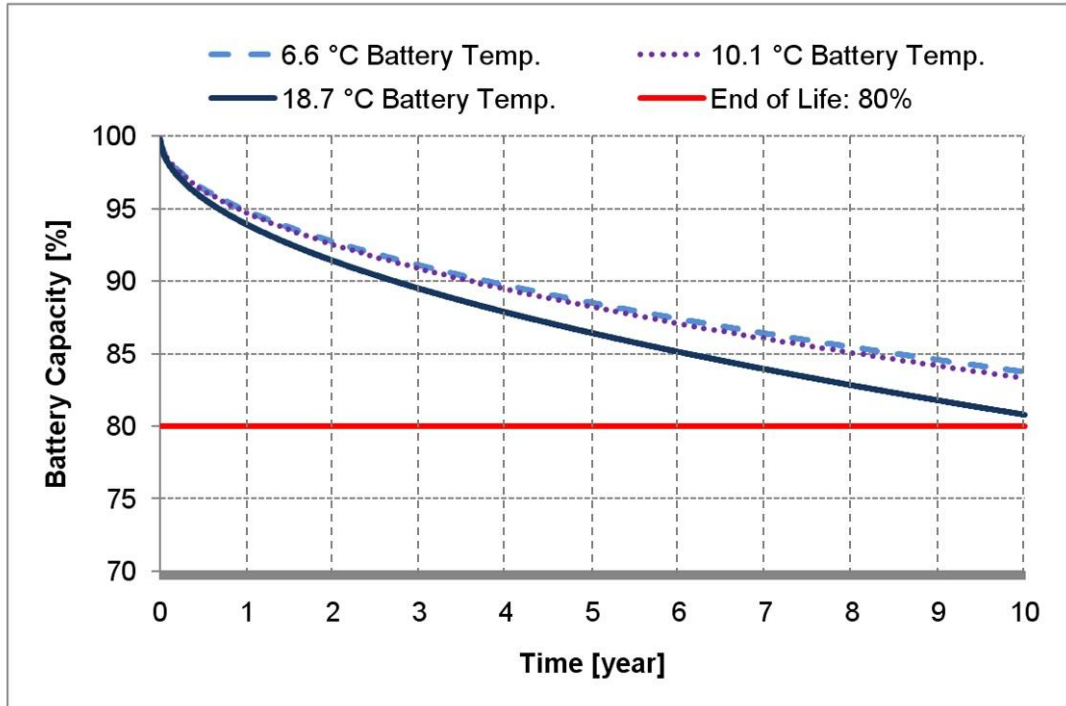


Figure 3.17 Battery capacity (calendarical and cyclic aging)

The figure shows that also in Malaga the target life of the battery of 10 years will be reached. To avoid that the range of the vehicle drops from 98 km (see chapter 3.3.2) to 78 km, the SOC range is increased from 80% to 90% at end of life. So the range of the vehicle after 10 years will still be 88 km, which is almost the target range of 90 km.

3.3.5 Battery cooling

As described in the chapter before the battery temperature is a very important parameter to influence the battery capacity and thus also the battery life. In the data sheet for the cell the maximum operating temperature is define with 60 °C [MAG10a]. At this temperature the battery aging strongly increases [TEC10]. Basically it is of course the target to use the battery without cooling to reduce the complexity of the battery and keep the vehicle costs low. Relevant for the temperature increase ΔT (formula 3-6) of the battery cells is the effective current I_{eff} (formula 3-5) square, the internal resistance of the battery cell R , and the thermal capacity of the cell C_{therm} . If the battery is not cooled the heat transfer can be neglected. As all the cells in the battery are connected in series, the internal resistance as well as the thermal capacity increases linear with the number of cells. Therefore the result is the same, weather the temperature increase is calculated for one cell or all the cells in the battery.

$$I_{eff} = \sqrt{\frac{1}{t} \cdot \int i^2(t) dt} \quad (3-5)$$

$$\Delta T = \frac{I_{eff}^2 \cdot R \cdot t}{C_{therm}} \quad (3-6)$$

The temperature increase is calculated for four different load cycles. In all four cases the battery is considered to be adiabatic:

- ΔT within 90 km NEDC at GVW: 10.6 K
- ΔT within 1 hour (32,6 km) NEDC at GVW: 3.8 K
- ΔT within full discharge of the battery (from 90% to 10% SOC) with maximum motor power of 15 kW (worst case): 19.2 K
- ΔT within full charge of the battery (from 10% to 90% SOC) with maximum power of onboard charger of 3.3 kW: 3.5 K

The results show that the maximum increase of battery temperature is less than 20 K in a very unlikely type of operation. The usual increase of temperature will be below 10 K. Nevertheless also in worst case the battery temperature will not come above 60 °C, because the battery temperature at the start would need to be above 40 °C, solely due to heating from ambient temperature. The conclusion is that it should be no problem to operate the battery in the E-MILA Student without any cooling. It is more important to isolate the battery to the vehicle interior, so that the hot air inside the vehicle does not heat up the battery.

4 Main Chassis Components / Modules

This chapter describes the concept layout of the main chassis modules (front- and rear suspension, steering system and brakes) for the E-MILA Student. The following characteristics of each of these modules will be investigated:

- Important functional requirements (as for example deceleration depending on the brake pedal force)
- Module weight
- Module costs per vehicle split up in part costs, development and tooling costs (if applicable)
- Design and package in the vehicle

It is necessary to focus on weight because of the limited kerb weight (without batteries) of the vehicle of 400 kg (see chapter 2.1). Based on a bill of material on the level of systems and main components a target weight for each of these systems and components is defined. The target weights are also checked for plausibility by benchmarking.

Costs per vehicle and especially the investment costs for development and tooling are especially relevant for this vehicle because of the low expected average volume of 10,000 vehicles per year during a production time of 6 years (see chapter 1 and for more details [Pre10] and [Wec11]).

Expectations from the customer

Before a benchmark is done and one compares the own product to products from competitors, it is important to understand what are the customers' expectations on a certain product. In case of chassis modules as parts of a car the expectations of the end customer will depend on the vehicle class. A driver of a sports car will have different expectations than the driver of a small city vehicle. But in both cases the main expectation is related to the function in relation to a reasonable price. The design or uniqueness will not be a selling argument. This is also a main reasoning for a platform strategy. The customer will accept or even not care if his/her car shares chassis parts with other (maybe also cheaper) cars. Of course this does not mean that the driving behaviour is not relevant. The tuning of the suspension must be optimized for every vehicle and is a very important characteristic. It is also clear that the driving behaviour is depending on the suspension design. So by choosing a certain design also the tuning is limited to a certain extend. It is

therefore necessary to choose the right design to be able to achieve a certain vehicle behaviour, but the design or/and the parts can be carried over from an existing vehicle.

When the E-MILA Student shall be compared to other existing vehicles with a similar purpose, it is obvious to compare it with a SMART Fortwo I. Table 4.1 shows the main relevant parameters. The outer dimensions of the two vehicles are very similar. The main purpose of both vehicles is driving in the city. The SMART has a higher engine power and a higher maximum speed. The demands concerning driving dynamic behaviour are therefore higher. Still the aim for the E-MILA Student is to achieve at least the same driving dynamic behaviour as the SMART.

Table 4.1 Comparison of SMART Fortwo I with E-MILA Student [SMA10]

Dimensions	E-MILA Student	SMART Fortwo I
Length [mm]	2550	2500
Width [mm]	max 1480	1515
Height [mm]	1550	1549
Wheelbase [mm]	1850	1812
Track Width front [mm]	1300	1272
Track Width rear [mm]	1300	1354
Weight		
Kerb weight [kg]	550	750
Design weight [kg]	625	825
GVW [kg]	800	990
Weight distribution @ design weight [f%/r%]	51 / 49	43 / 57
Performance		
Engine power [kW]	15	37
Top speed [kph]	90	135
Tires		
Tires front	155/70R13	135/70R15
Tires rear	155/70R13	175/55R15

A detailed comparison of the driving dynamic behaviour of the two vehicles cannot be given in this work. A basic vehicle dynamic measurement of the SMART and a vehicle dynamic simulation for the E-MILA Student are too much effort to be realized within this work. The following paragraph still tries to give arguments why it seems reasonable that the E-MILA Student with the chassis modules suggested in this chapter will be able to achieve at least the driving behaviour of the SMART.

The outer dimensions of both vehicles are almost the same. Track width and wheelbase together with the centre of gravity height influence the dynamic wheel load during braking or cornering. For the E-MILA Student the calculated CoG height is 437 mm

at design load. The heavy battery in the E-MILA Student that accounts for 27% of the kerb weight is positioned very low in the vehicle. The z-position of the battery centre of gravity is only 260 mm. Although there is no exact centre of gravity height known for the SMART, it can be estimated that it will be higher. Therefore also the wheel load change during cornering or braking will be higher in the SMART. A wheel load change reduces the brake force or side force potential of the tires (see Figure 4.1).

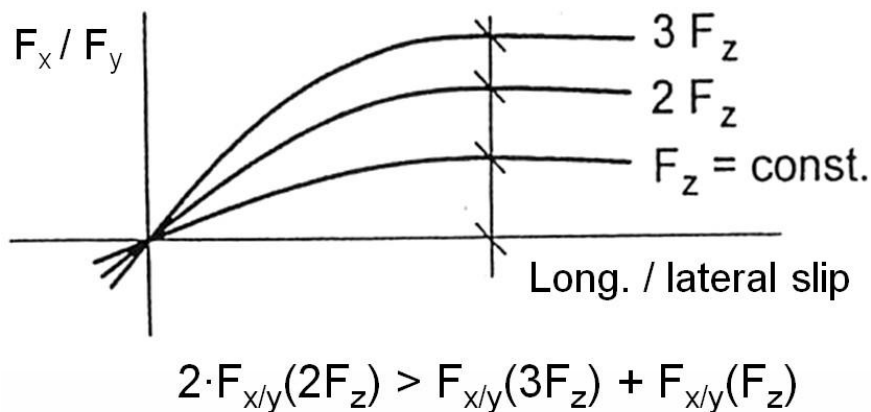


Figure 4.1 Wheel load influence on brake / side force potential [Hir99]

The following weight distributions were calculated for the E-MILA Student:

- Kerb weight: front 283 kg (52%), rear 262 kg (48%)
- Design weight: front 321 kg (51%), rear 314 kg (49%)
- Gross vehicle weight: front 337 kg (43%), rear 448 kg (57%)

The wheel load distribution is more balanced in the E-MILA Student. The load distribution for the SMART was measured at kerb weight with a used SMART Fortwo I. The front axle load is 317 kg (43%) and the rear axle load 424 kg (57%). The SMART has a higher rear axle load, which makes it necessary to use tires with different size on the front and rear axle, to realize an understeering behaviour of the vehicle. With the more balanced load distribution, it will most probably be possible to use the same tires on the front and rear axle of the E-MILA Student and still achieve a sufficient understeering behaviour.

An additional advantage for the E-MILA Student is the lower vehicle weight of approximately 200 kg. Due to the degressive behaviour of the tires brake and side force potential depending on the wheel load, the same tires would have relatively more grip in the lighter vehicle.

But the tires of the E-MILA Student have a bigger cross section height than the tires of the SMART (108.5 mm compared to 94.5 mm). The higher cross section will be

advantageous for the comfort, but will be a disadvantage for the side force potential of the tires. Still, as the static wheel load and the dynamic wheel load change will be smaller in the E-MILA Student, it is supposed that the driving dynamic behaviour will be similar to the SMART.

The reasoning given above shall be sufficient for this rough concept work, but needs to be supported by driving dynamic simulation of the full vehicle, if the vehicle concept is further developed.

4.1 Front Suspension

On the front axle there is not a big variety of different suspension systems on the world market. Four different types account for over 99% of all front axles built in vehicles with a weight of less than 3.5 to in 2005 [Hei08]:

- Rigid axle
- Mc Pherson
- Double Wishbone
- Multi link

The most common one is the Mc Pherson suspension system. It was used in 78% of all vehicles in 2005, followed by the double wishbone suspension, which was used in 20% of the vehicles. Rigid axle and Multi link suspension were used by only approximately 1% of the vehicles each. All four suspension system can be used as a driven or non driven axle. Apart from some exceptions like SMART Fortwo or TATA Nano small vehicles typically have front wheel drive. For front wheel drive vehicles the market share of the Mc Pherson suspension system is at 90%. And also the two small vehicles with rear wheel drive use a Mc Pherson suspension at the front axle. Generally it can be said that Mc Pherson suspension is the front suspension system for small vehicles [Hei08].

Therefore also the E-MILA Student shall get a Mc Pherson front suspension. To be able to compare the different variants of the Mc Pherson front suspension used in small cars a benchmark was carried out.

4.1.1 Benchmark: Front suspension of small vehicles

The following four different vehicles were chosen for the benchmark:

- SMART Fortwo I: A vehicle with very similar outer dimensions and the same purpose

- SMART Fortwo II: To see the changes/improvements that were made between the two generations
- Fiat Panda: A very cost efficient, popular small European car
- Tata Nano: It is the benchmark for low cost design and it has the same track width and a similar kerb weight

SMART Fortwo I

The pictures were taken by myself from a used SMART Fortwo I . As the vehicle could not be disassembled, there are no part weights available for the SMART Fortwo.

On this car the steering is in front of the wheel centre. The brake disk has an outer diameter of 280 mm, which requires the mounted 15 inch wheels. The wishbone is symmetrical and therefore the same part can be used on the left and right side (see Figure 4.3). The wishbone is made of 2.5 mm thick sheet metal. On the inner side there are two rubber bushings pressed in the wishbone. The supporting ball joint has a cuboid shaped housing which connects the two 2 mm thick sheet metal parts of the steering knuckle. Also the housing of the outer tie rod ball joint supports the two parts of the steering knuckle. The suspension strut is mounted to the steering knuckle with three screws. The stabilizer link is connected to the wishbone and not as usual to the suspension strut.

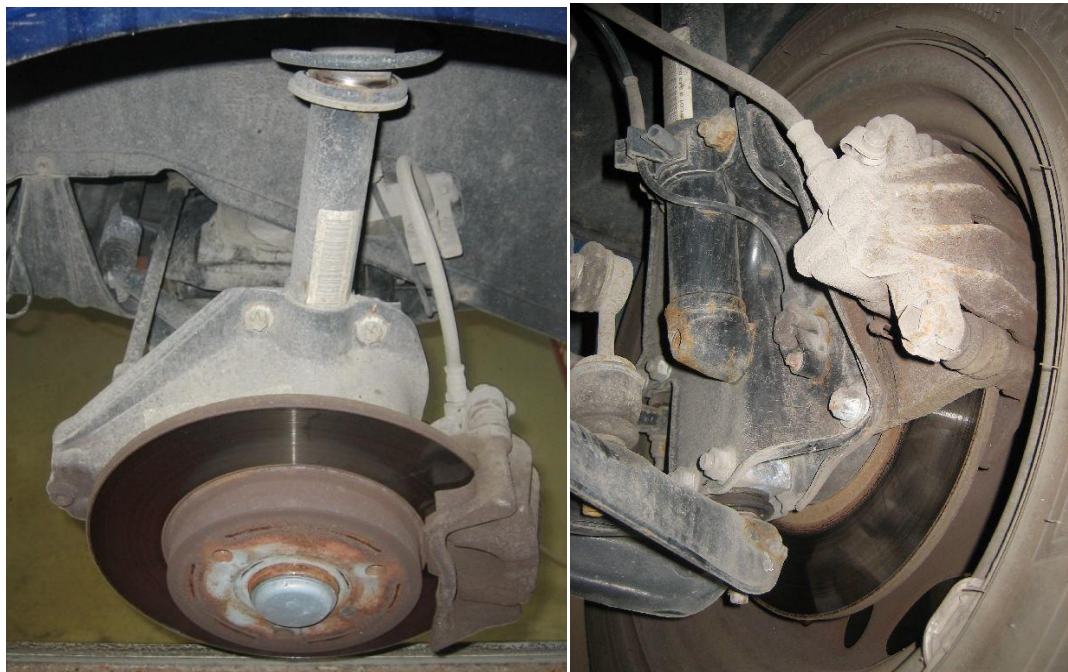


Figure 4.2 SMART Fortwo I disk brake and steering knuckle



Figure 4.3 SMART Fortwo I wishbone

SMART Fortwo II

The picture was taken from a used car by myself.



Figure 4.4 SMART Fortwo II steering knuckle and wishbone

The design of the front suspension was changed pretty much between the two SMART generations. The wishbone is still a sheet metal part and it is still one part for the left and right side, but it was redesigned and it now carries the supporting ball joint. The wheel carrier is completely new and is now a steel cast part. The suspension strut is clamped to the wheel carrier. The stabilizer link is not connected to the wishbone anymore, but directly to the suspension strut.

Fiat Panda

The pictures and weight information on the vehicle is from A2Mac1 homepage [A2M10] who do vehicle benchmarking. The teardown of the Fiat Panda 1.2 was done in the year 2003.

Table 4.2 Weights of Fiat Panda front suspension components [A2M10]

Fiat Panda 1.2	Weights per axle [kg]
Wishbone	7.0
Steering knuckle assy (incl. wheel bearing and hub)	9.1
Suspension Strut	12.7
Stabilizer Bar	5.0
Brakes	14.3
Steering Bar incl. Tie rods w/o power steering	5.4
Sum	53.5



Figure 4.5 Fiat Panda front suspension [A2M10]

As this vehicle has front wheel drive the steering system is positioned behind the front wheel centre, due to package reasons. The brake disk has a diameter of 240 mm and allows the use of 13 inch wheels. The wishbone has an L-shape and is produced as a steel cast part. Due to the L-shape it is possible to clearly separate the function of the two inner rubber bushings. The front rubber bushing, which is almost at the same x-position as the supporting ball joint, has a high stiffness for good lateral control. The rear rubber bushing is responsible for the longitudinal springing and thus for the rolling comfort. The

wishbone is a mirrored part on the left and right side. The steering knuckle is clamped in a sheet metal bracket welded to the suspension strut. The stabilizer link is connected to the suspension strut.



Figure 4.6 Fiat Panda wishbone [A2M10]

Tata Nano

The Tata Nano is up to now only produced for the Indian market, for a price of only EUR 1,700.- [AUT10]. It is therefore the benchmark for low cost design. The pictures and the weight information on the Tata Nano are from [A2M10].

Table 4.3 Weights of Tata Nano front suspension components [A2M10]

Tata Nano	Weights per axle [kg]
Wishbone	3.6
Steering knuckle assy (incl. wheel bearing and hub)	3.3
Suspension Strut	9.4
Stabilizer Bar	-
Brakes	13.6
Steering Bar incl. Tie rods w/o power steering	3.8
Sum	33.7

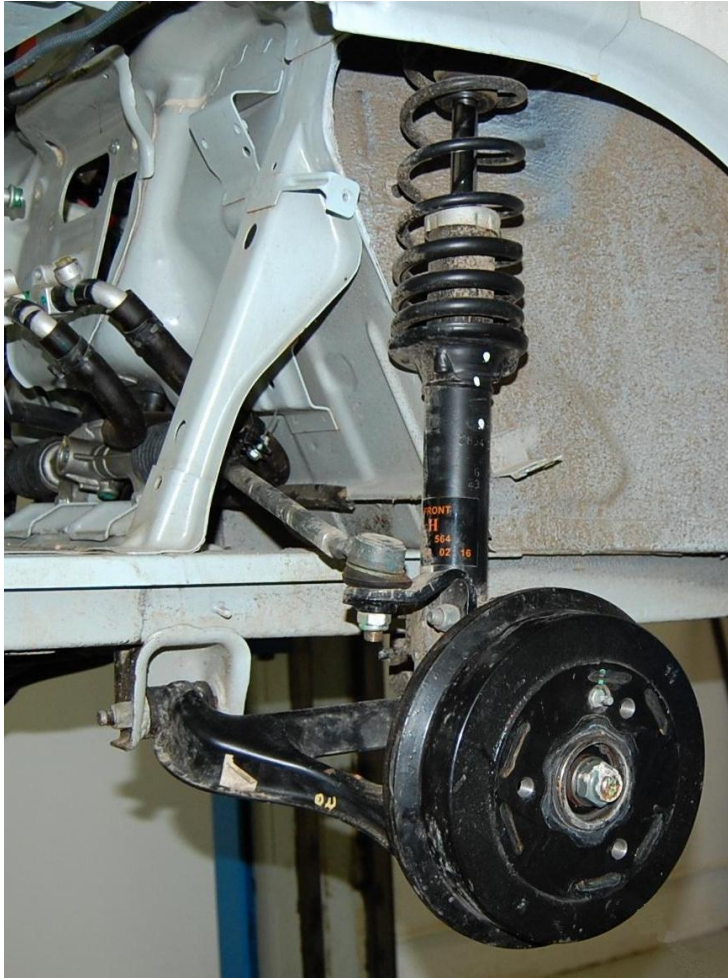


Figure 4.7 Tata Nano front suspension in vehicle [A2M10]

The Tata Nano is like the SMART Fortwo a rear wheel driven car. In the front there is therefore enough space to package the steering in front of the front wheel centre. The Tata Nano has drum brakes not only at the rear but also at the front axle. One reason for using drum brakes at front axle might be the higher C^* brake value compared to disk brakes [Hei08]. The base version of the Tata Nano is not equipped with a brake booster. The higher C^* brake value helps to still achieve low actuation forces. The wishbone is directly supported by the vehicle body and not by a subframe. The wishbone is an A-shaped sheet metal part with two inner rubber bushings. The supporting ball joint is mounted to the wishbone by two rivets. The sheet metal part is the same part on the left and right side, but the assembled part (with the supporting ball joint) is different. The steering knuckle is a steel cast part, which is the same for the left and right side. This is possible because the steering lever is a separate part that is bolted to the steering knuckle. Important to mention is also that the Tata Nano has no stabilizer bar on the front axle. As the vehicle has independent suspension on the front and rear axle, the parallel and the

opposite spring rate will be the same [Rei00]. It is necessary to find a compromise between the reduction of the maximum body roll angle and the springing comfort.



Figure 4.8 Tata Nano front suspension without steering [A2M10]

4.1.2 E-MILA Student front suspension

As described in the introduction of chapter 4 the expected volume of the E-MILA Student is only 10,000 units per year (see [Pre10] and [Wec11]). Thus investment costs have a big influence on the part costs. As it is not possible to carry over a complete front suspension module from the benchmark vehicles due to package reasons, it is investigated whether single parts of existing suspension systems can be used to save development and tolling costs.

4.1.3 New front suspension design

Based on the benchmark and on the package requirements of the full vehicle the following prerequisites for the suspension system were defined:

- Position of the steering system in front of the wheel centre: To have sufficient legroom for the centre positioned driver, it is necessary to position the steering as far front as possible. Of course also the steering kinematics need to be considered (see chapter 4.3.1)

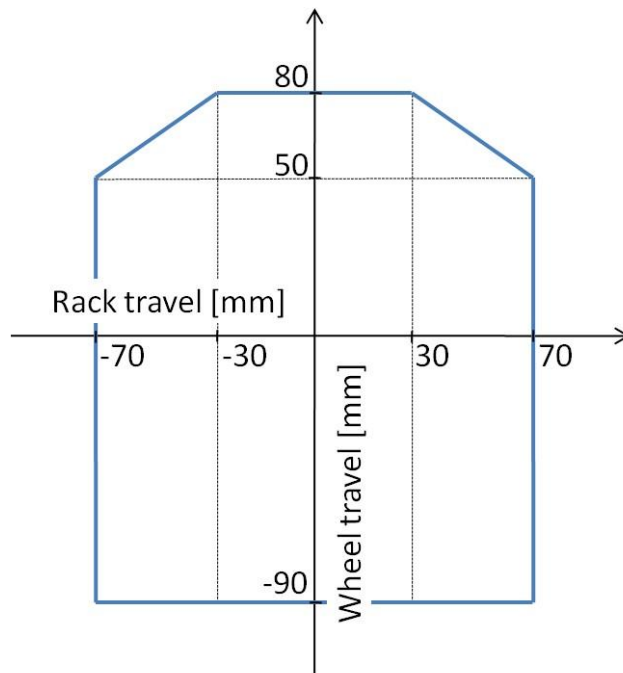


Figure 4.10 *Wheel envelope front suspension*

The relation between the rack travel and the steering angle of the front wheels is described in chapter 4.3.1. The tire dimensions are 155/70R13 (see chapter 4.5). The geometry of the tire model used for this simulation in CATIA is defined by the ETRTO standard [ETR03].

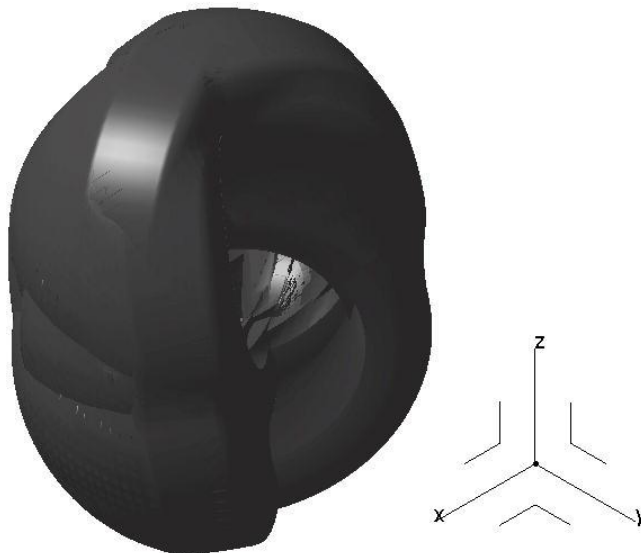


Figure 4.11 *Front wheel space demand in wheel house*

After the kinematics of the suspension system is defined, it is possible to design the components. When deciding on the component design and production technology, it is very important to consider the following prerequisites.

- Low volume production (see introduction of chapter 4) requires low tooling costs
- Low weight of the parts, due to the maximum kerb weight of 400 kg (see chapter 2.1.1)
- Low part price, to achieve an affordable price for the vehicle (but always considering the tooling costs)
- Carry over parts where possible

The rough tooling costs are provided by the MAGNA STEYR purchasing department. An overview of the estimated costs and the target costs is given in chapter 5.1.1.

In the following paragraphs the parts of the front suspension concept, which can be seen in Figure 4.12, are described briefly.



Figure 4.12 E-MILA S front suspension

Front suspension subframe

The suspension design and the vehicle frame design were optimized that no additional front suspension subframe is necessary. The wishbone is directly mounted to the vehicle frame. The top mount of the suspension strut is mounted to a bracket that supports the connection of the upper longitudinal beam and the fire wall.

Wishbone

The wishbone which is integrated in the concept is from a Dacia Logan, because it has the right dimensions to fulfil the package and kinematic requirements. Nevertheless the Dacia Logan is a vehicle with a significantly higher front axle load than the E-MILA S, therefore the part strength is higher than necessary and also the part weight is higher. Still to save the additional development and tooling costs the Dacia Logan wishbone is used.

Knuckle

The knuckle is a completely new designed part. There are three main reasons why this makes sense:

- A new knuckle offers big freedom to define the kinematics of the suspension. The steering axis (top mount position and supporting ball joint) and the outer tie rod joint can be defined to optimize the kinematics behaviour.
- It is possible to use the Fiat Panda front wheel brakes, because the knuckle can be adapted to carry the Panda callipers. The use of the Fiat Panda knuckle is not possible because the steering is positioned behind the front wheel centre.
- It can be designed to the needs of the vehicle, e.g. lightweight design.

The knuckle is designed as a gravity die casting part made from steel. It is possible to realize the part with a simple tool made from two dies and without any sliders. Thus the tooling costs will be acceptable.

Suspension strut

The spring and the damper will need to be adapted to the needs (especially the weight) of the vehicle. For the concept it is assumed that it is possible to use the Fiat Panda suspension strut with a modified damper and new spring. It will also be necessary to modify the top mount to fit to the weight of the vehicle. But it is likely that the same tools can be used and only the shore-hardness of the rubber is changed.

Wheel hub and wheel bearing

The wheel bearing can be carried over for instance from the SMART Fortwo, because it has a similar front axle weight. The wheel hub will need to be a new part, as the brakes are used from the Fiat Panda. The wheel hub and wheel bearing from the Fiat Panda cannot be directly carried over, because these are front wheel drive parts. The new wheel hub will need to support the 4 x 100 mm bolt pattern of the Fiat Panda. As this is very common it has the advantage that many different rims will be available for the car.

Anti roll bar

The anti roll bar as the spring must be fitted to the vehicle and is therefore a new part. Anti roll bars for smaller vehicles can be produced in a cold bending process, of which tooling costs are acceptably low. Only stiff anti roll bars with large diameters for bigger cars need to be produced with the more expensive hot bending process. To save weight it is suggested that the anti roll bar is not formed from a bar but from a tube, which significantly increases the material utilization and reduces the part weight [Hei08]. The anti roll bar links also need to be fitted to the vehicle. The adaption is very simple as these links usually consist of standard ball joints that are connected by a straight rod in the right length.

4.2 Rear Suspension

The variety of rear suspension systems in passenger cars is a lot higher than the variety of front suspensions. In the year 2005 over 99% of the worldwide available vehicles with a maximum weight of 3.5 t were equipped with 9 different rear suspension types. In comparison on the front axle there are only 4 types, of which only 2 types account for already 98% of all installed front suspensions (see chapter 4.1.1). On the rear axle 3 different types (rigid axle, twist beam and multi link) are installed in 72% of the vehicles. The other 6 types are used in the remaining 28% of the vehicles [Hei08].

For non-driven axles the twist beam suspension has the highest share with 34%. It is especially dominant in smaller vehicles up to the lower middle class, due to its low cost and space-saving design. For driven rear suspensions rigid axles still have the highest market share with 57% of the vehicles in 2005. They are used in SUVs and light trucks in non European countries [Hei08].

The twist beam suspension is not used as a driven rear suspension, because of the package problem of the torsion beam and the prop shaft. Only the Fiat Sedici and the

Suzuki RX4, which are the same vehicles only with a different branding, do have a twist beam suspension on a driven axle. The torsion beam is bended around the prop shaft (see Figure 4.13) [MAG06].



Figure 4.13 Suzuki SX4 rear suspension [MAG06]

Although the E-MILA Student has rear wheel drive, a twist beam suspension might be the right concept, because there is no prop shaft needed. The electric motor especially in the coaxial layout requires not much package space. The torsion beam can therefore have a simple and cost efficient straight design.

4.2.1 Benchmark: Rear suspension of small vehicles

For the benchmark the same four vehicles as for the front suspension are investigated. Interestingly the three different models have three different rear suspension types. All benchmark vehicles have a drum brakes on the rear axle

Smart Fortwo I

The rear axle of the SMART Fortwo is a rigid axle type. The variant is called De-Dion axle and was already used in the 1930ies to avoid the disadvantage of the high unsprung masses of a standard rigid axle. Contrary to the standard rigid axle, the differential is not integrated in the axle body at the De-Dion axle. In the SMART the De-Dion is used because space is needed between the wheels for the engine and transmission.



Figure 4.14 SMART Fortwo I rear suspension

The strong De-Dion axle body is made of a bended steel tube. Wheel carrier, spring and stabilizer support are sheet metal parts welded to the steel tube. The De-Dion axle body is connected to the vehicle body with a large centre positioned rubber bushing. The bushing is positioned in front of the steel tube, which is relatively far in front of the rear wheel centre and also not very high in z-direction, thus the lift and the dive angle are small. This results in a strong pitch movement of the vehicle during acceleration or braking [Hei08]. The lateral forces are supported by two simple lateral links made of sheet metal.

Smart Fortwo II

The SMART Fortwo II rear axle is basically the same as of the Fortwo I, but to improve the anti dive behaviour of the vehicle during acceleration or braking, the central bushing was moved up (in z-direction) and closer to the rear wheel centre. The bushing is now positioned above the De-Dion tube (and not in front of it as in the predecessor).

Characteristics of De-Dion axle [Hei08]:

Advantages:

- Constant wheel to street camber angle
- Lower unsprung masses compared to other rigid axles
- High roll centre (in the height of the front centre bushing)
- Sturdy design

Disadvantages:

- Influence on the opposite wheel at one side wheel travel
- Higher unsprung masses compared to independent wheel suspension
- Higher weight
- Additional lateral links necessary

Fiat Panda

The Fiat Panda is the only front wheel driven car in the benchmark. Like most other cars in that vehicle class, the Panda has a twist beam rear suspension.



Figure 4.15 Fiat Panda twist beam suspension [A2M10]

The twist beam suspension is a very simple suspension type. There is only one axle body which is connected to the vehicle by two large rubber bushings and supported by two coil springs and dampers. The axle body is a welded structure consisting of two longitudinal arms, one transversally positioned torsion beam, two wheel carriers and two spring supports. The longitudinal arms are bended steel tubes. The torsion beam is a simple sheet metal part with an open, U-shaped profile. Wheel carrier and spring support are sheet metal parts.

Due to the connection of the two longitudinal arms with the torsion beam, the suspension behaves partly like a rigid axle and partly like an independent wheel suspension. The twist beam suspension is a so called semi independent wheel suspension or also semi solid axle [Hei08]. As described in the characteristics the twist beam suspension has small package requirements especially in z-direction. In a conventional vehicle layout, like the Fiat Panda, the torsion beam can be positioned between the fuel tank and the spare wheel pan. In the E-MILA Student, as described in chapter 4.2.3, the torsion beam can be placed between the battery and the motor.

Characteristics of twist beam suspension [Hei08]:

Advantages:

- Very simple concept: Only one part and two rubber bushings
- Small package space requirements, especially in z-direction.
- Simple assembly
- Torsion beam can replace a stabilizer bar in small vehicles
- Small unsprung masses
- Good brake pitch reduction

Disadvantages:

- Not usable for high axle loads, due to high stresses in weld seams between longitudinal arm and torsion beam
- Limited optimization potential concerning ambitious handling and ride behaviour
- Low lateral stiffness

Tata Nano

The Tata Nano has a semi trailing arm rear suspension, which is a planar independent wheel suspension type.

Figure 4.16 shows the Tata Nano semi trailing arm suspension seen from under the vehicle and looking in driving direction. A semi trailing arm suspension is mainly used as a driven and less often as a non driven rear suspension. In many cases, like for instance in the BMW Z3, a subframe, which is mounted to the vehicle by rubber bushings, is used to improve the compliance behaviour of the suspension. Soft subframe bushings enable a comfortable longitudinal springing and allow using stiff bushings for the semi trailing arm and thus improving the lateral stiffness and steering behaviour [Hei08]. Nevertheless the subframe of the Tata Nano is rigidly mounted to the vehicle body and thus does not improve the suspensions behaviour. It is rigidly mounted because it also has to support the engine and transmission.



Figure 4.16 Tata Nano semi trailing arm suspension with subframe [A2M10]

The semi trailing arm of the Tata Nano suspension is welded structure consisting of several sheet metal parts. Each trailing arm is connected to the subframe by two rubber bushings. Spring and damper are separated. The spring is a cylindrical coil spring with a changing pitch to achieve a progressive behaviour. The dampers are positioned relatively far in front of the rear wheel centre and have therefore an unfavourable damper to wheel travel ratio.

Characteristics of semi trailing arm suspension [Hei08]:

Advantages:

- Good compromise of longitudinal and pendulum axle
- Possibility to optimize kinematic behaviour by the position of the two bushings of the semi trailing arm
- Small package space requirements in z-direction.

Disadvantages:

- Unfavourable steering behaviour under lateral force
- Stiff bushings necessary
- Good ride comfort only with a subframe which is supported (to the vehicle) by rubber bushings
- Big camber angle change at parallel wheel travel
- Usually a stabilizer bar is necessary

4.2.2 Suitability of benchmark suspension systems for E-MILA S

It was investigated if one of the suspension systems of the benchmark vehicles could be used in the E-MILA Student. Therefore the following main criteria need to be evaluated:

- Rear axle load: If the maximum rear axle load of the “donator” vehicle is higher than of the E-MILA Student, it can be assumed that the axle will be strong enough to withstand the loads in the E-MILA Student.
- Track width: In case of rigid or twist beam axle the track width of the “donator” vehicle must be similar to the E-MILA Student so that it is adjustable with the wheel offset.
- Package: The suspension to be carried over must fit into the package of the E-MILA Student.
- Drivable: The suspension must be suitable as a driven suspension.
- Weight: The suspension weight should ideally be within the weight target

SMART De-Dion axle:

The package of the SMART De-Dion axle is the reason why this axle cannot be used in the E-MILA Student. The axle body needs too much space in x-direction and collides with the battery (see Figure 4.17). It is not possible to position the axle body above or below the battery housing, because the lower position of the battery is limited by the required ground clearance and the upper position of the battery is limited by the driver and passenger seats (see chapter 3.3).

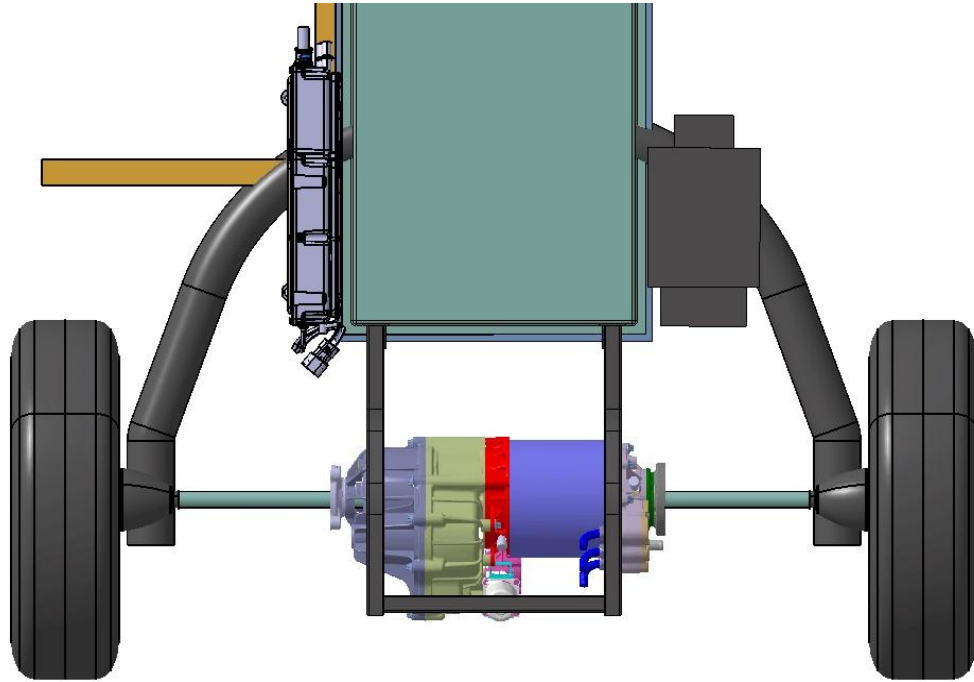


Figure 4.17 Sketch of SMART De-Dion axle body in the E-MILA S package

As the package is a knock out criteria for the SMART rear axle the other main criteria do not need to be evaluated.

Fiat Panda twist beam axle

Figure 4.18 shows the rear package of the E-MILA S with the Fiat Panda twist beam axle. The first thing that can be seen from the figure is that the Panda axle was not designed to be used on a driven axle. The spring (red circle) and the damper (blue filled circle) are positioned so close to each other in x-direction, that there is not enough space for the drive shaft. The damper maybe tilted backwards for sufficient clearance to the drive shaft bellow, but the collision with the springs is not avoidable. Additionally the twist beam, which would basically have enough space between the battery and the motor, is positioned to far in front, so it collides with the battery and the high voltage ECUs. The ECUs may be moved forward, but the battery cannot be moved further to the front, because there would be too less legroom for the driver. All in all it is not possible to use the Fiat Panda twist beam axle in the E-MILA Student.

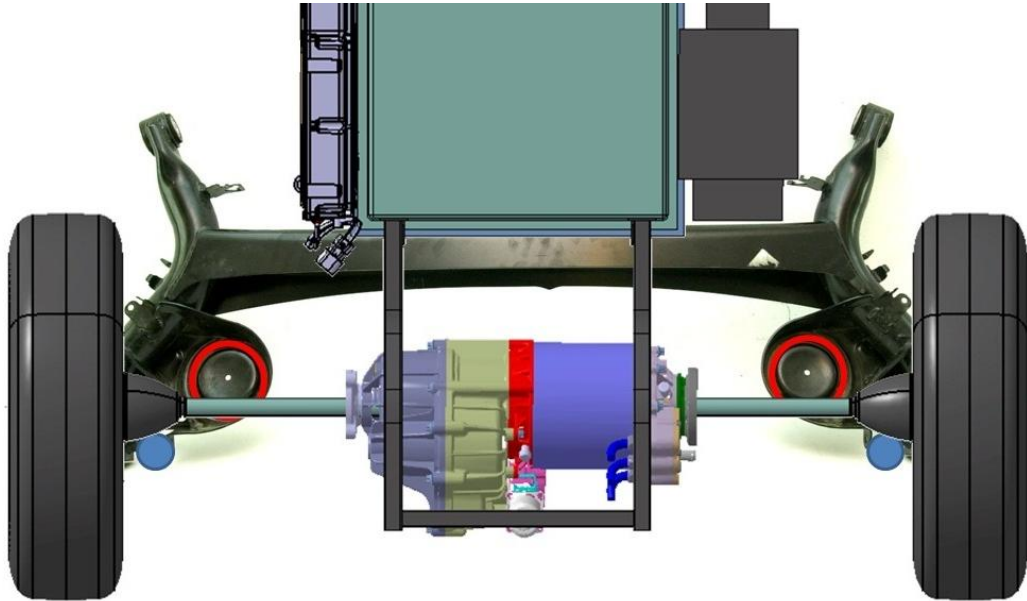


Figure 4.18 Fiat Panda twist beam axle in the E-MILA Student package

Tata Nano

The package is also the problem with the Tata Nano semi trailing arm suspension as it can be seen in Figure 4.19. The damper and the spring are positioned too far in centre and in front and collide with the rear passenger seats. Additionally the inner bushing of the left semi trailing arm collides with the charger and the inner bushing of the right semi trailing arm collides with the inverter. Therefore also this suspension cannot be used in the E-MILA S.

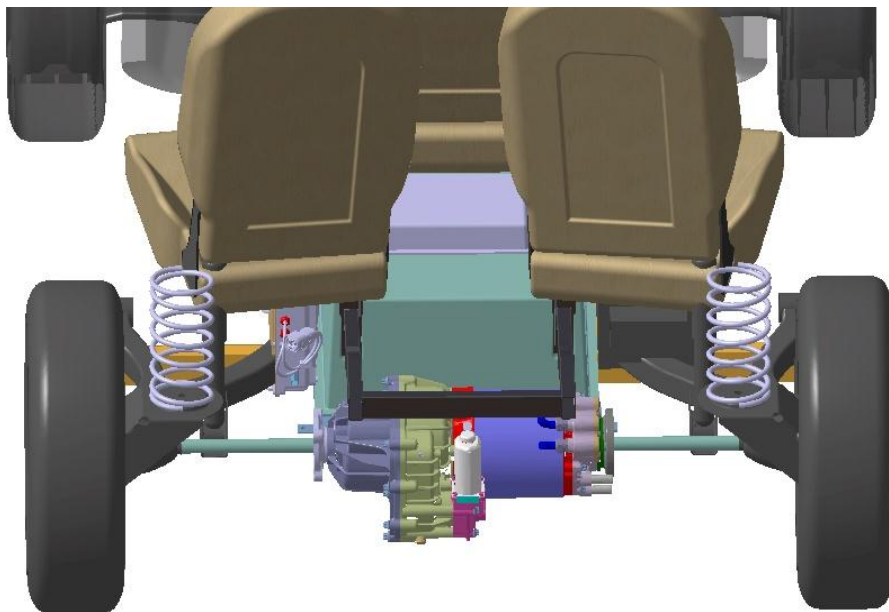


Figure 4.19 Tata Nano semi trailing arm in the E-MILA S package

4.2.3 E-MILA Student rear suspension

Besides the investigated suspension systems of the benchmark vehicles, other suspension systems of small, low cost cars like the Kia Piccanto, Suzuki Alto and Dacia Logan were considered for the use in the E-MILA Student. But none of the suspension systems fulfilled all criteria listed in chapter 4.2.2, mainly due to package problems or non-suitability as a driven axle. So it was necessary to design a new suspension system.

The basic concept for the new design is a twist beam suspension, as it is a low cost design with sufficient performance that fits very well to the package. Figure 4.20 shows the new suspension design in the rear package of the E-MILA Student.

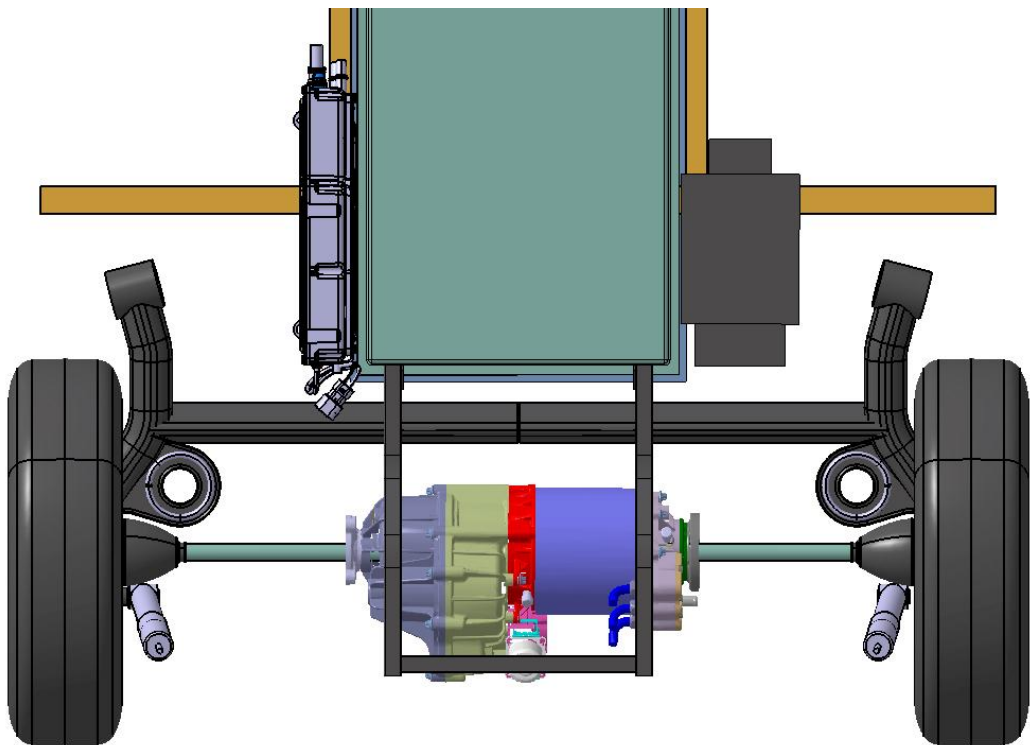


Figure 4.20 E-MILA Student package with twist beam suspension

The torsion beam can be positioned between the motor and the battery. The position of the torsion beam is relevant for the behaviour of the twist beam suspension, especially when the vehicle is cornering. Therefore it was necessary to make a kinematics analysis to see if an acceptable toe and camber angle change of the wheels can be achieved.

Kinematics analysis

As already mentioned in chapter 4.2.1 the twist beam suspension is partly behaving like a rigid axle and partly like an independent suspension. At parallel wheel travel (e.g.

both wheels compressing due to loading the vehicle) the axle behaves like a rigid axle and the toe and camber angle stay constant (despite a small influence of the static camber angle on the toe angle and vice versa due to the rotation around the axis (1) in Figure 4.21). At opposite wheel travel, which happens for instance when the vehicle body rolls during cornering, the twist beam suspension behaves similar to a semi trailing arm suspension (rotation axis (2) in Figure 4.21) [Hei08].

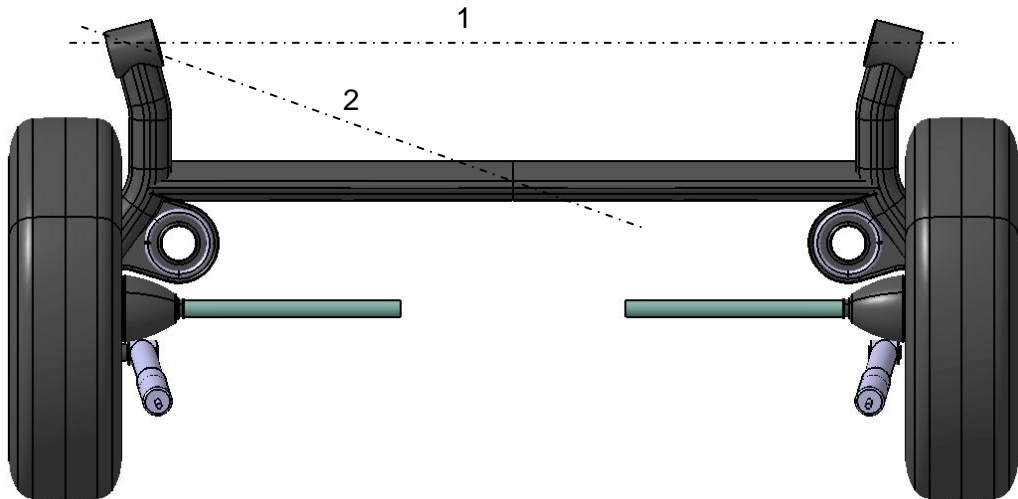


Figure 4.21 Twist beam top view with rotation axis (according to [Hei08])

The kinematics model of the twist beam suspension was therefore made like a semi trailing arm. The outer hardpoint of the semi trailing arm is the same as the hardpoint of the twist beam suspension bushing. The inner hardpoint of the semi trailing arm is the shear centre of the torsion beam profile in the vehicle centre plane.

Figure 4.22 shows the resulting toe- and camber-angle change depending on the wheel travel. The result seems reasonable and will support understeering vehicle behaviour.

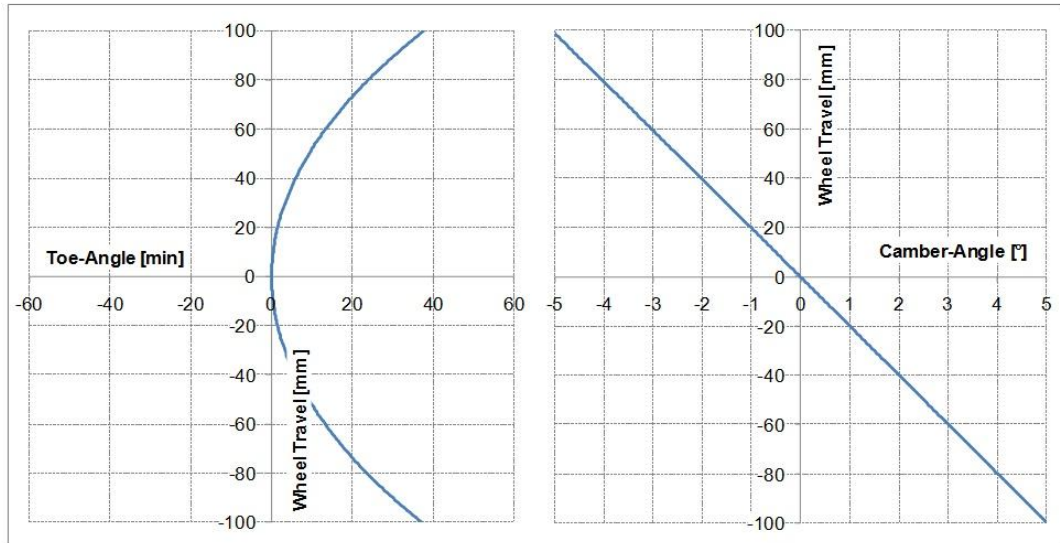


Figure 4.22 Toe- and camber-angle change

Suspension design

The target was to choose a suspension design, which does not require high tooling costs. The longitudinal arm is a steel tube bended in two dimensions, which allows a simple bending tool. The torsion beam is a simple sheet metal part with a V-shaped cross section, which should be possible to form on an edge bending machine. Probably the most complex and expensive tool for this suspension will be the fixture for the weld assembly of the axle body. In this assembly the static toe and camber angle are defined, this is why it needs to be very accurate. The estimated tooling and part costs and the part weight are listed in chapter 5.1.

4.3 Steering System

The steering system needs to fulfil the following basic demands:

- Large steering angles while fulfilling the Ackermann condition (see chapter 4.3.1)
- Acceptable steering uniformity (see chapter 4.3.2)
- Minimal steering wheel torque, for drivers comfort. Steering operation forces must at least fulfil European directive 70/311/EWG (see chapter 4.3.3)

4.3.1 Steering kinematics

The target for the turning circle diameter is maximum 7.5 m. This is less than for instance a Smart Fortwo with 8.75 m [SMA10], an Aixam Roadline (Microcar) with 8 m [AIX10] or the Tata Nano with 8 m [TAT10].

The small turning circle is possible because of the driver position in the vehicles centre and thus sufficient package space for large wheelhouses. A small turning circle is very convenient for the driver because parking is easier and it enables a U-turn without reversing the car already on a wider two track road.

At large steering angles it is essential that the Ackermann condition is fulfilled or respectively that the Ackermann error is not too big. The Ackermann error is zero, when the rotation axis of all four wheels intersect in one point (M) (see Figure 4.23). Therefore it is necessary that the steering angle of the inner wheel δ_i is bigger than the steering wheel angle of the outer wheel δ_a

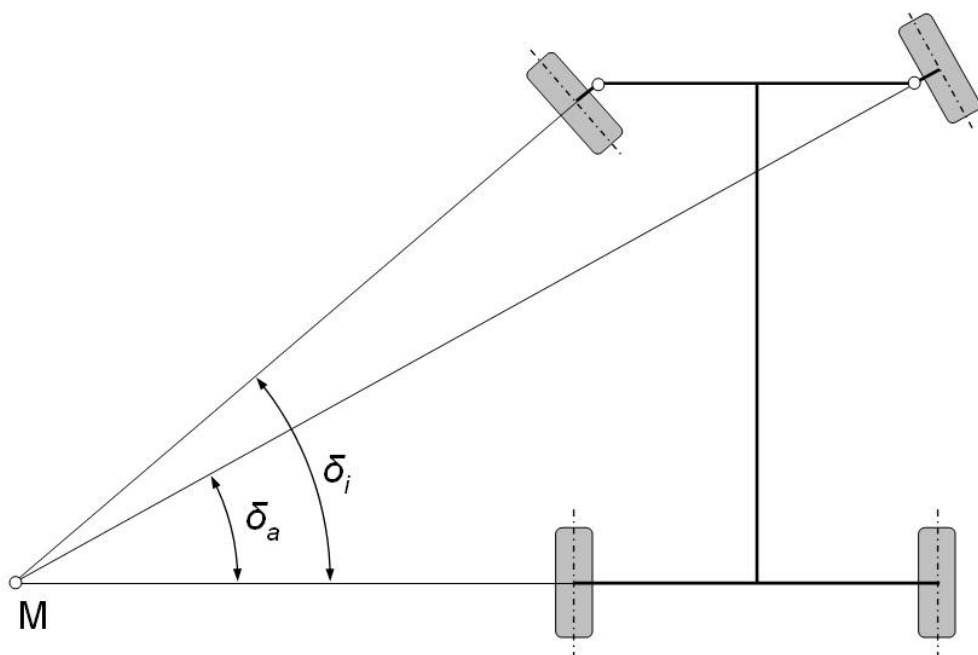


Figure 4.23 Ackermann condition [Rei00]

The optimization of the steering kinematics is carried out by the use of the kinematics module of CATIA. The results are visualised in Excel. Basis for the investigation is the front suspension described in chapter 4.1. Due to the method of simulation, forces and resulting elastic deformations in chassis bushings are not considered. Still this shall be sufficient for a first evaluation of the steering kinematics.

A steering position in front of the wheel centre has two main advantages. One advantage is generally valid for all vehicle concepts. When the steering position is in front of the wheel centre the steering gear can be rigidly mounted to the vehicle. Together with the compliance of the rubber bushings in the wishbone, the outer front wheel will make an advantageous toe-out steering movement under lateral force in a corner. The self steering behaviour of the vehicle thus becomes more understeering, which is easier to control for

the driver. The second advantage of a steering position in front of the wheel centre is especially important for this vehicle concept. As the driver is positioned in the vehicle's centre, the x-position of the driver is not restricted due to the wheel houses, but due to the required leg room and the steering gear. Therefore the steering gear position shall be as far front as possible.

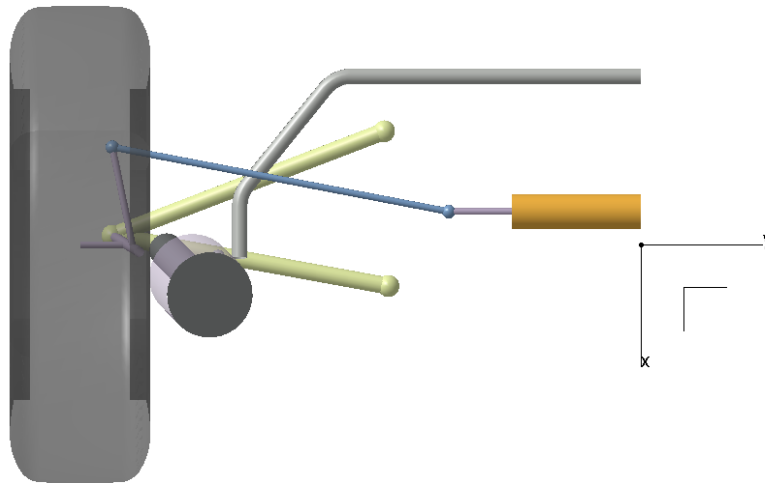


Figure 4.24 Kinematics model of front suspension

Figure 4.24 shows the kinematics model of the front suspension from top view. It can be seen that the steering gear position is in front of the wheel centre, but to satisfy the Ackermann condition it was necessary to move the steering gear relatively far back. The results of this optimization are shown in Figure 4.25.

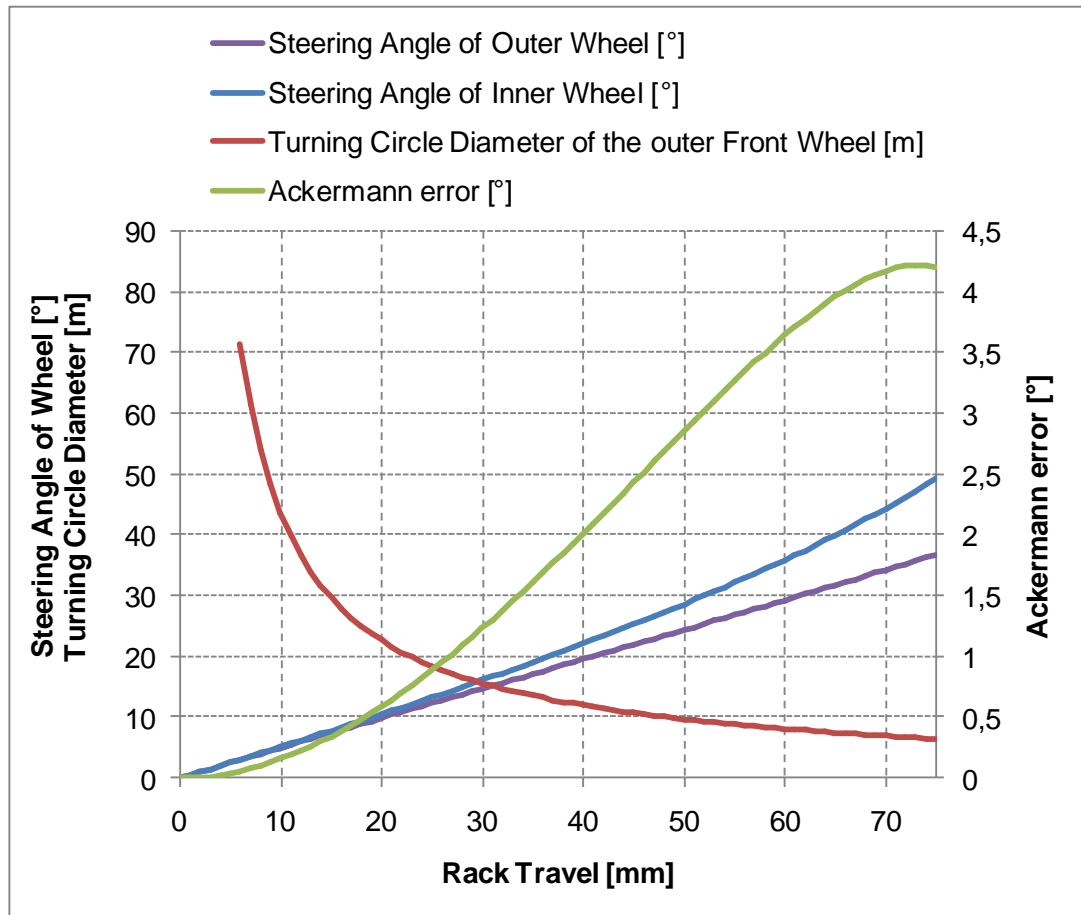


Figure 4.25 Steering kinematics

At a rack travel of 70 mm the inner wheel has a steering angle of 44.5 deg and the outer wheel has a steering angle of 34.3 deg. With this inner wheel steering angle the Ackermann condition would be fulfilled with a steering angle of the outer wheel of 30.1 deg. The Ackermann error is therefore 4.2 deg. As to [Sto92] it is usual to realize the steering kinematics with an Ackermann error between 2 and 6 deg. This has the advantage that the turning circle diameter can be reduced by approximately 0.1 m per degree of Ackermann error. The resulting turning circle diameter of the outer front wheel is therefore 7 m instead of 7.4 m.

4.3.2 Steering wheel position / Steering uniformity

The steering wheel position is defined according to ergonomic requirements. The recommendations given in SAEJ1517 concerning the steering wheel angle A18 and the distance L7 (see Figure 4.26) are considered. A detailed description of the position of the driver and the steering wheel is given in [Mad11]. With this steering wheel position the target was now to define the steering column position with especial focus on the bending angles of the two universal joints.

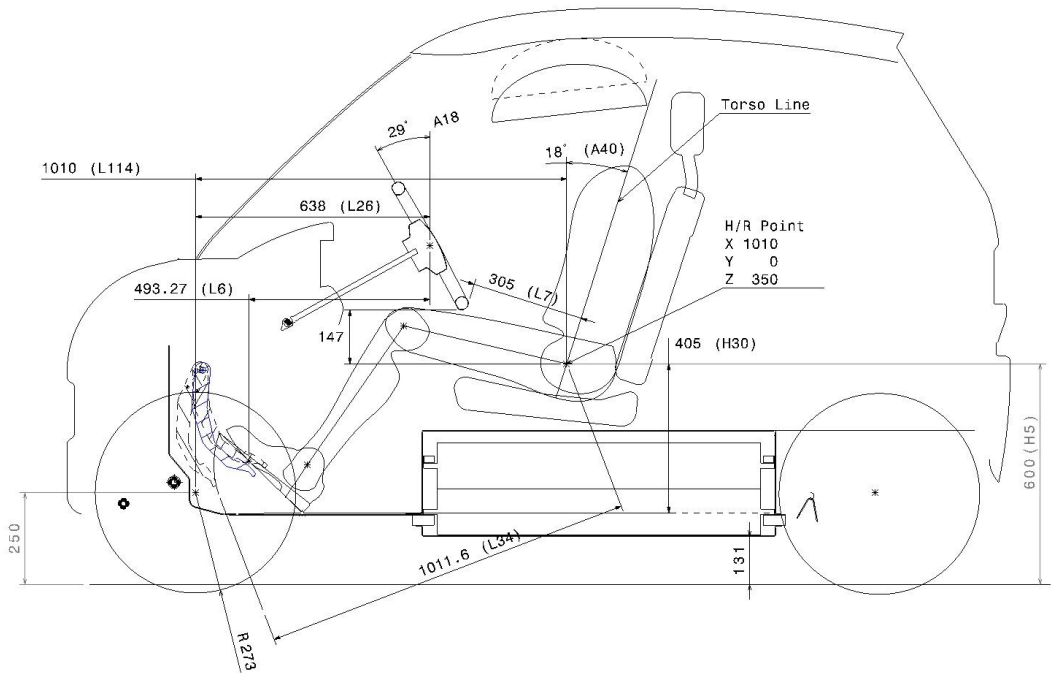


Figure 4.26 Seating position – steering wheel position [Mad11]

Depending on the angle of the input and output shaft, the universal joint will influence the rotational speed of the output shaft compared to the input shaft. Above angles of 15 deg this would result in a non-uniformity of the steering, which is detectable for the driver. Therefore it is necessary to use two universal joints so that the non-uniformity of the first universal joint can be equalized by the second one. Only the intermediate shaft (shaft 2 in Figure 4.27) will rotate in at a different rotational speed. To achieve the equalization the angle β_1 between shaft 1 and 2 must be the same as angle β_2 between shaft 2 and 3. The axis of each universal joint must be in the plane or respectively perpendicular to the plane of the two shafts that it connects [Bra01].

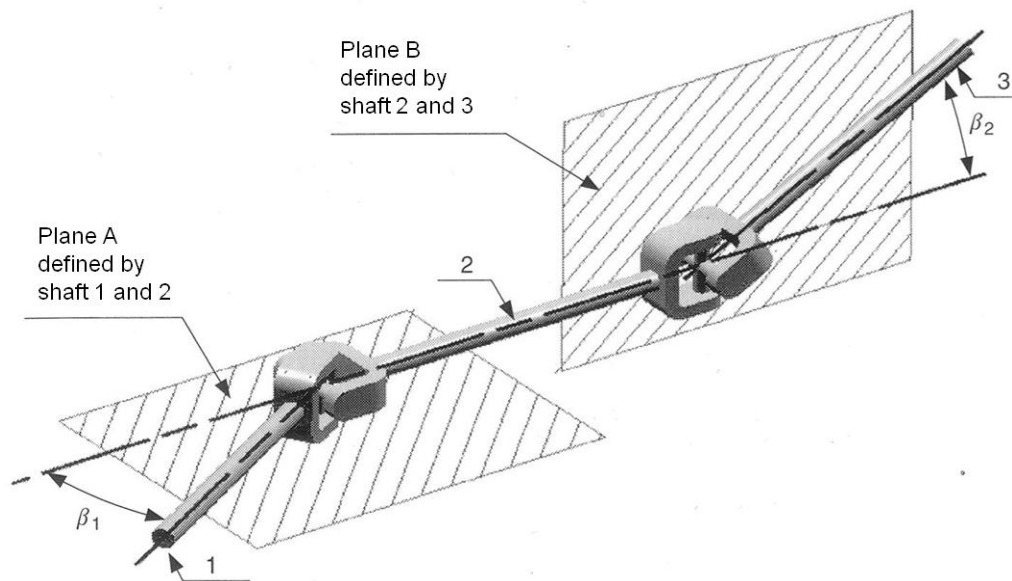


Figure 4.27 Equalisation of universal joint rotational non-uniformities [Bra01]

Additionally, the angle β generally should not exceed a value of 30 deg, because then the bending torque, which results from the change of the torque direction in the universal joint, becomes too high. The bending torque results in shear forces in the bearings and so due to elasticity and additional friction again to non-uniformities in the steering [Bra01].

The steering uniformity was investigated with two different steering designs. First it was investigated if the Tata Nano steering gear could be used. The Tata Nano steering gear is the only steering gear from the benchmark vehicles that fits to the front suspension kinematics. When an existing steering gear is used the position of the pinion and the angle of the input shaft are fixed. This allows very little optimization of the universal joint angles. As the Figure 4.28 shows the non-uniformity of the steering system with the Tata Nano steering gear is too big and is therefore not acceptable. Within 90 deg from the centred position of the steering wheel the steering ratio changes from 17.2 to 23.3. This means at 90 deg steering wheel angle the driver would need to steer 1.4 times more than in the centred position to achieve the same steering angle change at the wheels.

If the steering housing is a new part, the design can be optimized in a way that a perfect uniformity of the steering system is achieved. The still existing steering ratio change from the centred position to the maximum steering wheel angle is due to the steering kinematics of the suspension and not due to the non-uniformity of the steering column. The slow change of the steering ratio from a more indirect to a more direct steering has the advantage that at small steering wheel angles has a good directional stability and at high steering angles the steering effort is reduced.

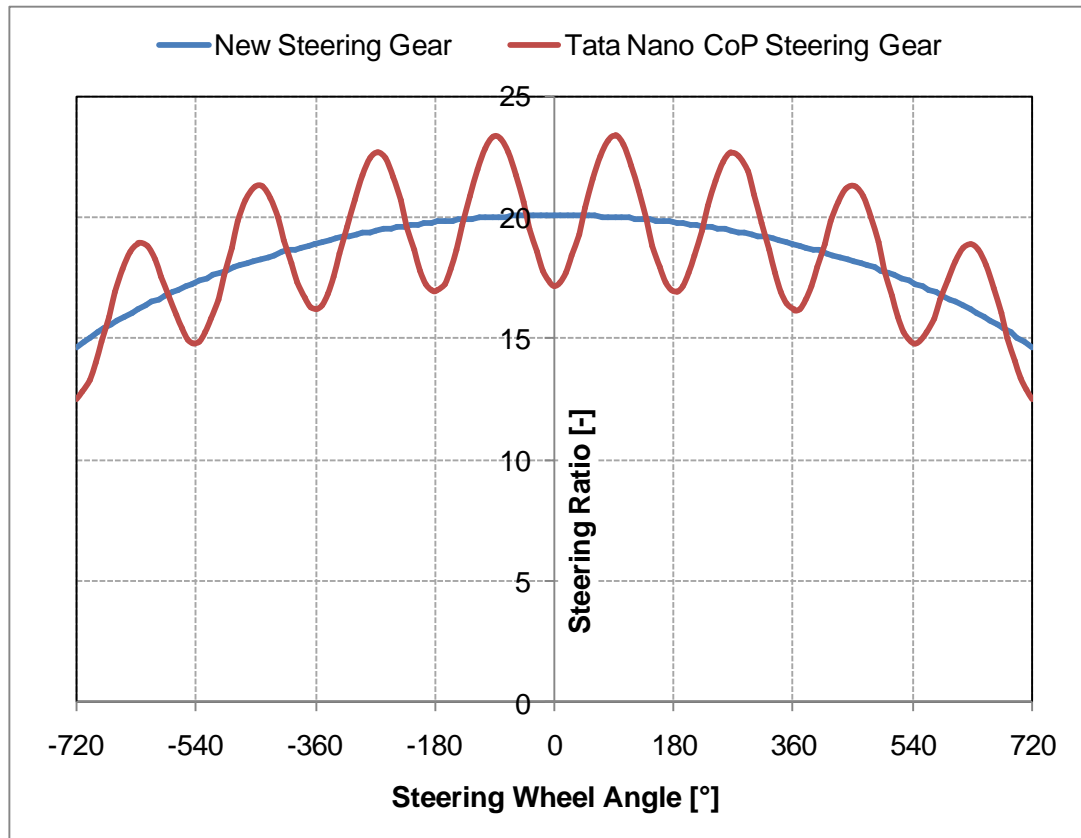


Figure 4.28 Comparison of two steering gears

4.3.3 Steering wheel torque

The target is that the vehicle gets a simple mechanical steering without power assistance. Therefore it is necessary to check how high the necessary steering forces might get and if this is acceptable for the driver and also fulfilling the European directive [70/311/EWG]. Usually the highest steering forces are necessary to steer the fully laden vehicle while standing. The main resistance comes from the drilling torque of the tires. In [Ril94] a formula (4-1) is given to estimate the drilling torque M_D of one tire:

$$M_{D \max} = \frac{1}{4} \cdot w \cdot \mu \cdot F_{z \text{ axle}} \quad (4-1)$$

w is the width of the tire, μ the grip coefficient, and F_z the front wheel load at gross vehicle weight.

$$F_{StW \max} = \frac{2 \cdot M_{D \max}}{i(\delta_{StW}) \cdot R_{StW}} \quad (4-2)$$

The maximum required actuation force $F_{StW \max}$ to steer the front wheels at standstill can be calculated with formula (4-2). Due to the steering kinematics (see Figure 4.28), the ratio $i(\delta_{StW})$ between the steering wheel angle and the steering angle at the wheels is depending on the steering wheel angle. The ratio is changing from 20.2 at zero steering

wheel angle (centre position) to 14.4 at the maximum steering wheel angle of 720 deg. The actuation force at the maximum steering wheel angle with a steering wheel diameter R_{SW} of 370 mm is 45.6 N. This is within the acceptable maximum actuation force of 150 N defined in [70/311EWG]. Around the centre position the required steering force is only 32.5 N. From these results it is estimated that the vehicle does not need to be equipped with a power steering. This argument is also supported by the fact that the SMART Fortwo I, which has a similar front axle load, had no power steering [SMA10a].

4.4 Brakes

For an electric vehicle it is necessary to differentiate between two different possible ways to reduce the vehicle speed. The conventional way is to use friction brakes at the front and rear wheels. Additionally it is possible to use the electric motor as a generator to produce a brake force at the driven wheels. This second way has the big advantage that most of the kinetic energy, which is usually transformed into heat at the friction brakes, can be stored to the battery. The recuperation reduces the energy consumption of the vehicle and increases range. Therefore the recuperation brake shall be used as often as possible. But due to the limited motor/generator power, due to the grip limit of the driven wheels, and also due to the battery, which might be fully charged and cannot take up more energy, the recuperation brake performance is limited. Thus a conventional friction brake, which fulfils all the legislative requirements as a standalone brake system, is still required.

4.4.1 Recuperation brake

The maximum deceleration, which is possible with the recuperation brake is depending on the maximum power and torque of the motor and on the grip coefficient between the tire and the road. At a high grip coefficient the maximum motor torque is limiting the deceleration at low speeds (constant deceleration until 20 kph) and at speeds above 20 kph the maximum motor power is limiting the deceleration (see Figure 4.29). At a low grip coefficient and at low speeds the limiting factor is not the motor torque, but the grip. To avoid locking of the wheels, it is important that the motor torque is reduced. This is especially important, when the rear wheels are driven like in the E-MILA Student, to avoid destabilized vehicle behaviour. Therefore it is necessary to have wheel speed sensors to detect a high wheel slip. As the transmission only has one fixed gear it could be investigated, if the wheel speed sensors at the rear wheels could be saved, because the motor speed is known anyways from the motor control. But such an investigation is too much into detail to be covered in this thesis.

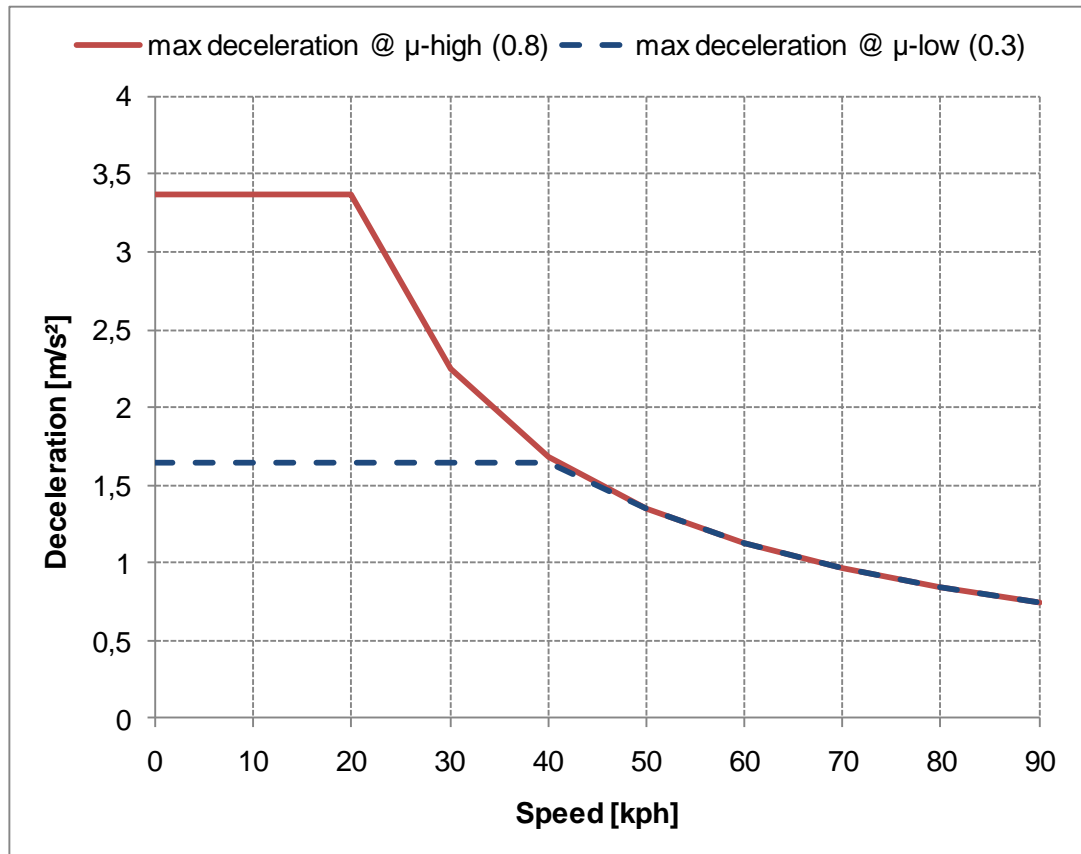


Figure 4.29 Maximum deceleration with recuperation brake

As a figure in [Hei08] shows, most of the braking manoeuvres occur at decelerations lower than 3 m/s². This is also the case for the NEDC, of which the maximum deceleration is 1.39 m/s² [ECE-R101]. So at low speeds during city driving it will be possible to get along with regenerative braking in most of the cases. Only at higher speeds due to the low motor power it will be necessary to use the friction brake more frequently.

To actuate the recuperative brake it was decided to use a comparably simple technical solution. The accelerator pedal, which must be an electronic pedal anyways, has two different pedal force characteristics depending on the stroke. A suggestion of the characteristics is shown in Figure 4.30. For the definition of the force level, figures given in [Hei08] were used.

The recuperation is done in a pedal stroke from 19 mm (0%) to 0 mm (100% recuperation) (see Figure 4.30). From 21 mm to 50 mm the accelerator pedal is used in its conventional sense to define the motor traction torque. Of course the dependency does not need to be linear and can also be progressive. This needs to be defined later in series development.

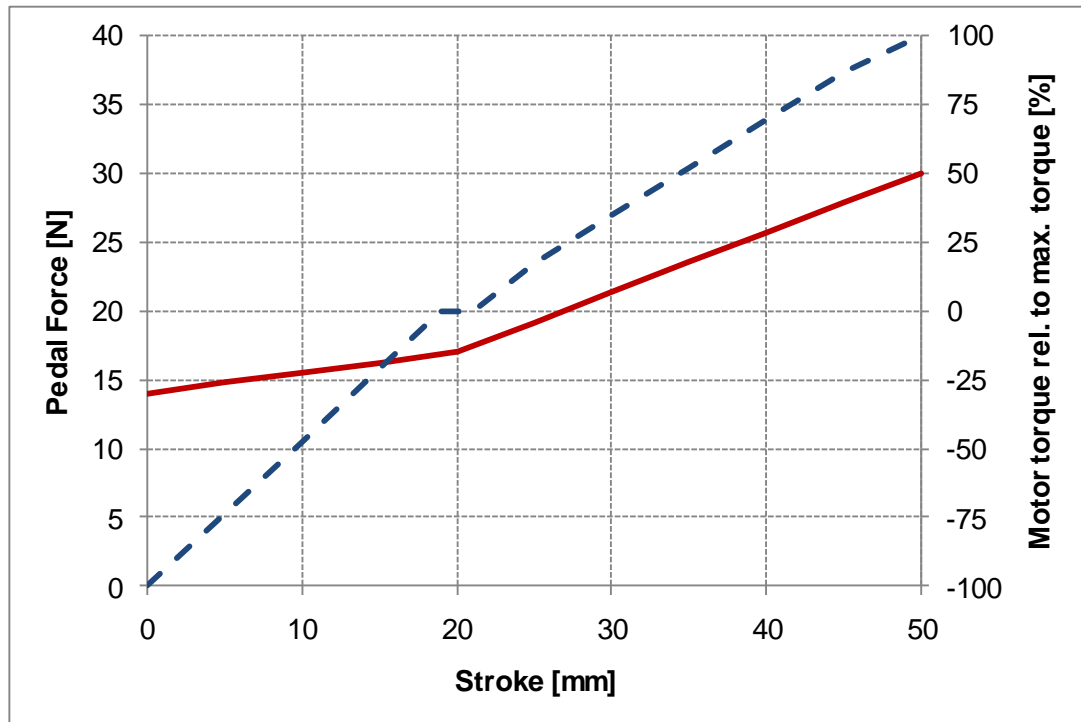


Figure 4.30 Accelerator pedal force characteristics

4.4.2 Friction brake

For an L7e class vehicle the friction braking system must fulfil the same requirements as for an M1 class vehicle [Mad11]. The requirements are described in the EU directive [71/320 EEC] and in the ECE regulation [ECE-R13]. Here only the most important requirements from the directive and the regulation are described.

Passenger vehicles must have 3 different braking systems, a service-, a secondary- and a parking braking system, which may have common components. And they must have at least 2 mutually independent control devices.

The apportioning of braking force among the individual axles is prescribed (see chapter 4.4.3). When the service- or secondary braking system is actuated it is important that, up to a deceleration of 0.8 g the wheels of the front axle must always lock before the wheels of the rear axle, for driving stability reasons.

A dual circuit transmission is able to fulfil the requirements of the law regarding the service- and the secondary braking system. According to DIN 74000 there are 5 possible variants. Type II (scheme a in Figure 4.31) and type X (scheme b in Figure 4.31) are the variants used in modern cars. Compared to the others their installation effort is smaller and due to the lower number of parts and sealings also their failure probability is lower. Basically Type II is used for vehicles with a higher rear axle load and type X for vehicles

with higher front axle load, to achieve the requirements of the directive and the regulation concerning the secondary braking system performance [BOS07]. Although the E-MILA Student has a neutral to rather rearward weight distribution, it was decided to use the X-type distribution pattern because of the short wheelbase and the resulting high dynamic wheel load change to the front while braking.

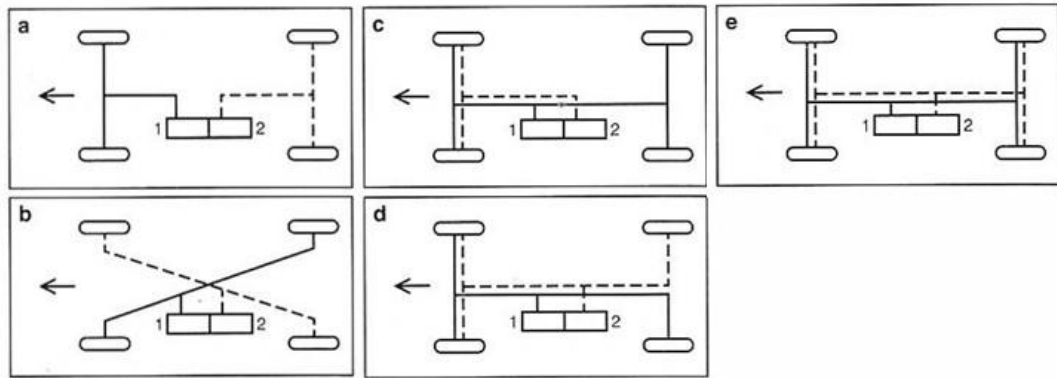


Figure 4.31 Brake circuit configuration [BOS07]

In the following the brake components and the targets concerning the E-MILA Student are described.

Wheel brakes

The benchmark investigation in chapter 4.1.1 and 4.2.1 showed that all investigated vehicles, except the Tata Nano, which has drum brakes at the front and the rear axle, are equipped with disk brakes for the front wheels and drum brakes for the rear wheels. Based on the following reasons it was decided to also use disk brakes for the front and drum brakes for the rear wheels in the E-MILA Student:

- Drum brakes have a cost advantage, but it is not very high (see chapter 5.1.1)
- It is assumed that simply for marketing reasons to sell the vehicle in Europe, a disk brake on the front axle is required.
- The proportioning and the friction uniformity of a disk brake is better than a drum brake. This is especially relevant on the front axle, because brake force differences between the left and the right wheel would result in a steering torque [Hei08].
- As an option the vehicle shall be equipped with ABS or ESP. For the brake control systems it is also important that the brake friction coefficient is constant [Hei08].

As described above the wheel brakes shall be disk brakes at the front and drum brakes at the rear wheels. To save investment costs and to profit of economies of scale the wheel brakes shall be carried over from a high volume production car. Besides cost of course the weight of the parts is important to consider. Table 4.4 shows a comparison of different wheel brake system weights from existing production cars. For comparison also the weights of the Tata Nano wheel brakes are listed, although these components are not suitable for the E-MILA Student (see above). Additionally to weight and costs also the size of the wheel brakes, especially the size of the disk brake, is relevant. The drum brake usually fits in every common wheel size, but the disk brake must be fitted to the smallest wheel size. Therefore for every disk brake also the smallest wheel size that can be mounted is given in the table. The wheel size is estimated from the brake disk size.

Table 4.4 Benchmark wheel brake systems, data from [A2M10]

		Fiat Panda 1.2	Smart ForTwo I/II	Suzuki Alto 1.0	Kia Piccanto 1.1	Tata Nano 0.6
Wheel brakes front	Type	Disk	Disk	Disk	Disk	Drum
	Size	13"	15"	13"	13"	12"
	Weight	14.3kg	na	15.8kg	16.8kg	13.6kg
Wheel brakes rear	Type	Drum	Drum	Drum	Drum	Drum
	Weight	9.3kg	na	12.3kg	13.9kg	8.0kg

The benchmark shows that the Fiat Panda disk brake has the right size and that the weight of wheel brakes is the lowest (despite of the Tata Nano). But the wheel brakes of the Fiat Panda are still oversized for the E-MILA Student as the Fiat has a kerb weight of 953 kg compared to 550 kg and a gross vehicle weight of 1305 kg compared to 800 kg [FIA10]. A weight optimized solution would have to be designed especially for the E-MILA Student. It was also considered to use brakes from an L6e category vehicle ("Mopedauto") like the Aixam Roadline, but the brakes of such a vehicle are too weak for the E-MILA Student. The kerb weight of the Aixam is only 380 kg and the gross vehicle weight is 675 kg [AIX10]. A test drive with the Aixam showed that the brakes are even too weak for this low weight. To lock the wheels during braking was hardly possible, even with a very high pedal force. Therefore it was decided to accept the higher weight of the Fiat Panda brakes and use this wheel brakes for the further concept investigations.

Brake actuation

The vehicles in the benchmark, except the Tata Nano, have a vacuum brake booster as standard equipment. The vacuum booster itself is a relatively simple mechanical part, which is used in almost every passenger vehicle. It is therefore a mature

technology produced in a high volume and would not contribute extensively to the vehicles cost and weight. But as the E-MILA Student has an electric drive and no internal combustion engine, it would be necessary to install an electric driven vacuum pump for the brake booster. Such a pump is only produced in a low volume for some electric and hybrid vehicles and is therefore expensive. The price for the pump is estimated with EUR450.- from MAGNA STEYR purchasing department. Thus the target is to design the brake system that can be actuated without a brake booster.

The master cylinders of the benchmark vehicles are designed to work with a brake booster and therefore do have too big piston diameters. To have the chance to find a suitable master cylinder in the shelf of a brake supplier, it was taken care that a common piston diameter was used.

The brake pedal used for the package was taken from the Tata Nano. The bracket to support the brake pedal and hold the brake switch and mount them to the fire wall will need to be a new designed part.

Important for the brake pedal positioning is the ergonomics for the driver and that there is enough space for the pedal travel also in case if one brake circuit fails. The simulation program (see chapter 4.4.3) calculates the maximum possible pedal travel, when the maximum stroke is limited by the master cylinder and not by the brake pedal and the firewall or the carpet on it. Figure 4.32 shows the brake pedal in design position and in worst case position (pedal with dotted lines) at maximum master cylinder stroke.

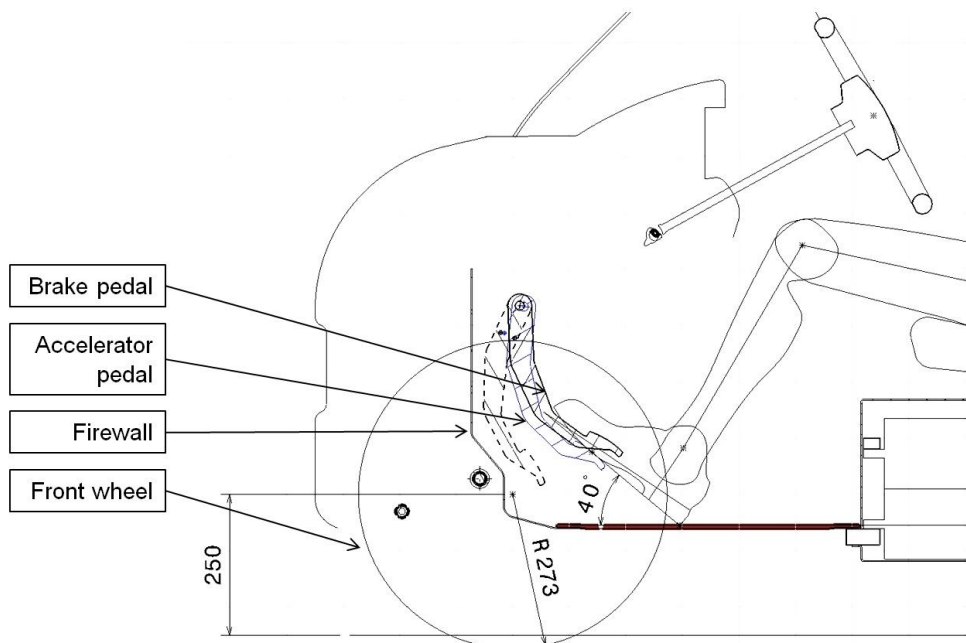


Figure 4.32 Brake pedal position

Brake force limiter

The simulation (see chapter 4.4.3) shows that for the rear axle a brake force limiter is necessary. As there is no big difference between laden and unladen rear brake force, a simple pressure dependant brake force limiter can be used. The limiter shall reduce the brake force on the rear axle starting from a threshold pressure of 11 bar with a factor of 0.35.

ABS / ESC

The electronic stability control system (ESC) is mandatory in Europe for M1 cars since the 1st of November 2011 [SPI11]. For L7e vehicles there is no regulation concerning brake control systems [Mad11]. But as wheel speed sensors are necessary to control the wheel slip during regenerative braking anyways, and as ABS and especially ESC essentially contribute to the vehicles active safety, it makes sense to consider these systems for the vehicle. But to stay within the cost targets it is decided to offer ABS or ESC as optional equipment.

4.4.3 Brake simulation

At MAGNA there is a simulation tool available which runs in Matlab/Simulink and which can be used for a basis brake system design. The parameters given in the annex in Table A.1 define the necessary input for the simulation. The simulation was done for several reasons:

- Target is to carry over the brake system parts from an existing vehicle. Thus it was necessary to investigate which parts will fit and which parts need to be new.
- Define the parameters for the brake force limiter for the rear axle
- Investigate if a sufficient brake performance can be achieved without a brake booster for service- and secondary brake function.
- Calculate the maximum pedal travel at maximum master cylinder stroke.

The brake force diagram shows the vehicles deceleration in dependency of the front and rear brake force. The ideal brake force distribution shows the distribution at which the grip coefficient of the front and rear axle is equally used. According to the regulation [ECE-R13] the installed brake force distribution must always be below the ideal distribution until a deceleration of at least 0.8 g. In that case the grip coefficient of the rear axle is used less and thus the wheels at the front axle lock before the wheels at the rear axle. This ensures a stable braking behaviour. For brake performance reasons (e.g. stopping distance) it is

important that the installed distribution is as close as possible to the ideal distribution [BOS07].

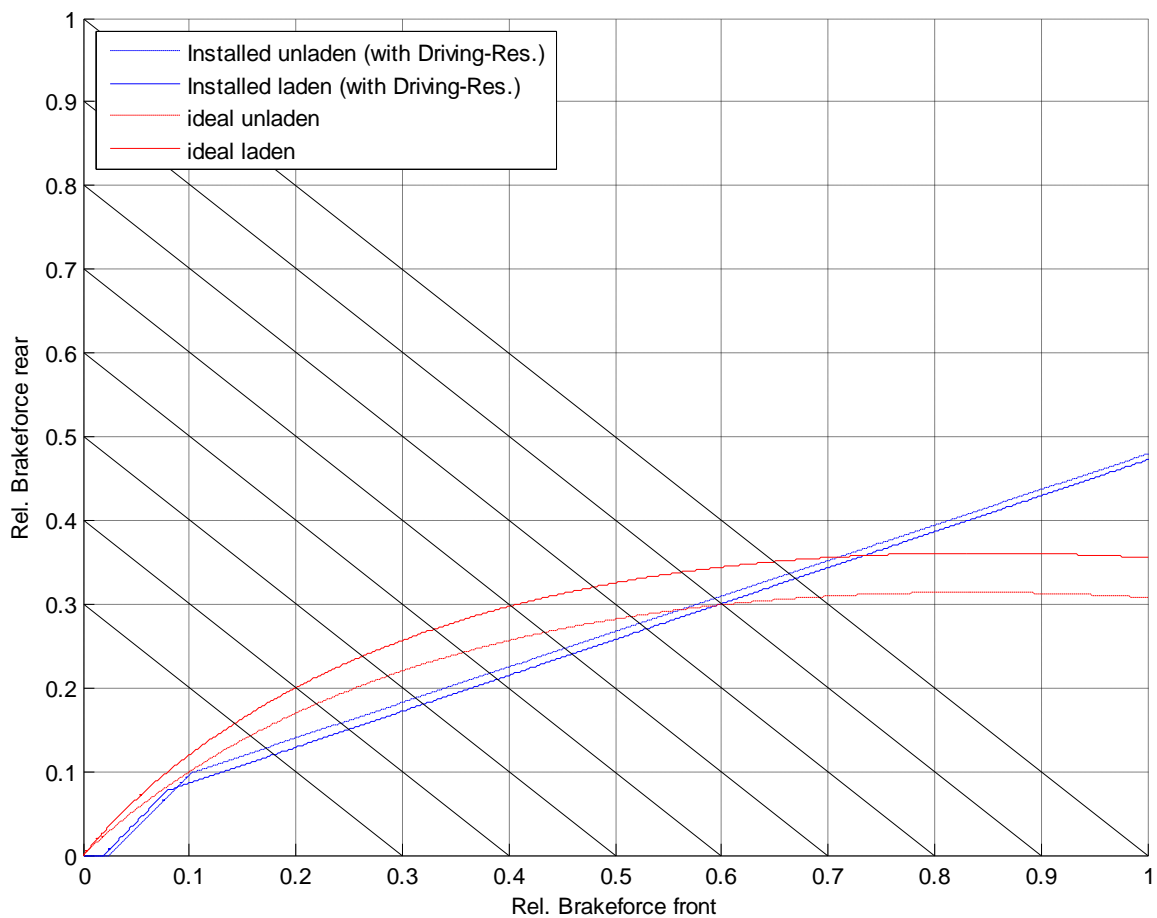


Figure 4.33 Brake force distribution

Figure 4.33 shows that it is possible to use the wheel brakes of the Fiat Panda and that it is necessary to use a pressure dependant brake force limiter.

The brake tests for the brake performance of the service brake required in [71/320 EEC] and [ECE-R13] require a mean fully developed deceleration of 5.8 m/s^2 with a maximum actuation force (at the brake pedal) of 500 N. Figure 4.34 shows the brake performance at the type O test from 80% of the maximum vehicle speed, which is 72 kph in case of the E-MILA Student. The stopping distance is 24.9 m (41.7 m would still be acceptable) and the mean full deceleration is 8.6 m/s^2 . These results do not only fulfil the law, but are also good results for small passenger vehicles. The brake system for the E-MILA Student therefore does not require a brake booster.

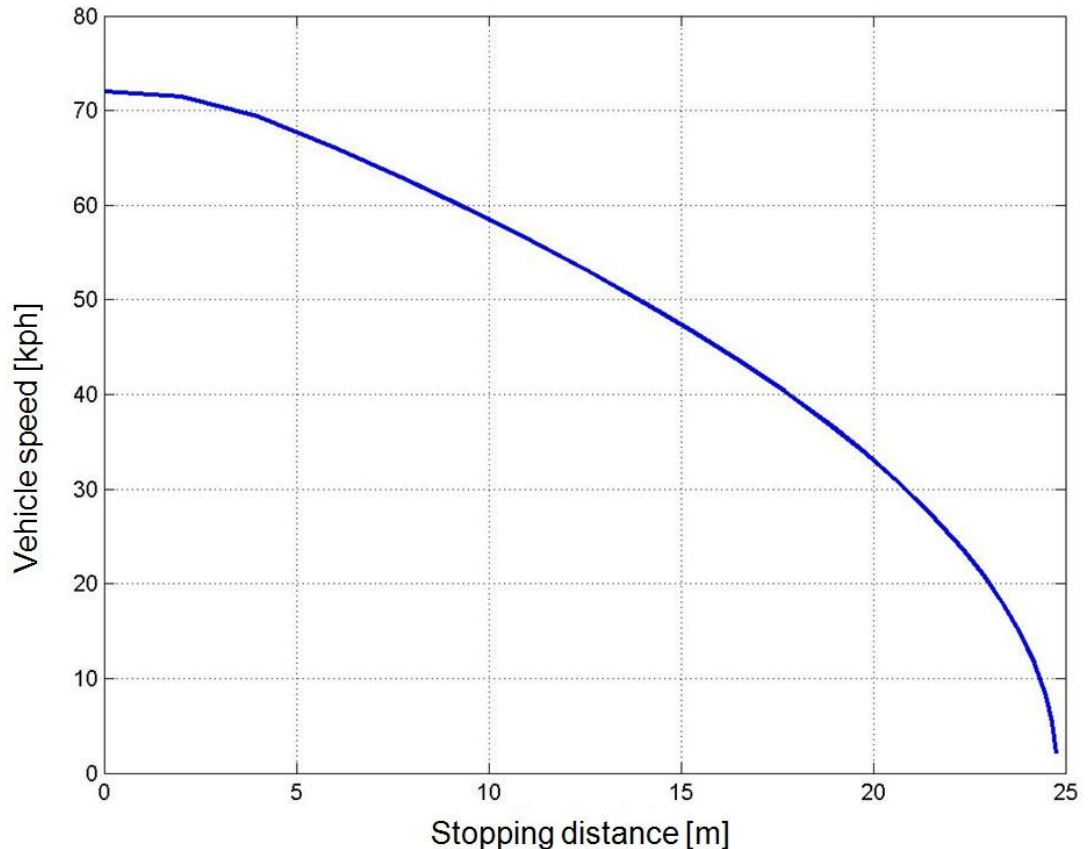


Figure 4.34 Vehicle brake performance

4.5 Tires

The tire size needs to be defined in a very early stage of the concept phase. On the one hand it is an essential parameter for the vehicle styling. On the other hand the tire size together with the suspension kinematics is defining the required space for the wheel house, and thus limiting the space for the passenger compartment.

For the styling and also for a good rolling resistance a large outer diameter of the tire and the rim would be of advantage. But large wheels are heavy and expensive which contradicts the main targets of the vehicle. The influence of the tire size on the rolling resistance is not very strong. An increase of 1cm in diameter improves the rolling resistance coefficient with 1%. To compare an increase of tire pressure of 0.05 bar or an increase of the ambient temperature of 1.7 K has the same effect [MIC03]. Therefore it was decided to use smaller tires in the common dimension 155/70R13 for the standard equipment, this has the advantage that the tire is comparably cheap and that the right tire can be chosen from different premium manufacturers. To use the “right” tire has a bigger effect on the rolling resistance than the tire size. A so called “green tire” can have a low

rolling resistance coefficient of 0.0085 whereas a “black tire” will have a rolling resistance coefficient of 0.012 [MIC03]. The difference is almost 30% less rolling resistance.

Another important advantage of the smaller tires is the lower weight and lower rotational inertia. The lower inertia of the smaller tires additionally reduces the advantage of the bigger tires concerning the fuel economy.

5 Vehicle Integration of Components

5.1 Fulfilment of vehicle targets

The package and the function of the selected components in the vehicle are described already in the chapters 4 and 5. This chapter focuses on the important targets on cost and weight of modules and components.

5.1.1 Costs

The target costs were defined on the level of 3 major modules (drivetrain, battery, and chassis) by Lukas Wechselberger [Wec11]. To define the target costs he used the method of quality function deployment (QFD). With this method the target costs for the full vehicle are split up to the modules, by the function they fulfil and the value of these functions for the customer. The target costs for the vehicle are derived from a top down approach from the estimated price a customer is willing to pay for the vehicle. The estimated price for the vehicle including the battery and taxes is EUR 15,400.-. The details for the price estimation and break down are explained in [Wec11].

The actual costs were estimated with the help of the MAGNA purchasing department, by comparing the components and modules to components and modules from other similar projects. The resulting price is a very rough estimate. The following assumptions are made for the price estimation:

- SOP of the vehicle is 2013
- Production life cycle is 6 years
- Volume average 10,000 per year (60,000 in total)

In the interest of readability the part number is not given in the tables that list the component costs. The part numbers for the components can be found in the weight tables.

Table 5.1 Drivetrain modules and components costs

Description	Pcs	Part price	Investment Costs	Part costs per car incl. Invest costs	Comment
Electric Drive Assembly	1			€ 1,655.-	MAGNA Powertrain MEA Class 1 Layshaft [MAG10b]
Electric Motor	1	€ 1,000.-	€ 2,000,000.-	€ 1,033.-	
Gear Box i=13	1	€ 580.-	€ 2,500,000.-	€ 622.-	incl. differential
Assy Drive Shaft	2	€ 20.-	€ 65,000.-	€ 41.-	Target costs incl. in Electr. Drive Assembly
HV Components				€ 1,625.-	High Voltage ECUs, VCU and HV-Cables
Inverter	1	€ 1,400.-	€ 3,000,000.-	€ 1,450.-	MAGNA E-Car Single Inverter (incl. DC/DC Converter) [MAG10c]
Charger 3.3kW	1	incl. above		€ 0.-	MAGNA E-Car 3.3kW Charger [MAG10d]
DC/DC Converter	0			€ 0.-	Component incl. in inverter (no seperate part)
HV Cable	1	€ 200.-		€ 0.-	
Charging Socket	1	€ 65.-		€ 65.-	
Vehicle Control Unit	1	€ 110.-		€ 110.-	only hardware, software incl. in MSF vehicle development costs see [Wec11]

The total actual costs of the drivetrain components is EUR 3,321.- which is 66% higher than the target costs of EUR 2,000.-.

Table 5.2 Battery module and components costs

Description	Pcs	Part price	Investment Costs	Part costs per car incl. Invest costs	Comment
Battery Assy	1	€ 4,338.-	€ 6,275,000.-	€ 4,442.-	
Battery Frame	1			€ 0.-	incl. in battery module
Upper Housing	1			€ 0.-	incl. in battery module
Lower Housing	1			€ 0.-	incl. in battery module
HV Distribution Unit	1	€ 400.-	€ 275,000.-	€ 405.-	
HVDU Cover	1			€ 0.-	Costs incl. in HVDU
Battery Module 10 Cells	6	€ 656.-	€ 6,000,000.-	€ 4,038.-	Costs incl. frame and housing

The total actual costs of the battery module is EUR 4,338.-. The costs are mainly influenced by the battery cell costs, which decline in the next years, due to production and material improvements (see Figure 5.1). For the cost calculation the estimated price for the battery is EUR 350.-/kWh. At the SOP in 2013 the price will not be down at this level, but during the 6 years of production until 2018 it is estimated that the price will drop even lower. Thus a price of EUR 350.-/kWh is a reasonable average. But with this battery price the total cost of the battery module does not meet the target of EUR 3,605.-.

The target would be met with a battery price of EUR 275.-/kWh as an average over the production period from 2013 to 2018. But this target does not seem to be realistic (compare Figure 5.1).

Table 5.3 Chassis modules and components costs part 1

Description	Pcs	Part price	Investment Costs	Part costs per car incl. Invest costs	Comment
Mc Pherson Front Axle	1	€ 180.-	€ 1,800,000.-	€ 216.-	
Sub Frame	0			€ 0.-	directly connected to vehicle frame
Knuckle left	1			€ 0.-	
Knuckle right	1			€ 0.-	
Wheel Hub Bearing	2			€ 0.-	
Wishbone	1	incl. above		€ 0.-	incl bushings and supporting ball joint
Wishbone	1			€ 0.-	incl bushings and supporting ball joint
Assy Suspension Strut	1			€ 0.-	
Assy Suspension Strut	1			€ 0.-	
Anti Roll Bar	1		€ 380,000.-	€ 6.-	
Stabilizer Link	2			€ 0.-	Investment costs incl. in costs for anti roll bar
Assy Twist Beam Axle	1			€ 161.-	
Weld Assy Twist Beam Axle	1	€ 80.-	€ 2,100,000.-	€ 115.-	
Wheel Bearing Unit	2	€ 10.-		€ 20.-	
Wheel Bearing	2	incl. above		€ 0.-	
Wheel Hub	2			€ 0.-	
Spring	2	€ 5.-	incl. in dev. costs for axle	€ 10.-	
Damper	2	€ 8.-		€ 16.-	
Assy Steering System	1			€ 168.-	
Rack and Pinion Steering	1	€ 80.-	€ 500,000.-	€ 88.-	
Tie Rod	2			€ 0.-	Weight incl in rack and pinion steering
Steering Column	1	€ 60.-		€ 60.-	
Steering Wheel	1	€ 20.-		€ 20.-	
Assy Wheel 155/70R13	4	€ 48.-		€ 192.-	
Assy Wheel 155/70R13 Alloy	0	€ 60.-		€ 0.-	Optional equipment alloy wheel
Tire 155/70R13	4	€ 35.-		€ 140.-	MICHELIN Energy Saver
Wheel 4,5Jx13 ET35 Steel	4	€ 13.-		€ 52.-	
Wheel 4,5Jx13 ET35 Alloy	0	€ 25.-		€ 0.-	Optional equipment alloy wheel

Table 5.4 Chassis modules and components costs part 2

Description	Pcs	Part price	Investment Costs	Part costs per car incl. Invest costs	Comment
Braking System				€ 189.-	
Master Braking Cylinder	1	€ 15.-		€ 15.-	Without brake booster
Assy Hand Brake Lever	1	€ 22.-	€ 40,000.-	€ 23.-	Incl cables
ABS System	0	€ 130.-	€ 900,000.-	€ 0.-	Incl sensors, optional equipment
Brake Booster (optional)	0	€ 25.-		€ 0.-	Optional equipment
Electric Vakuu Pump (opt.)	0	€ 450.-		€ 0.-	Optional equipment
Brake Disk	2	€ 10.-		€ 20.-	
Calliper	2	€ 20.-		€ 40.-	
Brake Pads front	4	incl. above		€ 0.-	
Brake Drum	2	€ 20.-		€ 40.-	
Brake Baking Plate	2	incl. above		€ 0.-	
Brake Pads rear	4	incl. above		€ 0.-	
Brake Cylinder	2	incl. above		€ 0.-	
Brake Lines and Hoses	1	€ 50.-	€ 100,000.-	€ 52.-	Incl brakets
Pedals incl. Braket				€ 43.-	
Accelerator Pedal inkl. Braket	1	€ 15.-	€ 100,000.-	€ 17.-	
Brake Pedal	1	€ 25.-	€ 50,000.-	€ 26.-	Price incl braket
Braket for Brake Pedal	1	incl. above		€ 0.-	

The total actual costs of the chassis components is EUR 969.- which is above the target costs of EUR 798.-.

The sum of the actual costs for the three major modules exceeds the target costs by EUR 2,225.-.

5.1.2 Weight

In cooperation with the other students of the E-MILA Student team a target weight for each module was set in order to achieve the target of 400 kg for the kerb weight of the vehicle without the battery. The 400 kg target is necessary for the homologation of the vehicle in the L7e category (see chapter 2.1.1). The process to find the target weight was as follows: All the modules necessary for the full vehicle were split up amongst the students according to their thesis topics. Every student made a list with estimated weights of his modules and components. The module weights of all modules were summed up to get the vehicle weight. As the resulting vehicle weight exceeded the 400 kg, it was agreed in the team for which modules the weight targets are reduced. The result was a weight target for each module.

In the tables below the actual weight of each module and its components is shown. Additionally the target weight for the modules is given in brackets. For the definition of the actual weight the weight of a component (e.g. the inverter) is taken from a datasheet if

available. The datasheet is then given as a source in the table. Else if no specific component is yet defined or no datasheet is available, the weight is estimated by a comparison of similar components in a benchmark using the benchmark platform A2Mac1 [A2M10]. The benchmarked vehicles are Fiat Panda 1.2, Suzuki Alto 1.0, Kia Piccanto 1.1 and Tata Nano 0.6.

Table 5.5 Drivetrain modules and components weights

Part Number	L/R	Description	Pcs	Weight pP [kg]	Weight (target) [kg]	Comment
204	001	Electric Drive Assembly	1		39 (40)	MAGNA Powertrain MEA Class 1 Layshaft [MAG10b]
	010	Electric Motor	1	25	25	
	030	Gear Box i=13	1	15	15	incl. differential
319	001	Assy Drive Shaft	2	4.5	9 (9)	
499		HV Components			18.6 (17.1)	High Voltage ECUs, VCU and HV-Cables
	010	Inverter	1	8.5	8.5	MAGNA E-Car Single Inverter (incl. DC/DC Converter) [MAG10c]
	020	Charger 3.3kW	1	7	7	MAGNA E-Car 3.3kW Charger [MAG10d]
	030	DC/DC Converter	0	0	0	Component incl. in inverter (no separate part)
	050	HV Cable	1	2.1	2.1	
	060	Charging Socket	1	0.3	0.3	
	101	Vehicle Control Unit	1	0.7	0.7	

The sum of the drive component weights is 0.5 kg higher than estimated. But for the electric drive assembly there is a weight saving potential. The MEA Class I Layshaft drive assembly is equipped with an electromechanical actuated parking pawl, as described in chapter 3.2.2 the parking pawl shall be actuated mechanical, which would save weight and costs. As the exact design and functionality of the mechanical parking pawl is not yet known, the electromechanical actuator is still considered in the weight and costs list. The estimated weight saving potential is 1 kg.

Table 5.6 Battery module and components weights

Part Number	L/R	Description	Pcs	Weight pP [kg]	Weight (target) [kg]	Comment
310	001	Battery Assy	1		145 (150)	
	010	Battery Frame	1	18	18	
	021	Upper Housing	1	2.5	2.5	
	022	Lower Housing	1	2.3	2.3	
	040	HV Distribution Unit	1	1.5	1.5	
	041	HVDU Cover	1	0.7	0.7	
	050	Battery Module 10 Cells	6	20	120	

The battery weight is 5 kg lower than estimated. But the battery weight is not that important as the weight is not considered in the limited kerb weight of the vehicle of 400 kg (see chapter 2.1.1). Nevertheless the battery weight is important for the driving performance and the range of the vehicle. The lighter battery helps to achieve the targets set in the chapter 2.2.

Table 5.7 Chassis modules and components weights part 1

Part Number	L/R	Description	Pcs	Weight pP [kg]	Weight (target) [kg]	Comment
301	001	Mc Pherson Front Axle	1		28.2 (28)	
	010	Sub Frame	0		0	directly connected to vehicle frame
	020	1 Knuckle left	1	2	2	
		2 Knuckle right	1	2	2	
	031	Wheel Hub Bearing	2	1.3	2.6	
	041	1 Wishbone	1	2.2	2.2	incl bushings and supporting ball joint
		2 Wishbone	1	2.2	2.2	incl bushings and supporting ball joint
	060	1 Assy Suspension Strut	1	6.2	6.2	
		2 Assy Suspension Strut	1	6.2	6.2	
	070	Anti Roll Bar	1	4	4	
	071	Stabilizer Link	2	0.4	0.8	Investment costs incl. in costs for anti roll bar
302	001	Assy Twist Beam Axle	1		18.4 (18.6)	
	010	Weld Assy Twist Beam Axle	1	10	10	
	030	Wheel Bearing Unit	2		0	
	031	Wheel Bearing	2	0.5	1	
	032	Wheel Hub	2	1	2	
	040	Spring	2	0.7	1.4	
	041	Damper	2	2	4	
303		Assy Steering System	1		10.7 (12)	
	010	Rack and Pinion Steering	1	5	5.5	
	030	Tie Rod	2	0	0	Weight incl in rack and pinion steering
	040	Steering Column	1	4	4	
	050	Steering Wheel	1	1.2	1.2	
304	002	Assy Wheel 155/70R13	4	11	44 (42)	
	005	Assy Wheel 155/70R13 Alloy	0	11.3	0	Optional equipment alloy wheel
	012	Tire 155/70R13	4	5.5	22	MICHELIN Energy Saver
	022	Wheel 4,5Jx13 ET35 Steel	4	5.5	22	
	023	Wheel 4,5Jx13 ET35 Alloy	0	5.8	0	Optional equipment alloy wheel

Table 5.8 Chassis modules and components weights part 2

Part Number	L/R	Description	Pcs	Weight pP [kg]	Weight (target) [kg]	Comment
306		Braking System			24.1 (25.6)	
	001	Master Braking Cylinder	1	0.5	0.5	Without brake booster
	010	Assy Hand Brake Lever	1	2.8	2.8	Incl cables
	020	ABS System	0	3	0	Incl sensors, optional equipment
	030	Brake Booster (optional)	0	2	0	Optional equipment
	040	Electric Vakuum Pump (opt.)	0	2	0	Optional equipment
	051	Brake Disk	2	3	6	
	052	Calliper	2	2.9	5.8	
	053	Brake Pads front	4	0.2	0.8	
	061	Brake Drum	2	2.3	4.6	
	062	Brake Baking Plate	2	0.3	0.6	
	063	Brake Pads rear	4	0.275	1.1	
	064	Brake Cylinder	2	0.2	0.4	
	070	Brake Lines and Hoses	1	1.5	1.5	Incl brakets
307	001	Pedals incl. Braket			3 (3)	
	002	Accelerator Pedal inkl. Braket	1	0.6	0.6	
	003	Brake Pedal	1	1.5	1.5	Price incl braket
	004	Braket for Brake Pedal	1	0.9	0.9	

The sum of the chassis components weight is 0.8 kg less than estimated. The reason for the good results of the estimation is that already for the estimation some benchmark investigation was done. With this result the weight limit of 400 kg for the kerb weight without batteries shall be achievable. Except other modules like the body frame, which is more difficult to estimate, has a higher weight than estimated.

5.2 Outlook for optimization potential

Of course there is optimization potential in the basic chassis components especially concerning weight. In some cases, as for instance for the wishbone, this potential is already roughly described in chapter 5. Still to really find the potential there, a more detailed investigation of all parts rear would need to be carried out. As this thesis shall provide a basic concept for a chassis-, drivetrain and energy storage layout for an electric city vehicle, this detailed investigation could not be provided here.

For the drivetrain components it is easier to find optimization potential concerning cost and weight. The inverter that is used for the vehicle is over dimensioned concerning power (see chapter 3.2.3). An inverter that fits perfectly to the vehicles requirements could not be found. As from [Rei10] there might be a suitable inverter in development, but detailed data was not available. If such an inverter is available in the future it will reduce

weight and costs. For the DC/DC converter it is the same case. The DC/DC converter integrated in the inverter has a constant power of at least 2.1 kW, which will not be needed for this vehicle, as there is for instance no electric power steering, no big multimedia equipment, no electric vacuum pump for the brake booster and so on. The exact required power would need to be calculated and then in case it is available the inverter could be equipped with a smaller DC/DC converter. As described in chapter 5.1.2 there is also weight and cost saving potential for the electric drive unit by using a mechanical instead of an electromechanical parking pawl.

The main optimization potential in the future can be hopefully found in the battery, as this is the heaviest and most expensive component in the vehicle. Main potential here will be the battery costs, but this will take time as Figure 5.1 shows. For the planned production start in 2013 there is not much hope that the real achievable battery price will be lower than the estimated price in chapter 5.1.1.

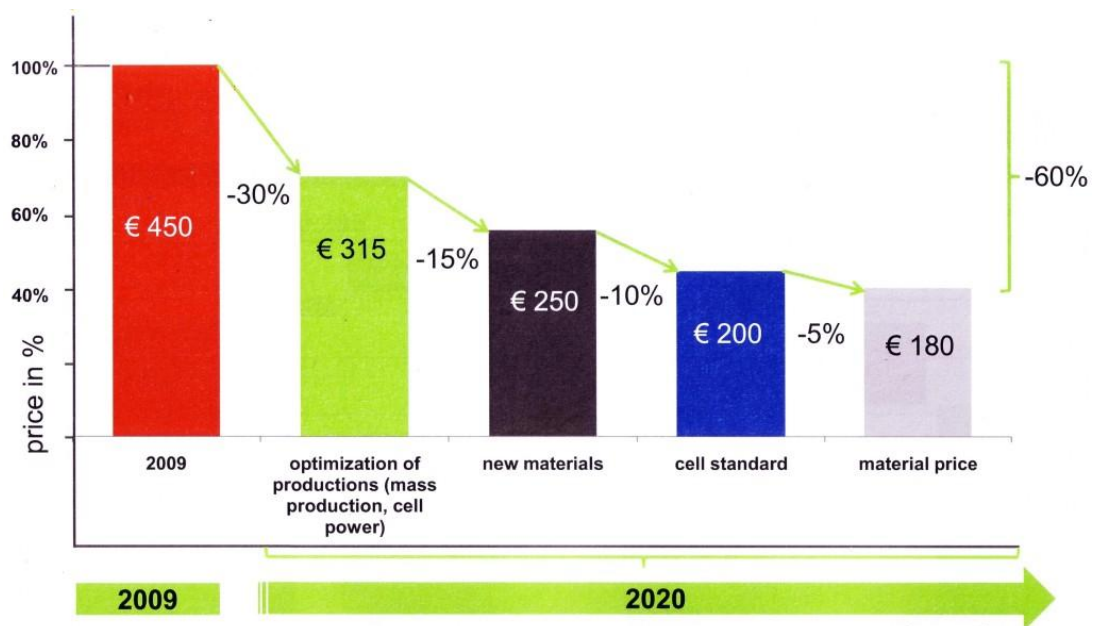


Figure 5.1 Battery price (supplier to OEM) development [Rei10]

6 Conclusion

This thesis shows the definition of a chassis, drivetrain and battery system layout for a small battery electric vehicle concept, which was designed from scratch. For the three major modules it is possible to achieve the technical targets defined by the vehicle specification. Besides the relevant functions like driving and braking performance, range, packaging and ergonomics also the weight target could be met. The result is a vehicle concept that perfectly fulfils the technical requirements. Within an outer length of only 2.55 m, which is the length of the first Smart Fortwo, and a vehicle weight of 400 kg (without batteries), it is possible to comfortably accommodate one driver and two adult passengers. The vehicle will have sufficient performance for convenient city driving.

Although the main focus was on low costs, when selecting or designing the components this important target could not be met. The main reason for that is the low estimated volume of 10,000 vehicles per year. Tooling and engineering costs therefore have a major impact on the part price. To avoid this it is necessary to carry over existing parts. Further this is only helpful in some cases, for instance for chassis parts, where parts can be used from high volume production vehicles. For the electric drivetrain components the problem is that the existing components are either not yet available or produced in a low volume. In the following paragraphs the results for the three major modules are summarized.

For the drivetrain it was possible to find existing modules like a motor-transmission module or an inverter that can be integrated into the vehicle. The problem is that the existing components often do not exactly fit the specifications. The inverter and the DC/DC converter that is integrated in the charger are oversized in terms of performance. Therefore these parts do not represent the best solution concerning size, weight and costs. Still it was possible to package the components into the vehicle without any negative impacts on the interior space. The weight target is only exceeded by a very small amount and this excess could be compensated by a weight reduction in the chassis parts. The overall weight target therefore is met. Concerning costs at present it will be cheaper to carry over the existing components than to develop new components solely for this vehicle. Nevertheless more suitable components might be available in the near future. Here it is worth keeping an eye on the market and doing further, more detailed investigations.

The battery module including battery cells, frame, housing and the HVDC needs to be newly designed to fit to the vehicle. Although the development and tooling costs are

comparably high, the pro rata investment costs account for only 2.4% of the part price. The battery cell price still has a major impact on the overall battery price. The battery costs besides the costs for the cells could be reduced to a minimum, because as the permanent discharge power is low, no complex battery cooling system is required. As a consequence the reduction of the battery price is more or less only a question of time (compare Figure 5.1).

The situation for the chassis modules is different, because there are a high number of different existing components that are produced in a high volume. Here the challenge was to find components that perfectly fit to the vehicle. For the wheel brakes and the wheels adequate existing parts could be found. In case of the front or rear suspension it was not possible to find existing modules that fit in the vehicle. The reason is that these modules have a big impact on the vehicle layout and vice versa. The layout of the vehicle is not common, because of the centrally positioned driver, the battery under the seats that influences the rear package and the small track width. Therefore it was only possible to carry over single parts like the Dacia Logan wishbone and not a whole module. The same is also valid for the steering system where the centrally positioned steering column requires a new steering gear. A drawback of the carryover parts like the wheel brakes of the Fiat Panda is that these parts are usually oversized because they are used in vehicles with higher weight. These parts are therefore heavier than required to fulfil their function in the E-MILA S. Nevertheless it was possible to meet the given weight target.

The results of the thesis showed that the idea of a small electric city vehicle, with a focus on a very low vehicle weight is worth following up. The vehicle weight has a significant influence on the energy consumption of the vehicle. Reducing the vehicle weight means reducing the energy consumption and thus reducing the required size of the battery, which again saves weight and costs. Saving 10 kg on the vehicle reduces the battery weight by 1 kg and the battery costs by EUR 25.-. Additionally it could be shown that due to the low vehicle weight a power steering and a brake booster are not required. As these are high price parts, the cost advantage for the full vehicle is significant. All in all it can be said that the light weight strategy is one step into the right direction of an acceptable market price for a battery electric vehicle.

Future investigations can be based on this feasible concept and focus on improving single components in detail. The main cost drivers are the battery and the drivetrain. The costs for the battery almost solely depend on the battery cells and can hardly be influenced. But the drivetrain components have a high cost savings potential. Further work should concentrate on the optimization and cost reduction of these components.

References

[70/156/EEC] Type-approval of motor vehicles and their trailers, council directive, 1970

[70/311/EEC] Steering equipment, council directive, 1970

[71/320/EEC] Braking devices, council directive, 1971

[A2M10] Internet source :

<http://www.a2mac1.com/AutoReverse/reversepart.asp?ProductType=2&ProductId=&Clientid=1>

visited 2010-11-23

[AIX10] Internet source: <http://www.aixam.co.uk/roadline.html>

visited 2010-11-02

[AMS10] Internet source: <http://www.auto-motor-und-sport.de/eco/spritsparpotential-leichtbau-ist-nicht-das-wichtigste-1478244.html>

visited 2010-09-30

[AUT10] Internet source: <http://www.autobild.de/artikel/volksauto-tata-nano-519741.html>

visited 2010-11-24

[BOS07] BOSCH, Automotive Handbook, Bosch, SAE 2007

[Bra01] Braess H., et.al.: Handbuch Kraftfahrzeugtechnik, Verlag Vieweg 2001

[BRU10] Internet source: http://www.brusa.biz/products/g_pa_k16129.htm

visited 2010-7-21

[Bie10] Biermann J., Scholz-Starke K.: Elektrofahrzeuge – Historie, Antriebskomponenten und aktuelle Fahrzeugbeispiele, Handbuch Elektromobilität, Verlag EW Medien und Kongresse GmbH 2010

[Can04] Canders W.-R., Wöhl-Bruhn H., Rius-Sambeat B.: Charakterisierung und gezielter Entwurf von Elektromotoren für Fahrzeugantriebe, 2. Braunschweiger Symposium "Hybridfahrzeuge und Energiemanagement" 2004

[Cha99] Chau K.T., Wong Y.S., Chan C.C.: An overview of energy sources for electric vehicles, Energy Conversion & Management 40 (1999)

[DIE10] Internet source: http://www.dieselnet.com/standards/cycles/ece_eudc.html

visited 2010-10-13

References

- [ECE-R 101] Emission, regulation, 2010
- [ECE-R13] Braking, regulation, 2010
- [EUR10] Internet source:
<http://www.eurosolar.at/Drucksorten/ElektroAuto%20Presse%20INFO.pdf>
visited 2010-11-10
- [FIA10] Internet source : http://www.alle-autos-in.de/flat/flat_panda_12_8v_ktb381.shtml visited 2010-12-26
- [Hei08] Heising B., et.al.: Fahrwerkhandbuch, Verlag Vieweg + Teubner 2008
- [Hir99] Hirschberg W.: Skript zur Vorlesung Fahrdynamik, FH Joanneum 1999/2000
- [ISO8767] Passenger car tyres - Methods of measuring rolling resistance, 1992
- [KFZ10] Internet source: <http://www.kfz-tech.de/Bilder/Kfz-Technik/Radaufhaengung/SmarrHAchse01.jpg>
visited 2010-11-26
- [Koe10] Köhler U.: Batteriesysteme für Elektro- und Hybridfahrzeuge, Handbuch Elektromobilität, Verlag EW Medien und Kongresse GmbH 2010
- [LEX10] Internet source: <http://www.lexus.de/hybrid/faqs.aspx>
visited 2010-11-10
- [Mad11] Madeshi P.: Homologation and packaging study of E-MILA Student, TU Graz, MSc Thesis, 2011
- [MAG06] MAGNA STEYR internal report on benchmark analysis of Suzuki SX4, 2006
- [MAG10a] MAGNA E-Car basic data sheet of 50Ah lithium-ion cell, 2010
- [MAG10b] MAGNA Powertrain internal report: 20100406 MEA Class I Definition DP, 2010
- [MAG10c] MAGNA E-Car internal report: ME Inverter DCDC Converter datasheet, 2010
- [MAG10d] MAGNA E-Car internal report: Charger&DCDC datasheet, 2010
- [MAG10e] MAGNA E-Car internal report: Description of bending beam battery module concept, 2010
- [Mat10] Mathoy A.: Grundlagen für die Spezifikation von E-Antrieben, MTZ 09/2010
- [MIC03] MICHELIN: The Tyre – Rolling resistance and fuel savings, Société de Technologie Michelin, 2003

References

- [Mut11] Muttumula V.: Study on recycling of an electric vehicle (E-MILA Student), TU Graz, MSc Thesis, 2011
- [Pre10] Preiss M.: Market Study for an electric city car (E-MILA-Student), TU Graz, MSc Thesis, 2010
- [PRI10] Internet source: <http://www.priuswiki.de/wiki/Hybrid-Batterie>
visited 2010-11-10
- [PSM09] Wechselberger L., et.al., MILA Student – MAGNA/PSM Project, Power Point Presentation presented at FSI 2009-09-24
- [Rei00] Reimpell J., Belzer J.: Fahrwerktechnik: Grundlagen, Verlag Vogel Fachbuch 2000
- [Rei10] Reif P.: MAGNA E-Car Systems – a new business unit, lecture notes: Management topics in automotive industry, TU Graz 2010
- [REV10] Internet source: <http://www.revaclub.com/reva-club-media-pack.pdf>
visited 2010-12-12
- [Ril94] Rill G.: Simulation von Kraftfahrzeugen, Verlag Vieweg 1994
- [Riz07] Rizzoni G., Cantemir C.-G.: Electric Motors for Hybrid Propulsion, FTZ Conference: Alternative Propulsion Systems for Automobiles, 2007
- [SAE83] Saeki N., Yamada N., Kojima R. : Japanese Minicars (Kei Jidosha) and Their Technical Characteristics, SAE Paper 830942, 1983
- [SMA10a] Internet source: http://www.alle-autos-in.de/smart/smart_fortwo_coupe_45_kw_mhd_ktb5001.shtml
visited 2010-11-02
- [SMA10b] Internet source : <http://www.reiseberichte.bplaced.net/auto-bahn-bus/sixti-smart-fortwo-coupe-mietwagen.html>
visited 2010-12-27
- [SPI11] Internet source : <http://www.spiegel.de/auto/aktuell/0,1518,612473,00.html>
visited 2011-01-21
- [Sto92] Stoll H. : Fahrwerktechnik : Lenkanlagen und Hilfskraftlenkungen, Verlag Vogel Fachbuch 1992
- [TAT10] Internet source:
http://tatanano.inservices.tatamotors.com/tatamotors/index.php?option=com_

- [whynano&task=experience&Itemid=303](#)
visited 2010-11-02
- [TEC10] Internet source :
http://www.tecchannel.de/pc_mobile/notebook/432097/akkus_notebook_lebensdauer_kapazitaet_ladezyklen_lithium_ionen_laufzeit/index3.html
visited 2010-12-16
- [THI10] Internet source:
<http://www.thinkev.at/preisetechnischdaten.php?m=preisetechnischdaten>
visited 2010-11-10
- [TOY10] Internet source :
http://www.toyota.at/innovation/design/concept_cars/prius_plugin/index.aspx
visited 2010-11-10
- [Wat10] Watzenig D.: LEISTUNGSFÄHIGE BATTERIEN – Schlüsselkomponente der Elektromobilität, ÖVK Vortrag TU Graz 2010
- [Wec11] Wechselberger L.: Concept for the development of an urban electric vehicle, TU Graz, MSc Thesis, 2011
- [WIK10a] Internet source: <http://en.wikipedia.org/wiki/Malaga> visited 2010-12-16
- [WIK10b] Internet source: <http://en.wikipedia.org/wiki/Oslo> visited 2010-12-16
- [Wil10a] Willberger J., Hirz M.: Energy Efficient Operation of In-wheel Motors for 4 Wheel driven Passenger Cars, FISITA 2010
- [Wil10b] Willberger J., Krischan K.: Untersuchung, Charakterisierung und Bewertung von Elektromotoren für deren Einsatz im Kraftfahrzeug, interner Bericht Institut für Fahrzeugtechnik, TU Graz 2010
- [ZAM10] Internet source: <http://www.zamg.ac.at/fix/klima/oe71-00/klima2000/daten/klimadaten/stm/16412.htm>
visited 2010-12-03
- [Zhu07] Zhu Z. Q., Howe D. : Electrical Machines and Drives for Electric, Hybrid, and Fuel Cell Vehicles, Proceedings of the IEEE, Vol. 95, No.4, April 2007

List of Figures

Figure 2.1 First vehicle layout – sideview [PSM09].....	7
Figure 2.2 First vehicle layout – top view [PSM09].....	7
Figure 2.3 Driving resistances at constant speed [BOS07].....	8
Figure 2.4 Vehicle speed influence on rolling resistance [MIC03]	9
Figure 2.5 Vehicle cross sectional area	11
Figure 2.6 Percentage of resistive forces in different driving cycles [MIC03]	12
Figure 2.7 Motor characteristic for driving performance calculation	14
Figure 2.8 Traction force diagram	15
Figure 2.9 Acceleration Performance (continuous torque).....	16
Figure 2.10 Acceleration Performance (peak torque – max. 30 sec).....	17
Figure 2.11 ECE 15 driving cycle [ECE-R 101]	19
Figure 2.12 EUDC for low powered vehicles [ECE-R 101]	19
Figure 3.1 Sketch drivetrain layout, side view and top view.....	23
Figure 3.2 Classification of alternating current machines [Bou07], [Riz07]	26
Figure 3.3 Idealized torque/power-speed characteristics [Zhu07]	27
Figure 3.4 Sketch of a simple 3-phase Switched Reluctance Machine [Zhu07].....	30
Figure 3.5 Motor characteristics compare [MAG10b].....	31
Figure 3.6 Motor and transmission in vehicle package	32
Figure 3.7 Package of high voltage ECUs.....	35
Figure 3.8 Energy and power demand for different drivetrain types [Koe10]	36
Figure 3.9 Performance of different cell types [Koe10]	37
Figure 3.10 Section cut of MAGNA battery module with 8 cells [MAG10e]	40
Figure 3.11 Package of 7 battery modules with 8 cells	41
Figure 3.12 Section cut of battery module with 10 cells	41
Figure 3.13 Battery frame with battery modules	42
Figure 3.14 Battery Housing.....	44

List of Figures

Figure 3.15 Weekly profile of the SOC	46
Figure 3.16 Battery capacity after 10 years (no cyclic aging)	47
Figure 3.17 Battery capacity (calendarical and cyclic aging)	48
Figure 4.1 Wheel load influence on brake / side force potential [Hir99]	52
Figure 4.2 SMART Fortwo I disk brake and steering knuckle	54
Figure 4.3 SMART Fortwo I wishbone	55
Figure 4.4 SMART Fortwo II steering knuckle and wishbone	55
Figure 4.5 Fiat Panda front suspension [A2M10]	56
Figure 4.6 Fiat Panda wishbone [A2M10].....	57
Figure 4.7 Tata Nano front suspension in vehicle [A2M10].....	58
Figure 4.8 Tata Nano front suspension without steering [A2M10]	59
Figure 4.9 CATIA kinematics model of front suspension	60
Figure 4.10 Wheel envelope front suspension	61
Figure 4.11 Front wheel space demand in wheel house.....	61
Figure 4.12 E-MILA S front suspension.....	62
Figure 4.13 Suzuki SX4 rear suspension [MAG06]	65
Figure 4.14 SMART Fortwo I rear suspension	66
Figure 4.15 Fiat Panda twist beam suspension [A2M10]	67
Figure 4.16 Tata Nano semi trailing arm suspension with subframe [A2M10]	69
Figure 4.17 Sketch of SMART De-Dion axle body in the E-MILA S package.....	71
Figure 4.18 Fiat Panda twist beam axle in the E-MILA Student package.....	72
Figure 4.19 Tata Nano semi trailing arm in the E-MILA S package.....	72
Figure 4.20 E-MILA Student package with twist beam suspension	73
Figure 4.21 Twist beam top view with rotation axis (according to [Hei08])	74
Figure 4.22 Toe- and camber-angle change	75
Figure 4.23 Ackermann condition [Rei00].....	76
Figure 4.24 Kinematics model of front suspension.....	77
Figure 4.25 Steering kinematics.....	78

List of Figures

Figure 4.26 Seating position – steering wheel position [Mad11].....	79
Figure 4.27 Equalisation of universal joint rotational non-uniformities [Bra01].....	80
Figure 4.28 Comparison of two steering gears.....	81
Figure 4.29 Maximum deceleration with recuperation brake	83
Figure 4.30 Accelerator pedal force characteristics	84
Figure 4.31 Brake circuit configuration [BOS07].....	85
Figure 4.32 Brake pedal position	87
Figure 4.33 Brake force distribution	89
Figure 4.34 Vehicle brake performance.....	90
Figure 5.1 Battery price (supplier to OEM) development [Rei10].....	99

List of Tables

Table 2.1 Basic vehicle specifications, compare to [Pre10]	6
Table 2.2 Inertia of rotating parts	11
Table 2.3 Vehicle parameters for traction force diagram	13
Table 2.4 Energy consumption from battery at NEDC	20
Table 3.1 Summary of characteristics of IM [Bou07].....	28
Table 3.2 Summary of characteristics of PM [Bou07]	29
Table 3.3 Summary of characteristics of SRM [Bou07].....	30
Table 4.1 Comparison of SMART Fortwo I with E-MILA Student [SMA10]	51
Table 4.2 Weights of Fiat Panda front suspension components [A2M10].....	56
Table 4.3 Weights of Tata Nano front suspension components [A2M10].....	57
Table 4.4 Benchmark wheel brake systems, data from [A2M10].....	86
Table 5.1 Drivetrain modules and components costs.....	93
Table 5.2 Battery module and components costs	93
Table 5.3 Chassis modules and components costs part 1	94
Table 5.4 Chassis modules and components costs part 2.....	95
Table 5.5 Drivetrain modules and components weights.....	96
Table 5.6 Battery module and components weights.....	96
Table 5.7 Chassis modules and components weights part 1	97
Table 5.8 Chassis modules and components weights part 2	98
Table A.1 Parameters for brake simulation	A

Annex

Table A.1 Parameters for brake simulation

Vehicle	Parameter	Unit
Wheelbase	1.85	m
Vehicle front projection area	2.1	m ²
cw-Value	0.35	-
Center of gravity unladen	0.44	m
Center of gravity laden	0.46	m
Axle load front unladen	278.9	kg
Axle load front laden	316.6	kg
Axle load rear unladen	336.1	kg
Axle load rear laden	473.4	kg
Static tyre radius	0.25	m
Dynamic tyre radius	0.265	m
Roll resistance at 1	0.008	-
Roll resistance at 2	8e-005	-
Moment of inertia frontaxle	0.9	kgm ²
Moment of inertia rearaxle	1.081	kgm ²
Speed	50	kph
Wheelbrakes	Parameter	Unit
Split	X-Split	-
Type front	Disk	-
Type rear	Drum	-
Caliper piston diameter front	0.035	m
Caliper piston diameter rear	0.019	m
Number of pistons / axle front	2	-
Number of pistons / axle rear	4	-
cStar front	0.8	-
cStar rear	2	-
Effective radius front	0.1025	m
Effective radius rear	0.089	m
Apply pressure front	0.5	bar
Apply pressure rear	3	bar
Pad area/axle front	129	cm ²
Pad area/axle rear	220	cm ²
Ventilation clearance front	0.2	mm
Ventilation clearance rear	1	mm
Pad compressibility pressure front	0 0.5 160	bar
Pad compressibility pressure rear	0 3 160	bar
Pad compressibility piston travel front	0 0 0.18	mm
Pad compressibility piston travel rear	0 0 1	mm
Caliper stiffness (pressure) front	0 0.5 13 20 40 80 160	bar
Caliper stiffness (pressure) rear	0 0.5 13 20 40 80 160	bar
Caliper stiffness fluid displacement front	0 0 0 0 0 1.1	mm
Caliper stiffness fluid displacement rear	0 0 0 0 0 1.1	mm

Brake Activation	Parameter	Unit
Pedal ratio	4	-
Hydraulic efficiency factor	0.99	-
Mastercylinder diameter	0.0178	m
Mastercylinder diameter 2	0.0	m
Mechanical efficiency factor	0.99	-
Mastercylinder stroke primary	16	mm
Mastercylinder stroke secondary	16	mm
Lost travel to breather hole	1.5	mm
Lost travel to pressure	1	bar
Mastercylinder type	Normal	-
Booster	No	Yes/No
Controller & Piping	Parameter	Unit
Type of controller	Breakpoint	
Change over pressure unladen	11	bar
Change over pressure laden	11	bar
Reduction ratio	0.35	-
Bypass	No	Yes/No
Pipe before controller Circuit 1	2.5	m
Pipe before controller Circuit 2	2.5	m
Pipe after controller Circuit 1	0.8	m
Pipe after controller Circuit 2	0.8	m
Hoses before controller Circuit 1	0.35	m
Hoses before controller Circuit 2	0.35	m
Hoses after controller Circuit 1	0.35	m
Hoses after controller Circuit 2	0.35	m
Pipe expansion	0.0036232	cm ³ /m
Hose expansion - Pressure	0 70 200	cm ³ /m
Hose expansion - Volume	0 0.7 1.5	bar